Università degli Studi di Parma
Dipartimento di Fisica e Scienze della Terra "Macedonio Melloni"
Dottorato di Ricerca in Scienze della Terra
Ciclo XXVI

Evoluzione 4D di sistemi di rift complessi: modellizzazione analogica ed applicazione a casi naturali.

Coordinatore:
Prof. Fulvio Celico

Tutor:
Prof. Fabrizio Storti

Co-tutor:
Dott. Fabrizio Balsamo
Dott. Cristian Cavozzi

Dottorando:
Yago Nestola

Yago Nestola
yago.nestola@gmail.com
+39 - 3336649370

Parco Area delle Scienze, 157/A
Campus Universitario - Parma
yago.nestola@unipr.it
+39 - 0521905356

Contents

Riassunto esteso

ABSTRACT

Il processo di rift ed i meccanismi che possono eventualmente portare alla rottura della crosta e della litosfera continentale sono complessi e non ancora pienamente conosciuti. La strutturazione dei margini di rift è il risultato della sovrapposizione di differenti processi geologici, propri del rifting o ereditati da precedenti fasi tettoniche. L'architettura del rift e del necking porta ad un differente assetto strutturale e termico dei bacini in funzione di parametri quali la strain-rate e la reologia dei vari componenti litosferici. Successivamente alla rottura continentale, in presenza di tassi di espansione oceanica differenziali, si può avere la riattivazione in trascorrenza dei margini passivi. Sono qui presentati i risultati dello studio sperimentale di alcuni fattori che influenzano il processo di rift, e dello studio di terreno per quanto riguarda la riattivazione post-rift del margine passivo brasiliano.

I.I. Introduzione

Il rifting continentale è un processo complesso, tipicamente prodotto dall'applicazione di un campo di stress tensionale su una litosfera longeva, strutturata da precedenti fasi tettoniche. La propagazione del rifting non è casuale ma segue il fabric metamorfico della placca riattivando sistematicamente antiche strutture litosferiche (Tommasi and Vauchez, 2001). Queste strutture preesistenti hanno quindi un ruolo chiave nell'architettura del rift. Lineamenti strutturali preesistenti ad alto angolo rispetto alla direzione di propagazione possono segmentare l'asse del rift, diventando successivamente il luogo di formazione preferenziale delle *Fracture Zones* e delle Faglie Trasformi (Wilson, 1965). Le *Fracture Zones* sono state classicamente descritte come settori di inattività tettonica. Recenti studi (Storti et al., 2007) hanno dimostrato che in presenza di tassi di espansione differenziali fra i centri di *spreading* a cavallo delle *Fracture Zones* è possibile la produzione di eccesso di taglio che può essere trasferito nel continente, portando alla formazione di nuove strutture deformative, o alla riattivazione di quelle preesistenti, ed inducendo anche un'importante attività sismica.

I processi di rifting ed i meccanismi con i quali la crosta e la litosfera continentale possono eventualmente frammentarsi e formare due margini coniugati sono complessi e non ancora pienamente conosciuti (Ebinger, 2005; Reston and Pérez-Gussinyé, 2007; Rosenbaum et al., 2008; Sawyer et al., 2007). Gli attuali margini di rift sono il risultato della sovrapposizione di differenti processi geologici che ne determinano la strutturazione finale una volta sopraggiunta la rottura. La risposta elastica ed isostatica della litosfera allo stiramento, le sue caratteristiche reologiche e termiche, unite alla presenza di zone di debolezza ereditate da deformazioni più antiche determinano l'andamento della deformazione durante il rifting e l'architettura finale dell'area sottoposta ad estensione.

Vari modelli sono stati proposti in bibliografia per spiegare la meccanica del rift e l'andamento della deformazione con la profondità (Beaumont et al., 1982; Kusznir and Karner, 2007; Mckenzie, 1978; Rowley and Sahagian, 1986; Ruppel, 1995; Wernicke, 1981). Per predire l'architettura profonda dei bacini, molti studi hanno correlato l'assottigliamento estensionale con le variazioni termiche prodotte dal rifting e registrate dai processi di subsidenza e sollevamento (Davis and Kusznir, 2002; Watts and Fairhead, 1999; Watts and Ryan, 1976; Watts and Torné, 1992). Parallelamente alle tecniche geofisiche classiche, un notevole contributo allo studio dei processi di rifting è stato apportato dalla modellizzazione analogica, permettendo lo studio separato delle singole variabili del processo (Autin et al., 2010; Brun and Beslier, 1996; Brun, 1999; Corti et al., 2003; Davy and Cobbold, 1991). In regioni come Il West Antartica Rift System o il margine del Togo nel sud Atlantico, zone di debolezza preesistenti possono essere riattivate come grandi sistemi trascorrenti dall'azione delle *Fracture Zones* oceaniche, le quali trasferiscono l'eccesso di taglio orizzontale dal *ridge* oceanico fin dentro il continente. Questa attività post-rift porta un ulteriore complicazione all'architettura strutturale dei margini passivi.

In questi tre anni sono state studiate sperimentalmente varie casistiche di rifting, volte a vincolare i parametri che possono determinare l'architettura strutturale e tettonica dei margini

di rift. Nello specifico, in questa tesi di dottorato viene presentata la messa a punto di una metodologia di laboratorio mirata a determinare l'andamento dell'assottigliamento nei vari strati della litosfera (§. I.II e Capitolo 2), applicando poi la stessa metodologia per monitorare l'effetto del tasso di divergenza sulla forma di necking e sulla distribuzione dei bacini in superficie (§. I.III e Capitolo 3). Sempre tramite modellizzazione analogica è stato studiato l'impatto di eventuali eterogeneità nella litosfera sull'evoluzione del rifting, applicando lo studio al caso del margine brasiliano nel segmento centrale del Atlantico meridionale (§. I.IV e Capitolo 4). Nel margine brasiliano è stato inoltre effettuato uno studio di terreno per verificare la possibilità di riattivazione post-rift del margine, ascrivibile a faglie trascorrenti di importanza regionale guidate dall'espansione oceanica (§. I.V e Capitolo 5).

I.II Evoluzione del necking (o strizione) litosferico tramite modelli analogici

I.II.I Introduzione

La geometria dei bacini di rift è funzione della risposta elastica ed isostatica della litosfera allo stiramento, ed è influenzata dalla variazioni reologiche e termiche della sua struttura (Cloetingh et al., 1995; van der Beek et al., 1994; Ziegler and Cloetingh, 2004). Molti modelli di rifting e di necking sono stati proposti assumendo differenti tipi di distribuzione della deformazione fra crosta e mantello (Beaumont et al., 1982; Kusznir and Karner, 2007; Mckenzie, 1978; Rowley and Sahagian, 1986). Numerose tecniche sono state messe a punto per determinare la storia tettonica dei margini di rift: retrodeformazione flessurale (1D, 2D, e 3D), modellazione gravimetrica, retrodeformazione delle faglie e modelli cinematici (Davis and Kusznir, 2002; Ranero and Pérez-Gussinyé, 2010; Reston, 2007; Watts and Fairhead, 1999; Watts and Ryan, 1976; Watts and Torné, 1992). Nonostante la grande mole di lavoro sui margini di rift, l'andamento incrementale e finito dell'assottigliamento e del necking litosferico non sono ancora stati pienamente vincolati. In questo contesto la modellazione analogica e numerica possono dare un notevole contributo alla comprensione

tridimensionale della risposta litosferica all'assottigliamento. In questo capitolo presentiamo i risultati di un programma sperimentale volto allo studio dell'evoluzione del necking litosferico in un rift ortogonale. In questo studio presentiamo i risultati sperimentali ottenuti da modelli analogici a scala litosferica progettati per analizzare l'andamento del necking durante l'estensione e per determinare la distribuzione finita della deformazione attraverso i diversi livelli che compongono la litosfera. I risultati mostrano una distribuzione della deformazione cilindrica nella crosta ed eterogena nel mantello. In generale, la deformazione durante il rifting tende a passare da delocalizzata nelle fasi iniziali a localizzata nelle fasi finali. Questo studio è servito a mettere a punto una nuova metodologia di laboratorio attraverso la quale è stato possibile studiare contemporaneamente l'andamento della deformazione in superficie ed in profondità.

I.II.II Modellizzazione analogica

L'apparato di deformazione usato per questo studio è costituito da una contenitore di plexiglas suddiviso a metà da una parete mobile a forma di U, le cui due braccia laterali costituiscono la discontinuità di velocità ortogonale agente sul modello. Il modello è costituito da un alternanza di livelli fragili (sabbia) e duttili (silicone) opportunatamente calibrati per simulare in scala le caratteristiche reologiche della litosfera. Il *multilayer* galleggia liberamente su uno strato di sciroppo di glucosio, che costituisce l'astenosfera analogica. Per mezzo di un motore a controllo numerico, la parete mobile viene spostata di 50mm a velocità costante di 10mm/h, estendendo il settore contenente la litosfera sperimentale a spese del settore serbatoio di astenosfera. Estendendo solo un lato della litosfera sperimentale, si è simulato un rifting asimmetrico. I dati del modello e dello *scaling* vengono forniti in tabella 1 e 2.

L'uso di un doppio laser scanner con risoluzione a 0.25mm, permette di monitorare in tempo reale l'andamento della superficie del modello e dell'interfaccia litosfera-astenosfera. Le scansioni sono state fatte ad intervalli programmati per avere una completa tracciatura dei percorsi deformativi del necking.

Una volta terminata la deformazione, i vari strati del modello che costituiscono la litosfera analogica sono stati rimossi. Per ogni strato sono state acquisite le scansioni della superficie e dell'interfaccia astenosfera litosfera. Dalle superfici ottenute sono stati calcolati i valori di assottigliamento (*Thinning Factor*, TF) per ogni *layer* litosferico.

I.II.II.I Evoluzione del modello

Fin dalle prime fasi di deformazione, tre depressioni tettoniche, separate da due alti strutturali, si formano adiacenti alla discontinuità di velocità. In questi tre bacini si localizza la deformazione estensionale, che nelle seconda metà del modello tende a concentrarsi nel bacino centrale. Parallelamente, il rigonfiamento dell'astenosfera nella litosfera meccanica mostra un risalita distribuita, asimmetricamente spostata verso il bacino sul lato fisso. La crescita del *necking* si localizza in due principali culminazioni astenosferiche, che isolano una porzione di mantello superiore indeformato. Nelle fasi finali della deformazione, i bacini tendono ad approfondirsi, soprattutto i due bacini laterali, mentre il bacino centrale è soggetto a sollevamento. Al termine della deformazione il bacino centrale ha uno sviluppo estensionale doppio rispetto ai bacini laterali ed il necking è penetrato all'interno della litosfera per due terzi del suo spessore. La sua forma è abbastanza simmetrica pur presentando una culminazione principale sul lato fisso ed una secondaria sul lato mobile. La culminazione principale mostra un trend di crescita a sviluppo verticale nella prima metà del modello, mentre nella seconda metà migra verso la direzione di estensione.

I.II.II.II Analisi della deformazione finita

La distribuzione 3D dell'assottigliamento calcolato per la crosta (TF_C), per il mantello litosferico (TF_M) e per l'intera litosfera (TF_L) sono illustrate in figura 3. Nella crosta questo parametro è caratterizzato da alti valori concentrati in un ristretto settore centrale, la cui ampiezza è coerente attraverso il modello. L'assottigliamento nel mantello litosferico mostra un andamento differente rispetto alla crosta, interessando un area più ampia e con una strutturazione più complessa. In,

particolare una regione allungata con bassi valori di assottigliamento viene enucleata da due settori molto stretti con TF molto alti. L'assottigliamento calcolato per l'intera litosfera meccanica mostra la combinazione dei valori di TF_C e TF_M. Il settore caratterizzato da bassi valori resta evidente, ma ha un'espressione più attenuata rispetto al mantello (TF_M).

I.II.III Discussione

Il setup presentato è stato progettato per simulare un processo di rifting asimmetrico (Aslanian et al., 2009; Ranero and Pérez-Gussinyé, 2010). In questo contesto un fianco del necking preserva la stessa posizione durante il rifting, mentre il fianco opposto viene spostato nella direzione di estensione. Di conseguenza, la crescita verticale del necking è asimmetricamente concentrata verso il fianco fisso. L'asimmetria è registrata anche a scala crostale dove i bacini con maggiore apertura sono i due verso la parete fissa, mentre il bacino verso la parete mobile mostra un minor tasso di apertura. I risultati del modello sono comparabili con i modelli già presentati in letteratura (Brun and Beslier, 1996; Brun, 1999; Callot et al., 2002), tenendo conto delle differenze dei principali parametri reologici e dello strain-rate. La forma finale del necking litosferico può essere comparata con quanto ricostruito per molti sistemi di rift in natura (Peron-Pinvidic et al., 2013), come anche per la struttura del margine della Tetide preservata nelle Alpi (Beltrando et al., 2010). L'andamento incrementale e finito della deformazione e dell'assottigliamento danno importanti indicazioni sulla distribuzione 4D del flusso di calore e del magmatismo legato al rift. Infatti l'asimmetrica posizione del necking rispetto ai bacini implica un maggiore flusso di calore ed un maggiore magmatismo nei bacini sul lato fisso rispetto a quelli sul lato mobile, che si sviluppano su di una litosfera sostanzialmente non assottigliata.

I.II.IV Conclusioni

Abbiamo messo a punto una configurazione di laboratorio mirata a studiare la forma del necking durante il processo di rifting e la distribuzione della deformazione. Il modello utilizzato per mettere a punto il metodo ha mostrato che nel con-

testo cinematico simulato, il necking ha uno sviluppo molto asimmetrico rispetto al rift in superficie, essendo più pervasivo verso il settore fisso rispetto a quello mobile. Questo ha portato alla crescita di bacini su settori di litosfera che hanno registrato una deformazione differenziale, con conseguenze importanti sulla distribuzione del flusso di calore e del magmatismo. La distribuzione della deformazione è quindi dipendente dalla profondità (*depth-dependent*) pur rimanendo in un sistema chiuso. Nello specifico, la crosta mostra una deformazione più cilindrica mentre nel mantello si ha un distribuzione asimmetrica. In ultimo, la deformazione passa da distribuita a localizzata con il progredire delle deformazione.

I.III. Architettura del rifting e del necking litosferico in funzione della strain-rate estensionale

I.III.I Introduzione

I margini di rift ed il processo di rifting sono stati oggetto di numerosi studi e tentativi di giungere ad una classificazione sempre più dettagliata, quanto più la tecnologia forniva nuove metodologie di studio. I vari margini sono stati così classificati in categorie a seconda delle caratteristiche prese in esame. La principale classificazione, ancora oggi molto in uso, definisce i rifts come passivi o attivi a seconda che, rispettivamente, l'estensione sia frutto di stati tensionali nella litosfera o di risalite di *plume* astenosferici (Ruppel, 1995). Buck (Buck, 1991) propose la classificazione in *Narrow*-rift, *Wide*-rift, e *Core-complex*, a seconda dello stile deformativo nella crosta e della sua reologia. La meccanica di estensione è classificata secondo vari modelli di taglio: *pure-shear* (Mckenzie, 1978), *simple-shear* (Wernicke, 1985), *combined-shear* (Lister et al., 1986). Lo studio della quantità di magma presente sul margine ha dato luogo alla classificazione del processo secondo due *end-member*: magma-*poor* e magma-*sustained*. Inoltre sono stati coniati nuovi termini per descrivere le caratteristiche morfologiche del rift, i vari domini del margine ed i processi agenti nelle differenti fasi (Peron-Pinvidic et al., 2013). La modellizzazione analogica ha dato un notevole contributo nello studio dei mar-

gini passivi e del processo di rift, potendo indagare l'effetto dei singoli parametri sulla deformazione prodotta (Autin et al., 2010; Benes and Davy, 1996; Brun and Beslier, 1996; Brun, 1999; Corti et al., 2003; Davy and Cobbold, 1991; Sokoutis et al., 2007). La modellizzazione analogica, come anche numerica e le osservazioni di terreno, ha evidenziato l'importanza della velocità di deformazione a prescindere dal contesto tettonico. In questo lavoro abbiamo testato l'effetto della velocità nel processo di rifting tramite modelli analogici a scala litosferica.

I.III.II Modellazione analogica

Abbiamo studiato la risposta della litosfera al variare della velocità di divergenza delle placche in un intervallo di un ordine di grandezza. In particolare, in questo paragrafo descriviamo i risultati ottenuti con tassi di estensione di 5mm/h (neck-05) ed 50mm/h (neck-50). L'intervallo di velocità è rappresentativo di tassi di divergenza per il prototipo naturale nell'ordine 2 - 20mm/y e strain-rate di 10^{-15} – 10^{-14} (s^{-1}) rispettivamente.

I.III.II.I Evoluzione dei modelli

La comparazione fra i due modelli mostra come il tasso di divergenza eserciti un forte controllo sul rifting fin dalle fasi iniziali della deformazione. La superficie del modello lento non mostra tracce di deformazione per faglia prima di essere giunti a 10mm di estensione; al contrario il modello veloce risponde immediatamente all'instaurarsi del regime estensionale, mostrando i primi lineamenti già dopo pochi mm di divergenza. Analogamente il necking litosferico assume fin da subito forme differenti fra i due modelli. Il neck-05 mostra una blanda antiforme ben sviluppata già a 10mm di estensione, mentre il modello neck-50 è caratterizzato da una vasta area di sollevamento con una blanda convessità.

Con l'aumentare dell'estensione, due bacini molto stretti separati da una vasto settore non fagliato si formano nel modello lento, mentre le zone di faglia sono molto più abbondanti e si sviluppano su una vasta area nel modello più veloce. Il necking evolve con un rapida crescita verticale nel model-

lo neck-05, mantenendo una definita forma a campana fino a circa 25mmm di divergenza. Il modello neck-50, a partire da 15mm di estensione, sviluppa un profilo del necking con tre corrugazioni antiformi le cui geometrie si accentuano al progredire della deformazione.

L'architettura del rift registrata nella prima metà del modello viene sostanzialmente preservata nella seconda metà di deformazione, mentre il necking evolve in forma molto differente negli ultimi centimetri di deformazione. Nel modello lento, il necking subisce un netto cambio di traiettoria in cui la crescita verticale si interrompe e viene sostituita da una migrazione laterale che accomoda l'estensione del modello. Al contrario, nel modello veloce il picco centrale subisce una forte migrazione verticale. Al termine della deformazione, l'espressione superficiale dell'allungamento e l'assottigliamento litosferico raggiungono dimensioni comparabili fra i due modelli, nonostante siano differenti le architetture strutturali dei due sistemi di rift. Nel modello lento l'assottigliamento viene accomodato da due bacini principali separati da un settore per lo più non fagliato. Il modello veloce mostra una deformazione più distribuita in una vasta depressione centrale.

I.III.II.II Rapporto d'aspetto del necking

Le differenze di crescita fra I vari modelli sono state parametrizzate per mezzo del rapporto d'aspetto (*aspect ratio*) H/L. L'altezza (H) è la massima penetrazione del necking nella litosfera, l'ampiezza (L) è la distanza lungo la direzione d'estensione dove il TF si attesta con continuità su valori maggiori o uguali a 0,1. L'andamento del rapporto d'aspetto durante la deformazione è molto differente fra i vari modelli. Il modello veloce inizia con valori elevati di H/L per poi decrescere durante la deformazione. Il modello intermedio (§II) comincia da valori alti per poi immediatamente decrescere attestandosi su un plateau. Il modello lento si attesta su valori bassi per poi incrementare durante deformazione. Al termine della deformazione sia il modello lento che il modello veloce convergono fino attestandosi sui valori di H/L del modello intermedio.

I.III.II.III Analisi della deformazione finita

La distribuzione dell'assottigliamento nella crosta (TF_C) è per lo più cilindrica in entrambi i modelli, meno ampio nel modello lento rispetto che nel modello veloce. Nel modello neck-05 TF_M è localizzato lungo il necking, al di fuori del quale non c'è assottigliamento del mantello. Nel modello neck-50 il TF_M è distribuito su di una vasta area con tre picchi di assottigliamento che individuano due settori di mantello superiore molto poco attenuato.

Il *thinning factor* calcolato per l'intera litosfera (TF_L) mostra le caratteristiche sia della crosta che del mantello nel modello neck-05, mentre la complessa struttura del mantello viene parzialmente mascherata nel modello neck-50. Quest'ultimo ha un area soggetta all'assottigliamento leggermente più ampia e con valori più alti rispetto al modello più lento che fatta eccezione per il picco centrale si attesta su valori molto più attenuati.

I.III.III Discussione e conclusioni

L'asimmetria cinematica del setup sperimentale produce un necking fortemente asimmetrico fin dal inizio della deformazione. Nello specifico, il disassamento esistente fra il necking e la superfice soggetta a deformazione è maggiore per bassi tassi di divergenza a causa dell'efficacia del disaccoppiamento della crosta inferiore duttile. Al contrario, la minore efficacia del disaccoppiamento porta a d una maggiore distribuzione della deformazione nei modelli ad alto tasso di divergenza. L'asimmetria causa una maggiore penetrazione del necking al di sotto dei bacini che si attestano sul lato fisso del modello, mentre quelli sul lato opposto giacciono su una litosfera per lo più non assottigliata.

Il tasso di divergenza incide sulla forma del necking. Nel caso di bassi strain-rate si produce un singolo necking con una sommità piatta e fianchi verticali. Nel caso di strain-rate elevati il necking influenza un'area più vasta e producendo rigonfiamenti astenosferici di secondo ordire al margine del necking principale.

Durante l'estensione, i rifts lenti mostrano un progressiva crescita dei valori H/L mentre i rifts veloci hanno una altrettanto veloce decrescita. Il rapporto d'aspetto dei differenti modelli converge verso valori moto simili indifferentemente dal velocità di divergenza, suggerendo che questo parametro sia funzione della stratificazione reologica della litosfera.

La forma finale della litosfera sperimentale estesa a differenti tassi di velocità mostra notevoli similitudini con i transetti ricostruiti per i sistemi di rift in natura. La peculiare architettura del rift lento con due bacini distinti che localizzano la deformazione, unitamente al disassamento del necking, è comparabile con il caso di blocchi di crosta più resistenti circondati da zone più deboli dove il rift può propagarsi, come nel "micro-continente" Jan Mayen fra la Groenlandia e la Norvegia nel nord Atlantico (Peron-Pinvidic et al., 2013). Modelli con strain-rate intermedi hanno geometrie della superficie, della moho e del necking che corcordano con quelle ricostruite per il margine Flemish Cap –Galicia Banks ed il suo analogo tetideo preservato nelle Alpi (Peron-Pinvidic and Manatschal, 2010; Peron-Pinvidic et al., 2013). Nel modello più veloce la distribuzione della deformazione come la forma della moho hanno una buona corrispondenza con i transetti ricostruiti per il sud Atlantico nel margine coniugato Brasile-Kwanza (Aslanian et al., 2009; Peron-Pinvidic et al., 2013).

I.IV Effetto delle eterogeneità litosferiche sull'evoluzione del rifting continentale, casi dal margine Atlantico meridionale.

I.IV.I Introduzione

I margini coniugati del Atlantico meridionale mostrano caratteristiche ascrivibili sia a tipologie magma-*poor* che magma-*sustained*. Per il suo segmento centrale (compreso fra la Rio Grande FZ e la Chain FZ), è stata proposta una classificazione di tipo magma-*poor* a causa della assenza di forti evidenze magmatiche (Contrucci et al., 2004; Moulin et al., 2005; Reston, 2009). I vari modelli di rifting proposti in letteratura (cfr. §II.I e §III.I) spiegano solo parzialmente i dati di geofisica e le os-

servazioni geologiche di questo settore del sud Atlantico. In questo studio abbiamo utilizzato un approccio volto ad integrare il dato geofisico con la modellizzazione analogica a scala litosferica al fine di caratterizzare l'effetto delle eterogeneità della litosfera sul evoluzione del rift. Nello specifico ci siamo concentrati sulla porzione meridionale del segmento centrale del sud Atlantico: i bacini di Santos e Campos.

I.IV.II Contesto geologico

I cratoni Sao Francisco e Congo sono stati interpretati come facenti parte di una porzione interna e stabile del settore occidentale del Gondwana, assemblata a seguito di una serie di collisioni tettoniche. Questa storia tettonica ha lasciato una serie di lineamenti strutturali ed eterogeneità nella litosfera che hanno avuto un controllo sulla messa in posto del rifting mesozoico dell'Atlantico meridionale. *Onshore* sono ancora distinguibili porzioni della sutura del Gondwana come l'Araçuai Belt, all'altezza del bacino di Campos, ad andamento NNE-SSW, collegata a sud con la Riberia Mobile Belt, ad andamento NE-SW. *Offshore* molti autori hanno evidenziato la presenza di un *ridge* oceanico abbandonato, l'Abimael *Ridge*, all'altezza della Florianópolis FZ. Questo sito è stato classificato come un aulacogeno o un centro di *spreading* abbandonato, prodotto dall'istaurarsi del rift su un settore reologicamente perturbato del Sao Paolo Plateau .

I.IV.III Modellizzazione analogica

Per simulare le eterogeneità presenti nella litosfera del margine brasiliano precedentemente descritte, sono stati introdotti nella litosfera sperimentale dei corpi con minore o maggiore resistenza. L'Araçuai Belt con le sue caratteristiche rappresenta un sito di alta resistenza della litosfera ed è stato simulato inserendo nella crosta duttile sperimentale un silicone a più alta viscosità (*strong lower crust*, SLC) rispetto a quello che lo circonda. Viceversa l'Abimael *Ridge* rappresenta una crosta assottigliata ed indebolita ed è stata simulata con un silicone a minor viscosità rispetto al contesto (*weak lower crust*, WLC). La differente orientazione del margine fra Campos (ortogonale) e Santos (obliqua) è stata studiata in alcuni modelli utilizzando

delle pareti laterali con lunghezze differenti ed inserendo una eterogeneità nella mantello superiore atta a deformare ortogonalmente il settore settentrionale di Campos ed obliquamente il settore meridionale di Santos.

I.IV.III.I Effetti delle eterogeneità

La presenza di eterogeneità all'interno della litosfera produce forti effetti sull'evoluzione strutturale del rift. I corpi a resistenza ridotta posti nel mantello superiore hanno un effetto regionale sulla deformazione della crosta fragile senza apportare significative localizzazioni. Viceversa l'indebolimento del mantello fragile guida la variazione di traiettoria del necking, seguendone l'andamento ortogonale ed obliquo. Inoltre i modelli con eterogeneità nel mantello non hanno raggiunto il breakup dimostrando la loro inefficacia nel localizzare lo stress estensionale, che viene per lo più dissipato negli strati a reologia duttile.

Le eterogeneità reologiche nella crosta inferiore duttile localizzano la deformazione producendo forti variazioni nella segmentazione del margine, in funzione della loro reologia. Nel caso di corpi con viscosità maggiore rispetto al contesto si producono bacini articolati ad *horst* e *graben* , mentre bacini più localizzati e profondi si formano al di sopra di corpi con viscosità inferiore rispetto al contesto. Una crosta con reologia indebolita promuove la formazione di *half-graben* con faglie listriche principali che portano alla formazione di spessi cunei sedimentari syn-rift. La presenza di corpi a resistenza maggiore rispetto al contesto della crosta inferiore duttile produce bacini controllati da faglie planari ruotate a domino con sequenze di basso spessore controllate direttamente dai singoli blocchi di faglia. La presenza di eterogeneità produce una differenziazione nell'ampiezza dei bacini prodotti nei margini. Nel caso del settore con la SLC, nel margine che giace al di sopra dell'anomalia di viscosità i bacini interessano un area più ampia e sono meno profondi ed in posizione strutturale più elevata rispetto al coniugato sul margine opposto, il quale presenta invece le caratteristiche tipiche dei settori indeboliti con bacini non molto ampi ma molto profondi. Nel caso dei

settori WLC, il margine che giace sull'anomalia produce bacini profondi e non molto ampi, rispetto al coniugato con bacini poco profondi che si sviluppano su una area più vasta.

I.IV.IV Conclusioni

Le eterogeneità ereditate da precedenti fasi tettoniche mostrano una notevole efficacia nel guidare la deformazione durante il rifting. Le anomalie profonde tendono a concentrare il loro effetto sul necking litosferico senza interferire sulla localizzazione della deformazione nella crosta fragile. Le anomalie nella crosta duttile mostrano invece una notevole efficacia nel segmentare il margine. Le anomalie WLC portano alla formazione di margini poco ampi con bacini profondi, la cui architettura ad *half-graben* porta a spessi cunei sedimentari. Le anomalie SLC producono faglie planari ruotate a domino, interessando un'aerea piuttosto estesa senza produrre forti spazi di accomodamento per i sedimenti. Laddove sia presente un margine interessato da anomalia reologica, il suo coniugato risponde alla localizzazione della deformazione rispettivamente come un margine indebolito se è coniugato di un margine SLC oppure come un margine con caratteristiche reologiche ad alta resistenza se coniugato con un margine WLC.

La presenza di eterogeneità reologiche è particolarmente rilevante nelle prime fasi del rifting durante le quali produce forti asimmetrie nel rift. Nelle fasi seguenti, a causa del loro assottigliamento, le anomalie diventano meno efficaci ed un successivo impulso estensionale localizza la deformazione in un area centrale formando bacini simmetrici con faglie immergenti verso oceano.

I modelli realizzati possono essere utilizzati per vincolare e ricostruire l'architettura strutturale delle sequenze pre-evaporitiche nel segmento centrale del sud Atlantico.

I.V Deformazioni intraplacca nel nordest del Brasile indotte da ripetute inversioni di taglio post-rift lungo la Pernambuco Fracture Zone.

I.V.I Introduzione

Le teoria della "Tettonica delle Placche" prevede che la sismicità sia confinata nei margini di placca. Questa attività nelle dorsali oceaniche è per lo più localizzata nelle faglie trasformi che connettono due assi di espansione adiacenti (Wilson, 1965), a causa dell'opposta direzione di accrezione della crosta oceanica nella regione di sovrapposizione. Esternamente rispetto alla zona di sovrapposizione, i corridoi di litosfera oceanica muovendosi nella stessa direzione ed alla stessa velocità, non dovrebbero dare luogo a sismicità. Nondimeno terremoti intraplacca avvengono in aree continentali stabili. Questo è il caso del NE-Brasile, dove sismicità e evidenze di tettonica attiva recente hanno luogo nell'interno del continente e lungo la costa (Bezerra et al., 2011). Classicamente questo stato di stress viene imputato ad una compressione E-W dovuta all'apertura dell'Atlantico ed alla subduzione del Pacifico sotto le Ande (Ferreira et al., 2008; Lopes et al., 2010). Le mappe di distribuzione della sismicità mostrano dei cluster lungo le *shear zones* neoproterozoiche (eg Pernambuco, Patos, and Sobral) (Bezerra et al., 2011), queste agiscono siti di debolezza preesistenti guidando la localizzazione di faglie trasformi durante il rifting (Wilson, 1965). Studi recenti (Storti et al., 2007) hanno evidenziato che una certa quantità di taglio può esistere oltre i settori di sovrapposizione delle trasformi, se fra i due *ridges* adiacenti esiste un tasso di apertura differente. Questa caratteristica si manifesta nell'Oceano Meridionale, dove la Tasman FZ mostra un eccesso di taglio destro che disloca la piattaforma continentale per centinaia di chilometri (Storti et al., 2007). Questo eccesso di taglio giustifica la presenza di terremoti e l'attività tettonica nei cosiddetti margini passivi. Per verificare la possibilità di attività tettonica recente nel margine brasiliano e le sue cause, abbiamo effettuato una campagna strutturale nella formazione Barreiras (Miocene) e nella formazione Post-Barreiras (Quaternario) comparandola con lo spreading differenziale del sud Atlantico giustapposto alla Pernambuco

FZ. Qui descriviamo in che modo le deformazioni nell'intorno dei lineamenti pre-rift siano strettamente correlate con il tasso di espansione dell'oceano.

I.V.II Pernambuco Shear Zone (onshore)

Abbiamo effettuato uno studio strutturale di terreno nella regione costiera dello Stato del Pernambuco (NE-Brasile), dove la formazione Barreiras e Post-Barreiras affiorano estesamente per centinaia di chilometri. La formazione Barreiras è un deposito continentale silicoclastico cdi 75-100 m di spessore, per lo più sabbie con intercalati livelli a conglomerati e argille, relazionato alla trasgressione miocenica. Il top della formazione è fornito da un ben sviluppato paleosuolo lateritico: una superficie di discontinuità regionale legata alla caduta del livello del mare del Tortoniano. La formazione post-Barreiras è un deposito sabbioso silicoclastico del Quaternario che giace al di sopra di questa discontinuità. Nell'aerea studiata si registrano deformazioni fragili per lo più estensionali in entrambe le formazioni, aventi direzioni N-S, WNW-ESE e NE-SW. Nella formazione Barreiras sono pervasive le faglie estensionali con direzione principale attorno a N300, meno pervasivi ma comunque presenti le faglie ascrivibili ai trend N040 e N360. Lo stesso non avviene nella formazione post-Barreiras dove le faglie estensionali sono per lo più organizzate attorno al trend N040. Faglie inverse e trascorrenti, sia destre che sinistre, sono state riscontrate solo nella Formazione Barreiras. I tre trend strutturali riscontrati sul terreno sono compatibili con un campo di stress cinematico prodotto lungo un lineamento trascorrente orientato N080, ovvero la direzione del lineamento Pernambuco nella area di studio. Nello specifico, il pattern deformativo nella formazione Barreiras è consistente con uno stress cinematico prodotto da un taglio destro del lineamento, mentre il pattern di deformazione nella formazione post-Barreiras è consistente con un'attività sinistra.

I.V.III Pernambuco Fracture Zone (offshore)

Per vincolare i tassi di espansione del *ridge* abbiamo misurato le ampiezze di segmenti coevi di crosta oceanica a cavallo della Pernambuco *Fracture Zone* (PeFZ). Le ampiezze sono sta-

te misurate a partire da un database preesistente (Müller et al., 2008) organizzato vincolando le età della crosta oceanica su 14 croni. Nello specifico di questo studio sono stati utilizzati gli 8 più recenti, che interessano la crosta oggetto di studio: 5o (10.9 Ma), 6o (20.1 Ma), 13y (33.1 Ma), 18o (40.1 Ma), 21o (47.9 Ma), 25y (55.9 Ma), 31y (67.7 Ma), 34y (83.5 Ma). L'ampiezza di crosta oceanica prodotta in un dato intervallo di tempo è stata misurata lungo due transetti paralleli alla PeFZ, a nord ed a sud. La differenza fra l'ampiezza del segmento nord e l'ampiezza del segmento sud restituisce l'eccesso di taglio e la sua polarità (destro-sinistro). Lungo la PeFZ sono state riscontrate 5 inversioni della polarità di taglio. L'inversione più recente, datata 10,9 Ma, segna il passaggio da un eccesso di taglio destro (20,4-10,9 Ma) ad un eccesso di taglio sinistro (10,9Ma-attuale).

I.V.IV Discussione

Il dato di terreno delle formazioni miocenico-quaternarie affioranti lungo la costa del NE-Brazil mostra la presenza di strutture ascrivibili alternativamente sia ad un taglio Dx che ad un taglio Sx del lineamento Pernambuco. Le prime sono presenti solo nella formazione Barreiras, miocenica; le seconde, presenti in entrambe, sono più pervasive nella formazione post-Barreiras, quaternaria. L'alternarsi delle due polarità di taglio per la Pernambuco *shear zone* mostra una singolare congruenza con l'alternanza di eccesso di taglio registrata negli centri di espansione adiacenti la PeFZ. Nei transetti offshore è stata individuato una inversione di polarità a 10,9Ma coerente con l'età tortoniana del paleosuolo lateritico che marca il passaggio dalla formazione Barreiras alla formazione post-Barreiras.

I.V.V Conclusioni

1) Le Anomalie magnetiche mostrano spreading rate differenziali a ridosso della Pernambuco *Fracture Zone*, producendo un'alternanza di taglio destro e sinistro.

2) I depositi Miocenici (Barreiras) e Quaternari (Post-Barreiras), nel bacino del Pernambuco, sono interessati da faglie con cinematica prevalentemente estensionale, orientate N300

e N040, congruenti con successive alternanze di cinematica destra e sinistra del lineamento Pernambuco.

3) L'integrazione dei dati geofisici e strutturali supporta la possibilità di un trasferimento di taglio dai centri di espansione oceanica all'interno del margine continentale passivo attraverso la faglia trasforme ed il lineamento Pernambuco.

4) L'eccesso di taglio accumulato dalla PeFZ può essere la sorgente della sismicità attuale associata al Lineamento Pernambuco nel continente

I.VI Conclusioni

Il dottorato di ricerca ha avuto come oggetto lo studio dei sistemi di rift e delle loro complessità. Per mezzo della modellizzazione analogica è stato possibile approfondire l'effetto di vari parametri sull'architettura del rift: la velocità di divergenza delle placche, la presenza di eterogeneità reologiche nella crosta e nel mantello litosferico. Lo studio di terreno è stato mirato allo studio della riattivazione in trascorrenza del margine brasiliano ad opera della accrezione differenziale di litosfera oceanica a cavallo della Pernambuco FZ.

La strain-rate estensionale ha un ruolo di primo ordine sull'architettura del rift e del necking litosferico in esperimenti analogici. Per tassi di divergenza bassi si hanno profili necking molto localizzati, viceversa all'aumentare del tasso di divergenza si ha un profilo di necking più frastagliato che produce rigonfiamenti astenosferici di secondo ordire al margine del necking principale. La configurazione cinematica simulata porta una marcata asimmetria del necking rispetto alla deformazione superficiale, che porta ad un maggiore assottigliamento verso il lato fisso del sistema di rift. Applicata al caso naturale questa asimmetria porta ad una maggiore risalita delle isoterme sul lato fisso del sistema di rift rispetto al lato mobile, con ricadute sulla produzione di magmatismo e sul flusso di calore a cui sono sottoposti i bacini ed i loro sedimenti. L'asimmetria si attenua all'aumentare dello strain rate portando quindi un flusso di calore più omogeneo fra i due

fianchi del rift.

La presenza di eterogeneità nella litosfera ha effetti differenti a seconda della loro natura e della loro posizione verticale nella litosfera. Anomalie di viscosità nel mantello portano ad una delocalizzazione della deformazione sia crostale che litosferica. La marcata segmentazione del rift prodotta da anomalie crostali porta ad una forte asimmetria fra i due lati del rift. Inoltre, a prescindere dalla resistenza intrinseca dell'anomalia, nel caso di due margini coniugati il margine che mostra una resistenza relativa maggiore produce bacini poco profondi con faglie a domino, mentre il margine coniugato con resistenza relativa inferiore produce bacini guidati da faglie listriche contenti cunei sedimentari anche di forte spessore.

Nello studio di terreno condotto nel margine Brasile si è riscontrata la riattivazione post-rift in trascorrenza sia destra che sinistra della zona di taglio Pernambuco, ad opera dell'eccesso di taglio prodotto dall'accrezione differenziale di litosfera oceanica a cavallo del PeFZ. Questa riattivazione per taglio del margine può produrre una ulteriore complicazione sulle geometrie dei bacini preesistenti riattivando precedenti depocentri o attivandone di nuovi. In ultimo, la riattivazione in trascorrenza delle linee di debolezza pre-rift porta ad una ulteriore complicazione nella distribuzione della fratturazione e quindi nella circolazione dei fluidi attesa per i bacini ed i margini di rift.

1

Introduction

Continental rifting is a complex process that results from the application of a tensional stress field to a long-lived and, hence, already structured lithosphere. Rifting propagation paths follow the trend of the pre-existing orogenic fabric, systematically reactivating ancient lithospheric structures, supporting an active role of lithosphere structure on rifting processes (Tommasi and Vauchez, 2001). Pre-existing lines of weakness that lies at high-angle with respect to the rifting propagation direction can segment the rifting axis, eventually becoming the preferential site of Transform Faults and, hence, Fracture Zones (Wilson, 1965). Classically, Fracture Zones are describe as tectonically inactive structures. Despite this, recent studies (Storti et al., 2007) demonstrate that differential spreading rate between two adjacent spreading centres can bear an excess of shear into the continent, forming or reactivating structures consistent with the shear kinematics.

1.1 Rifting

Rifting and the mechanism with which the continental crust is, through stretching and thinning processes, eventually broken are still far away to be completely understood (Ebinger, 2005; Reston and Pérez-Gussinyé, 2007; Rosenbaum et al., 2008; Rosendahl et al., 2005; Sawyer et al., 2007). Several generic models describing the above processes have been proposed during the end of the last century (such as the McKenzie (McKenzie, 1978) "pure-shear", the Wernicke (1981) "simple-shear", and the Barbier et al. (1986) "combined-shear" lithospheric shear models), and have defined the complex interaction of structural and magmatic relationships during the continental rifting and breakup. This interaction results in a wide variety of margin styles, ranging, among others, from "Narrow" to "Wide", and from "magma-poor" to "magma-sustained" conjugate-pair rifted margins (e.g. Blaich et al., 2011; Brun, 1999; Menzies et al., 2002; Peron-Pinvidic et al., 2013). "Narrow-rifts" and "Wide-rifts" differ in the mechanical instability type, namely necking versus spreading, which can

develop for a given lithospheric strength profile (Brun, 1999). Necking occurs preferentially in a stable lithosphere that has a four-layer strength profile where the greatest strength is located in the sub-Moho mantle. It gives birth to narrow rifts, from continental rifts to passive margins. Spreading occurs preferentially in a thickened lithosphere whose strength profile, after thermal relaxation, exhibits maximum strength at the base of upper brittle crust. It gives birth to wide rifts, such as the Basin and Range of the western United States or the Aegean (Brun and Beslier, 1996; Brun, 1999). "Magma-poor" rifted margins are those where volcanic products are sporadically distributed along the margin while the crust is affected by intense faulting (e.g. Brazil NE-West Africa margins (Aslanian et al., 2009); Iberia–Newfoundland margins (Péron-Pinvidic et al., 2007); Australian– East Antarctic margins (Close et al., 2009; Direen et al., 2007)). On the other hand, "magma-sustained" rifted margins are those where magma products are very well diffused and recognised along the rifted margins, and are characterised by seaward dipping reflector (SDR) sequences close to the continent–ocean boundary (COB), large igneous provinces both onshore and offshore, and voluminous along-margin crustal igneous intrusions (e.g. Namibia margin (Gladczenko et al., 1998); Lofoten-Vesterålen margin (Tsikalas et al., 2001); North-West Australia margin (Sawyer et al., 2007); East Greenland margin(Tsikalas et al., 2012)). Furthermore, despite the ocean spreading rate is well established by the oceanic magnetic anomalies (Müller et al., 2008) the actual extensional rate during rifting and its effect on the lithospheric structures is not yet fully constrained. Recent studies pointed out that many of the features of the passive margins can be reconciled by their different divergence rate rather than involving difference in magmatism or in the shear modes (Peron-Pinvidic et al., 2013), and that rifting could undergo change both in velocity field direction and magnitude (Heine et al., 2013).

The geometry of rifted basins is a function of both elastic and isostatic responses of the lithosphere to mechanical stretching and is influenced by rheological and thermal perturbations (Cloetingh et al., 1995; van der Beek et al., 1994; Ziegler and

Cloetingh, 2004). Many lithosphere stretching and necking models have been proposed assuming different deformation partitioning between crust and upper mantle (Beaumont et al., 1982; Kusznir and Karner, 2007; McKenzie, 1978; Rowley and Sahagian, 1986) (McKenzie, 1978; Beaumont et al., 1982; Rowley and Sahagian, 1986; Kusznir and Karner, 2007). Extreme lithospheric thinning can eventually lead to continental breakup and formation of a variety of diverging continental margins whose complex tectono-sedimentary and thermal architecture is imprinted during initial necking.

Several studies have been devoted to unravel passive margin history by relating tectonic thinning to thermal perturbations and subsidence/uplift in rifted regions. Basin architecture reconstruction attempts have been performed by using several techniques that include 1-D sediment and water Airy backstripping (Lin et al., 2003; Stewart et al., 2000; Watts and Ryan, 1976; Watts and Steckler, 1979), 2-D to 3-D flexural backstripping (Stewart et al., 2000; Watts and Torné, 1992), gravity modelling (Watts and Fairhead, 1999; Wyer and Watts, 2006), depth-of-necking calculation (Braun and Beaumont, 1989; Cloetingh et al., 1995), fault-heave restoration (Davis and Kusznir, 2002; Reston, 2007), and geometric forward modeling (e.g. Ranero and Pérez-Gussinyé, 2010).

Despite an impressive amount of work has been done on rifting and rifted regions (e.g. Aslanian et al., 2009; Corti, 2012; Corti et al., 2003), knowing incremental steps or the finite results of deformation does not typically provide enough information to univocally constrain the evolution of lithosphere thinning and necking. First-order features, such as the partitioning of thinning with depth (Davis and Kusznir, 2004; Ranero and Pérez-Gussinyé, 2010; Reston, 2007), are still a matter of debate. Analogue and numerical modelling can provide effective support on this side. In particular, analogue modelling is a well-established tool to investigate on the three-dimensional structural response of lithosphere to extension (Autin et al., 2010; Benes and Davy, 1996; Brun and Beslier, 1996; Corti et al., 2003; Davy and Cobbold, 1991; Sokoutis et al., 2007).

Along the South Atlantic margins there is evidence of both magma-sustained and magma-poor margin types. In this study, we focus on the conjugate margin pairs along the Central Segment (confined between the Rio Grande Fracture Zone to the south and the Chain Fracture Zone to the north) of the South Atlantic Ocean that have been proposed to have a magma-poor margin affinity as no major volcanic products are evidenced along the margin (Blaich et al., 2011; Contrucci et al., 2004; Moulin et al., 2005; Reston, 2009). The existing rifting models only partially explain the geophysical and geological observations along the Central Segment of the South Atlantic. In particular, the hyper-extended crust cannot be simply accounted by applying the McKenzie- or Wernicke-type models, thus, several other models were proposed to resolve the structural kinematic and extensional discrepancies that arise. The proposed models include, among other variants, considerations on depth-depending stretching (Kusznir and Karner, 2007), mantle exhumation (Blaich et al., 2010; Boillot et al., 1987; Manatschal and Bernoulli, 1999; Unternehr et al., 2010; Zalán et al., 2011), and polyphase faulting evolution (Reston, 2009, 2007). In this context, during the last decade complex lithospheric-scale analogue modelling rifting experiments of both magma-poor (Autin et al., 2010; Brun, 1999) and magma-dominated extension (Bonini et al., 2001; Corti et al., 2003) have been performed and have provided a valuable tool to address and analyse several of the issues dealing with the rifting processes. These include: the relationships between the rift kinematic and deformation patterns, the influence of lithospheric rheological structure on rift architecture, the mode of extension and the faulting evolution during the rifting process, and the rifting relations with inherited structures (Agostini et al., 2009; Bonini et al., 2007; Callot et al., 2002; Corti, 2012; Sokoutis et al., 2007).

In this study of the Central Segment of the South Atlantic, we utilize an integrated approach of structural restoration on regional crustal transects and lithospheric-scale analogue modelling in order to address the impact of divergence extensional rate and lithospheric heterogeneities on continental rifting

evolution. In particular, the studies concerning the aperture velocity have a general applicability to the Central Segment, whilst we concentrate the research on the lithospheric heterogeneities effect to the Santos and Campos basins offshore Brazil. The observations and considerations can be extrapolated to the West African conjugate margin, in order to better understand the generation, architecture and evolution of rift-basins in terms of subsidence and structural style, spanning from the initial phase of continental rifting to the breakup stage. Moreover, the applied integrated analysis provides insights on the observed along-margin segmentation and its relationship to pre-existing lithospheric weaknesses, the symmetry versus asymmetry of the conjugate rifted margin pairs, and the nature of the crust on the outer margin close to the continent–ocean boundary with related heat-flow considerations.

1.2 Inheritances

Geological and geophysical observation in both active (i.e. Pyrenees or Himalaya) and fossile (i.e. Borborema shear zone in Brazil or the Neoproterozoic belts in Madagascar) orogenic belts support the mantle rooting of the major shear zones (Vauchez and Tommasi, 2003). Shear zones as the Borborema SZ in Brazil have been eroded down to the level where deformation was accommodated under high-temperature (650-850°C), presenting a predominant low-angle metamorphic foliation outside the shear zones passing to steeply dipping attitude inside the shear zones. At such an high-temperature and, hence, low-viscosity conditions, a decoupling behaviour is expected, despite no evidence of faults rooting has been observed (Vauchez et al., 1995). Along with these geological observation, geophysical evidence, such as seimic profiling, seismic tomography, indicate that the shear zones can propagate into the upper mantle crosscutting the Moho discontinuity (Vauchez and Tommasi, 2003). The shear zone processes and products change with depth and the type of material being deformed. The nature of these processes and how they may be linked kinematically and mechanically, particularly across major geological and geophysical interfaces such as the Moho,

will deeply affect the overall rheological behaviour of the lithosphere during deformation on geological timescales (Alsop and Holdsworth, 2004).

By a mechanical point of view, the source of the structural inheritance lies in a mechanical anisotropy of the lithospheric mantle due to the preservation, within the uppermost mantle, of the olivine crystals lattice preferred orientation (LPO) formed during the main tectonic episode that shaped the plate. If the preservation of well-developed olivine LPO within the lithospheric mantle also generates a mechanical anisotropy at these larger scales, this may result in a directional softening that will control strain localisation in the uppermost mantle and, hence, crustal deformation (Tommasi and Vauchez, 2001). The anisotropy if located in the same direction of rifting propagation can guide the path follow by the aperture, conversely, if located at high-angle with respect to the aperture direction can segment the rifting axis, becoming the site of future major oceanic fracture zones (Storti et al., 2007; Wilson, 1965).

1.3 Thesis outline

The research activity during the Ph.D. work was addressed to the study of a variety of rifting cases, with the aim of constrain the parameters that determine the structural and tectonic architecture of rift margins. Specifically, here we show the development of a laboratory methodology focused on constraining the thinning pattern of the lithosphere layers (Chapter 2), applying the same methodology to monitor and constrain the effect of the divergence rate on the necking shape and on the basin distribution at the surface (Chapter 3). Similarly, using analog modelling we study the effects of lithosphere heterogeneities on rifting evolution, using as case study the Brazilian margin at the Central Segment of the South Atlantic Ocean (Chapter 4). Finally we present the result of a field-study carried out in the NE-Brazilian margin to verify the post-rift reactivation of the margin, attributable to major shear zones driven by oceanic spreading (Chapter 5).

2

Shape evolution and finite deformation pattern in analog experiments of lithosphere necking

Published in
Geophysical Research Letters (2013)
vol. 40, pp 1-6.

Shape evolution and finite deformation pattern in analog experiments of lithosphere necking

Yago Nestola,[1] Fabrizio Storti,[1] Enrico Bedogni,[1] and Cristian Cavozzi[1]

Received 8 August 2013; revised 18 September 2013; accepted 19 September 2013.

[1] Lithosphere necking evolution determines the 3-D architecture of crustal and upper mantle thinning and related basins, and the heat flow distribution in rifted regions. Despite a large number of studies, lithosphere necking evolution is still a matter of debate. We present the result from lithospheric-scale analog models designed for investigating the necking shape during extension and the vertical distribution of finite deformation in the mechanical lithosphere. In our experiments, lithosphere necking is asymmetric and, in particular, the 3-D distribution of thinning is cylindrical in the crust and very heterogeneous in the mantle. Overall, the evolution of rifting and necking progresses from delocalized to localized deformation.
Citation: Nestola, Y., F. Storti, E. Bedogni, and C. Cavozzi (2013), Shape evolution and finite deformation pattern in analog experiments of lithosphere necking, *Geophys. Res. Lett.*, *40*, doi:10.1002/grl.50978.

1. Introduction

[2] The geometry of rifted basins is a function of both elastic and isostatic response of the lithosphere to mechanical stretching and is influenced by rheological and thermal perturbations [*Van der Beek et al*., 1994; *Cloetingh et al*., 1995; *Ziegler and Cloetingh*, 2004]. Many lithosphere stretching and necking models have been proposed assuming different deformation partitioning between crust and upper mantle [*McKenzie*, 1978; *Beaumont et al*., 1982; *Rowley and Sahagian*, 1986; *Kusznir and Karner*, 2007]. Extreme lithospheric thinning can eventually lead to continental breakup and formation of a variety of diverging continental margins whose complex tectono-sedimentary and thermal architecture is imprinted during initial necking.

[3] Several studies have been devoted to unravel passive margin history by relating tectonic thinning to thermal perturbations and subsidence/uplift in rifted regions. Basin architecture reconstruction attempts have been performed by using several techniques that include 1-D sediment and water Airy backstripping [*Watts and Ryan*, 1976; *Watts and Steckler*, 1979; *Stewart et al*., 2000; *Lin et al*., 2003], 2-D to 3-D flexural backstripping [e.g., *Watts and Torné*, 1992; *Stewart et al*., 2000], gravity modeling [*Watts and Fairhead*, 1999; *Wyer and Watts*, 2006], depth-of-necking calculation [*Braun and Beaumont*, 1989a, 1989b; *Cloetingh et al*., 1995], fault-heave restoration [*Davis and Kusznir*, 2004; *Reston*, 2007], and geometric forward modeling [e.g., *Ranero and Pérez-Gussinyé*, 2010].

[4] Despite an impressive amount of work has been done on rifting and rifted regions [e.g., *Corti et al*., 2003; *Aslanian et al*., 2009; *Corti*, 2012], knowing incremental steps or the finite results of deformation does not typically provide enough information to univocally constrain the evolution of lithosphere thinning and necking. First-order features, such as the partitioning of thinning with depth [*Davis and Kusznir*, 2004; *Reston*, 2007; *Ranero and Pérez-Gussinyé*, 2010], are still a matter of debate. Analog and numerical modeling can provide effective support on this side. In particular, analog modeling is a well-established tool to investigate on the three-dimensional structural response of lithosphere to extension [*Davy and Cobbold*, 1991; *Benes and Davy*, 1996; *Brun and Beslier*, 1996; *Brun*, 1999; *Corti et al*., 2003; *Sokoutis et al*., 2007; *Autin et al*., 2010].

[5] In this paper, we present the results from an analog modeling program designed to simulate and comprehensively monitor 3-D lithosphere necking through time during orthogonal rifting. For this purpose, we equipped a sandbox with two laser-scanner devices providing in real time the evolution of surface topography and the corresponding geometry of the lithosphere-asthenosphere boundary. This data set is used to quantitatively analyze tectonic thinning at different scales.

2. Analog Modeling

2.1. Experimental Apparatus and Setup

[6] The deformation rig consists of a plexiglass box ($80 \times 30 \times 15$ cm) subdivided in two halves by a mobile U-shaped wall with 20 cm long lateral arms that define the orthogonal velocity discontinuity in the model (Figure 1a). The mobile wall does not reach the bottom of the box to ensure free flow of the viscous analog asthenosphere material. The motor side half of the box is the compensation reservoir; the opposite half hosts the experimental lithosphere multilayer floating on the asthenosphere. The mobile wall is pulled apart by a screw jack that progressively extends the model-side of the box at the expense of the reservoir-side. A paired laser-scanner device detects at the same time the free surface of the model and the mechanical base of the lithosphere through the experimental asthenosphere. Three-dimensional surface shapes are acquired as point clouds with 0.25 mm resolution. Experimental evolution is also monitored by time lapse photographing the model top. All the mechanical and electronic devices are connected to a

Additional supporting information may be found in the online version of this article.

[1]"Macedonio Melloni" Physics and Earth Sciences Department, University of Parma, Parma, Italy.

Corresponding author: Y. Nestola, "Macedonio Melloni" Physics and Earth Sciences Department, Università di Parma, Parco Area delle Scienze, 157/A, Parma, 43121, Parma, Italy. (yago.nestola@unipr.it)

0094-8276/13/10.1002/grl.50978

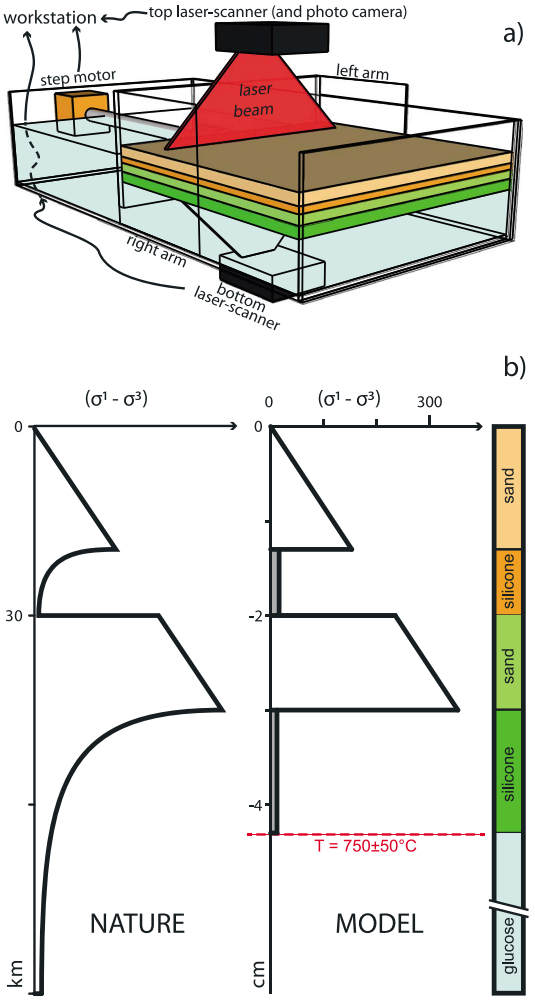

Figure 1. (a) Three-dimensional simplified sketch illustrating the architecture of the deformation rig. See text for details. (b) Comparison between natural and experimental yield-strength envelopes [e.g., *Brun*, 1999].

workstation. The scaling of the experiments is provided as supporting information (summarized in Table 1 and Table 2). Model evolution is commonly characterized by the presence of two regions adjacent to the opposite side walls, affected by boundary effects. Their width does not typically exceed the thickness of the undeformed multilayer. At the end of the experiments, these regions are removed from the acquired data sets before analyzing model results. Three experiments where extended 50 mm at plate divergence rate of 10 mm/h. Model results are consistent and well comparable. Consequently, in the following, we describe only the results from experiment "NECK03."

2.2. Model Evolution

[7] Since the very early stages of model evolution, three tectonic depressions start to develop adjacent to the velocity discontinuity line (Figure 2). After 10 mm of plate divergence, the rift architecture, consisting of three main basins separated by two intrabasinal high, is well established despite not fully developed. Two of the basins lie on the mobile side. The bottom of the lithosphere shows a broad and gentle doming that has the crestal region located below the basin on the fixed side (Figure 3a). The hinge point of the bulge on this side is well outside the stretched region at the surface, while the corresponding point on the mobile side roughly locates below the outer basin (basin 3). With increasing extension, the along-strike linkage of the basin boundary fault systems progresses, and at 25 mm of plate divergence, it is almost complete and the rift system shoulders undergo some uplift (Figures 2 and 3a). The central basin is the widest among the three ones and a well-developed asthenosphere bulge occurs below it (Figure 3b). In more detail, the lithosphere cross-sectional shape in the necking region is asymmetric: in the fixed side, it is steeper and culminates in a crestal area underneath basin1; the opposite side has a shallower slope and an additional, smaller culmination below basin 2 (Figure 3a). The second half of model evolution progresses along the same trend. Basins become deeper, particularly the lateral ones (1 and 3), while in the central basin stretching is more intense and subsidence is counteracted by some uplift of the floor. At the end of the experiment, the central basin is much broader than the

Table 1. Scale Ratios for the Silicone Putty Simulating the Lower Crust[a]

	Lengths	Densities	Gravity	Stresses	Viscosities	Strain Rates		
	(m)	(kg/m^3)	(m/s^2)	(N/m^2)	(Pa s)	(1/s)	Rm	Sm
Model(s)	0.007	1200	9.81	8.24E+01	4.00E+04	2.06E-03	5.19E-04	1.28
Nature	10500	2850	9.81	2.94E+08	5.00E+21	5.87E-14	5.19E-04	1.24
Scale ratio (M/N)	6.67E-07	4.21E-01	1	2.81E-07	8.00E-18	3.51E+10	1	1.03

[a]The "Ramberg number", Rm, and the "Smoluchowski number", Sm, ensure, respectively, the dynamic scaling of the model for ductile and brittle layers.

Table 2. Comparison Between Natural and Experimental Main Parameters in the Upper and Lower Crust, and Upper and Lower Mantle

	Thickness		Densities		Viscosities			
	Nature (km)	Model (cm)	Nature (kg/m^3)	Model (kg/m^3)	Nature (Pa s)	Model (Pa s)	n	
Brittle upper crust	19.5	1.3	2850	1200	-	-		Sand
Ductile lower crust	10.5	0.7	2850	1200	1.00E+21	40,000	1.053	Silicone (+ barite)
Brittle upper mantle	15	1	3300	1400	-	-		Sand
Ductile lower mantle	19.5	1.3	3300	1400	1.50E+21	60,000	1.067	Silicone (+ barite)

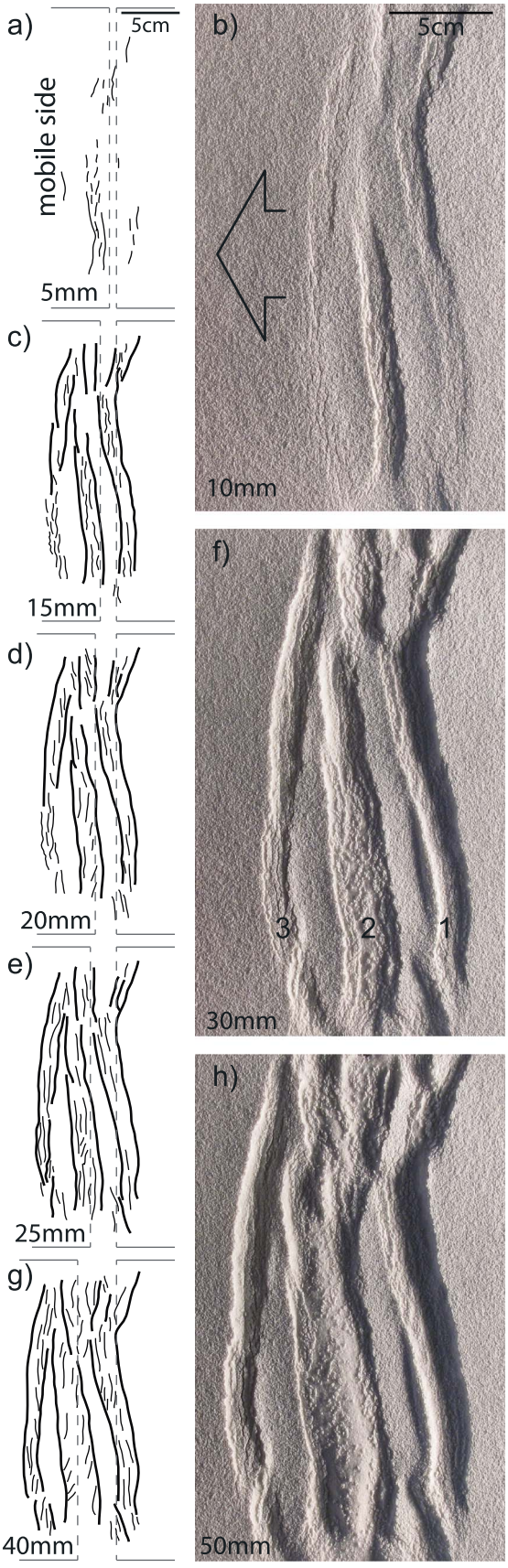

lateral ones (Figure 2h). The asthenosphere bulge is much more developed (Figure 3b) and its elevation reaches almost two thirds of the entire lithosphere thickness (Figure 3a). The final neck shape is more symmetric and preserves a main culmination on the fixed side, and a minor one on the mobile one (Figure 3a). Analysis of the synform hinge point incremental positions indicates an almost stable location through time on the fixed side (fixed hinge) and a progressive outward migration on the mobile side (mobile hinge). The elevation pattern of the antiform hinge points in the main culmination shows an almost vertical migration in the first half of the model evolution, followed by a progressive migration toward the mobile side. A similar trend characterizes also the minor culmination underneath the central basin (Figure 3a). The final cross-sectional picture of the rifted lithosphere shows a strongly asymmetric architecture: basins 1 and 2 overly a strongly thinned region while basin3 rest on an almost unstretched lithosphere (Figure 3a).

3. Finite Deformation Analysis

[8] The method for calculating the thinning factor is provided as supporting information. The final 3D pattern of the thinning factor calculated for the crust (TF_C) is characterized by a narrow central area of very high values, which has a coherent amplitude through the model (Figure 4a). Two belts of lower TF_C values bound the highly thinned sector on both sides. The thinning factor calculated for the mantle lithosphere (TF_M) shows a quite different pattern, dominated by a central belt of higher values, which is overall wider than the corresponding one in the crust and has a more complex architecture (Figure 4b). In particular, an elongated region of much lower values occurs within the central belt, separated from the almost undeformed region in the mobile-wall side of the model by a very narrow sector of higher values. The pattern of thinning factor values calculated for the whole lithosphere (TF_L) show the combination of TF_C and TF_M (Figure 4c). The elongated region characterized by low values is still evident but more smoothed with respect to the corresponding one in mantle (TF_M).

4. Discussion

[9] The experimental setup used in this work follows the majority of research papers on rifting in analog models. Despite significant limitations have to be accepted when

Figure 2. Top views of model NECK3 evolution. (a) Line drawing of main deformation features after 5 mm of extension, (b) photograph of model topography after 10 mm of extension (the arrow indicates the direction of extension), (c) line drawing of main deformation features after 15 mm of extension, (d) line drawing of main deformation features after 20 mm of extension, (e) line drawing of main deformation features after 25 mm of extension, and (f) photograph of model topography after 30 mm of extension; numbers indicate the inner (1), central (2), and outer (3) basins, respectively. (g) Line drawing of main deformation features after 40 mm of extension and (h) photograph of model topography at the end of the experiment (after 50 mm of extension).

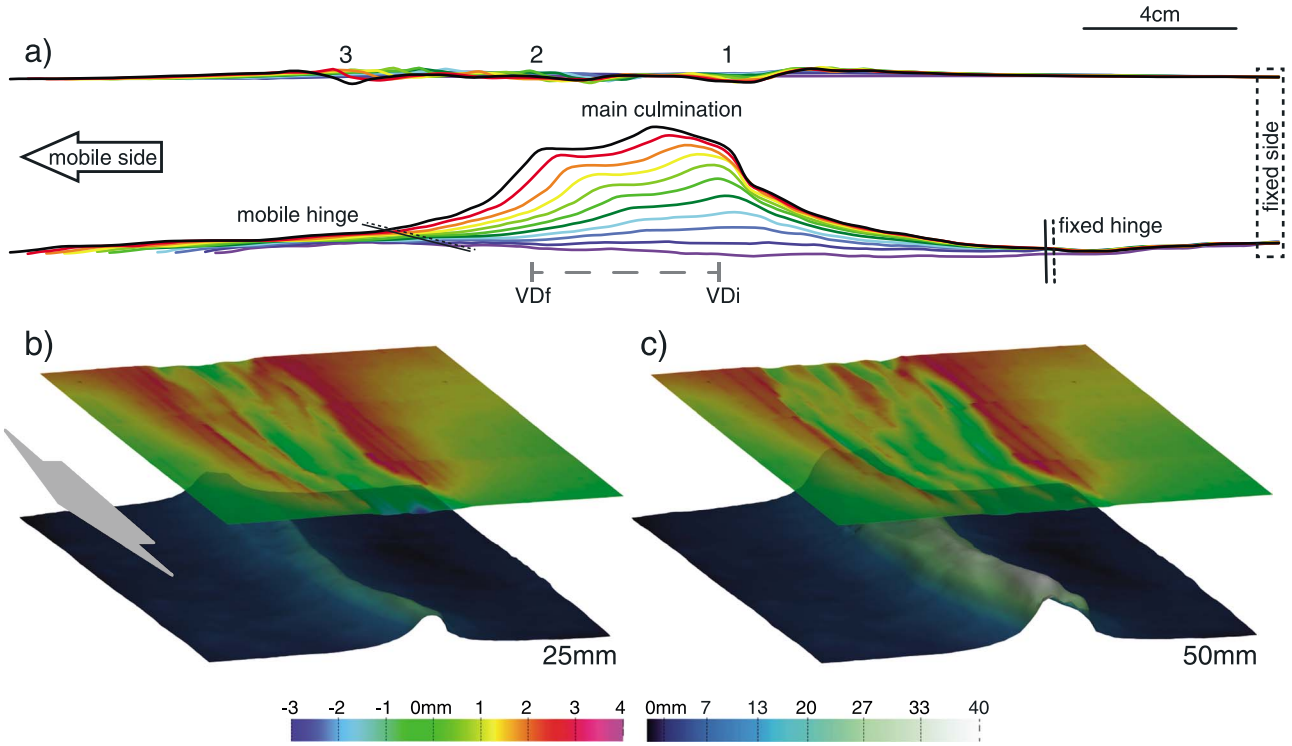

Figure 3. (a) Cross-sectional incremental shapes of the experimental lithosphere during rifting (cut in the central part of the model, along the extension direction; see Figure 4c for location). The undeformed stage is in purple, while the final one is in black; numbers 1, 2, and 3 in the surface topography refer to basins in Figure 2. VDi and VDf are, respectively, the initial and final position of the velocity discontinuity. See text for details. (b) 3-D view of the model topography and lithosphere base after 25 mm of extension; 3-D view of the model topography and lithosphere base at the end of the experiment. Note that in both figures, the distance between the top and the bottom of the lithosphere is exaggerated in order to minimize the overlap of the two layers and facilitate the view of the asthenospheric bulge in the necking region.

working at this geodynamic scale, the method has been proved to provide useful insights into the evolution of rifting [e.g., *Brun*, 1999; *Corti et al*., 2003; *Autin et al*., 2010]. In particular, the motion of only one of the two lateral walls makes our models appropriate for simulating asymmetric rifting [e.g., *Aslanian et al*., 2009; *Ranero and Pérez-Gussinyé*, 2010]. In this kinematic framework, one flank of the lithosphere necking system is preserved in the same position during rifting, while the opposite one is pulled apart. As a consequence, necking growth is enhanced at the fixed side of the experiments, where its slope is steeper and the maximum elevation of the asthenosphere is reached. The asymmetry of the necking system is evident also at the crustal scale: The three basins develop since the very early stages of rifting but the one on the mobile side is shallower than the others; moreover, the opening rate is maximum in the central basin and minimum in the one on the mobile side (basin 3 in Figure 2).

[10] A direct comparison of our experimental results with previous models available in the literature is not straightforward because of differences in model parameters such as the rheology of the deformed multilayers and the strain rate. Despite this, first-order features like the cross-sectional thinning distribution and necking shoulder dip in our models roughly compares with most previous results [*Brun and Beslier*, 1996; *Brun*, 1999; *Callot et al*., 2001]. The final shape of the stretched experimental lithosphere compares well with that reconstructed for natural rifts systems, including the Jurassic architecture of the Western Tethys, still preserved in the Alps [e.g., *Beltrando et al*., 2010]. In particular, the latter includes a main and a minor culmination at the top of the asthenospheric bulge, overlain by three rift basins (Figure 5). The first-order features of this cross-sectional geometry are similar to what produced in our models (Figure 3a).

[11] The incremental and finite asymmetric distribution of lithosphere thinning and necking illustrated in Figure 3a suggests important implications for the 4-D heat flow distribution and, hence, for rift-related magmatism. The basin on the fixed side of the rift system is located above the most stretched region since the very beginning of deformation, and this may imply higher heat flow and more abundant magmatism compared to the opposite rift margin, where formation of basin 3 is not accompanied by significant lithosphere thinning.

[12] The evolution of rifting and necking in our experiments progresses from delocalized to localized deformation: In the late stage of modeling, extension is mainly concentrated in the central basin where, eventually, uplift occurs preceding continental breakup. This is similar to what has been described in natural rift systems [e.g., *Moulin et al*., 2010; *Aslanian et al*., 2009].

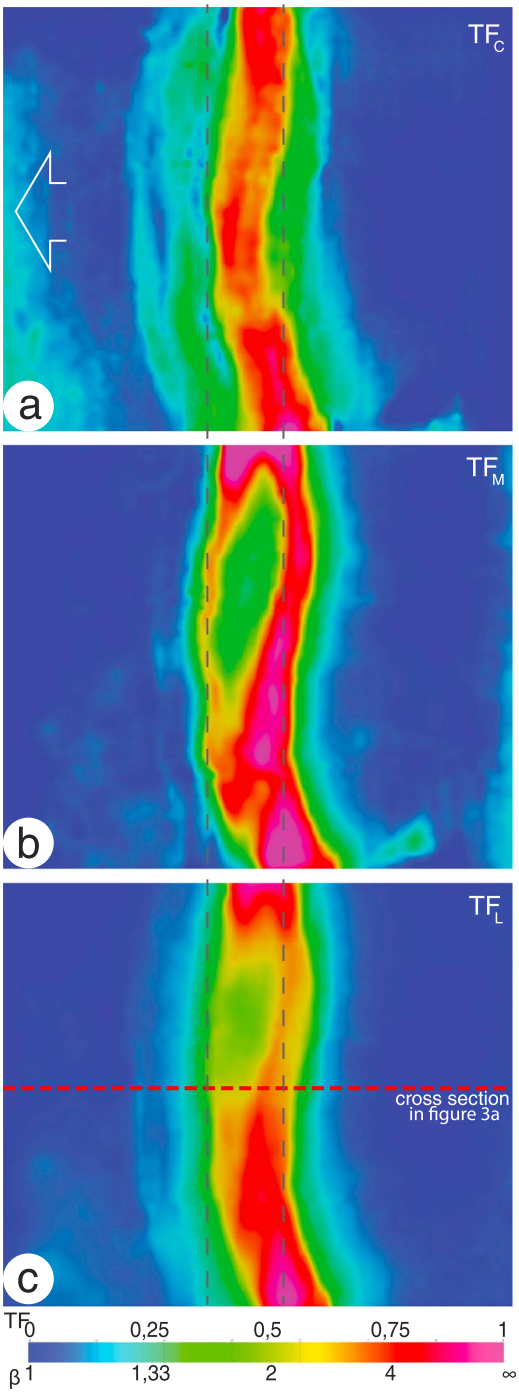

Figure 4. Map views of the distribution of the thinning factors calculated for (a) the crust, (b) the mantle, and (c) the whole lithosphere. The trace of the cross section in Figure 3a is indicated. See text for details. Two vertical dashed lines marks the final position of the velocity discontinuities.

5. Conclusions

[13] We studied the incremental evolution of rifting in analog models where the top and the bottom of the experimental lithosphere were simultaneously monitored by time-lapse laser scanning. This experimental setup allowed us to follow the geometry of lithosphere necking through time. The following three points can be drawn to summarize our main results.

[14] 1. In our experimental kinematics, where a mobile plate is pulled apart from a fixed one, the process of lithosphere necking is strongly asymmetric since the onset of deformation. In particular, thinning is more severe on the rift shoulder located in the fixed plate where, before continental breakup, the asthenosphere can penetrate from about 1/3 to more than 4/5 of the entire lithosphere thickness. On the other hand, the opposite rift shoulder lies on an almost unstretched lithosphere. This has important implications for the distribution of heat flow and, eventually, on rift-related magmatism that is expected to be more abundant on the "fixed side" of asymmetric rift systems.

[15] 2. The experiments produced a depth-dependent 3-D distribution of lithosphere thinning despite deformation occurred in a "closed system": it is more "cylindrical" in the crust and strongly asymmetric in the upper mantle, where regions of low strain are preserved in between strongly thinned belts.

[16] 3. Crustal deformations progressed from distributed to localized extension. The rift basins architecture was established in the very early stages of model evolution and remained basically preserved with increasing crustal stretching. However, partitioning of the fault activity varied from widespread faulting in the first evolutionary steps to focused tectonic activity on the central basin when continental breakup was approaching.

[17] Finally, the experiment described in this work, despite being very simple, clearly illustrate the validity of the top-bottom time-lapse paired scanning the model lithosphere to monitor its shape during deformation. Application to more complex experimental programs will provide a valid support to future physical models of geodynamic processes.

[18] **Acknowledgments.** This paper is dedicated to the memory of Elisabetta "Betti" Costa, who established the analog modeling laboratory at our department in 1998. Constructive criticism and suggestions from M. Bonini and an anonymous reviewer helped us to significantly improve the manuscript. Journal Editor A. Newman is thanked for handling this manuscript. We are deeply in debt with ENI S.p.A. for financial support to our experimental work. Suggestions and constructive discussions of modeling result with F. Salvi, C. Magistroni, and G. Spadini (ENI - GEBA, Milan), and J.P. Brun, M. Pérez-Gussinyé, and C. Ranero are gratefully acknowledged. Thanks to M. Vettori for technical support.

[19] The Editor thanks Marco Bonini and Giacomo Corti for their assistance in evaluating this paper.

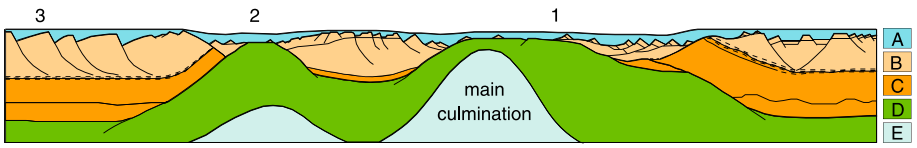

Figure 5. Cross-sectional architecture of the Western Tethys in the Alps as reconstructed by *Beltrando et al.* [2010]. Note the correspondence with our experimental results of both asthenosphere culminations and rift basin number and geometrical position. A means sedimentary cover, B is the brittle crust, C is the ductile crust, D is the lithospheric mantle, and E is the asthenosphere.

References

Aslanian, D., et al. (2009), Brazilian and African passive margins of the Central Segment of the South Atlantic Ocean: Kinematic constraints, *Tectonophysics*, *468*, 98–112.

Autin, J., N. Bellahsen, L. Husson, M. O. Beslier, S. Leroy, and E. d'Acremont (2010), Analogue models of oblique rifting in a cold lithosphere, *Tectonics*, *29*, TC6016, doi:10.1029/2010TC002671.

Beaumont, C., C. E. Keen, and R. Boutilier (1982), On the evolution of rifted continental margins: Comparison of models and observations for the Nova Scotia Margin, *Geophys. J. R. Astron. Soc.*, *70*, 667–715.

Beltrando, M., D. Rubatto, and G. Manatschal (2010), From passive margins to orogens: The link between ocean-continent transition zones and (ultra-) high-pressure metamorphism, *Geology*, *38*(6), 559–562.

Benes, V., and P. Davy (1996), Modes of continental lithospheric extension: Experimental verification of strain localization processes, *Tectonophysics*, *254*(1–2), 69–87.

Braun, J., and C. Beaumont (1989a), A physical explanation on the relation between flank uplifts and the breakup unconformity at rifted continental margins, *Geology*, *17*, 760–764.

Braun, J., and C. Beaumont (1989b), A physical explanation on the relation between flank uplifts and the breakup unconformity at rifted continental margins, *Geology*, *17*, 760–764.

Brun, J. P. (1999), Narrow rifts versus wide rifts: Inferences for the mechanics of rifting from laboratory experiments, *Philos. Trans. R. Soc., A*, *357*(1753), 695–712.

Brun, J. P., and M. O. Beslier (1996), Mantle exhumation at passive margins, *Earth Planet. Sci. Lett.*, *142*(1–2), 161–173.

Callot, J.-P., C. Grigné, L. Geoffroy, and J.-P. Brun (2001), Development of volcanic passive margins: Two-dimensional laboratory models, *Tectonics*, *20*(1), 148–159.

Cloetingh, S., J. D. Van Wees, P. A. Van der Beek, and G. Spadini (1995), Role of pre-rift rheology in kinematics of basin formation: Constrains from thermo-mechanical modelling of Mediterranean basins and intracratonic rifts, *Mar. Pet. Geol.*, *12*, 793–808.

Corti, G. (2012), Evolution and characteristics of continental rifting: Analog modeling-inspired view and comparison with examples from the East African Rift System, *Tectonophysics*, *522–523*, 1–33.

Corti, G., M. Bonini, S. Conticelli, F. Innocenti, P. Manetti, and D. Sokoutis (2003), Analogue modelling of continental extension: A review focused on the relations between the patterns of deformation and the presence of magma, *Earth Sci. Rev.*, *63*(3–4), 169–247.

Davis, M., and N. Kusznir (2004), Depth-dependent lithospheric stretching at rifted margins, *Rheology and Deformation of the Lithosphere at Continental Margins*, edited by G. D. Karner et al., pp. 92–137, Columbia University Press, New York.

Davy, P., and P. R. Cobbold (1991), Experiments on shortening of a 4-layer model of the continental lithosphere, *Tectonophysics*, *188*(1–2), 1–25.

Kusznir, N. J., and G. D. Karner (2007), Continental lithospheric thinning and breakup in response to upwelling divergent mantle flow; application to the Woodlark, Newfoundland and Iberia margins: Geological Society Special Publications, v. 282, p. 389–419.

Lin, A. T., A. B. Watts, and S. P. Hesselbo (2003), Cenozoic stratigraphy and subsidence history of the South China Sea margin in the Taiwan region, *Basin Res.*, *15*, 453–478.

McKenzie, D. (1978), Some remarks on the development of sedimentary basins, *Earth Planet. Sci. Lett.*, *40*, 25–32.

Moulin, M., D. Aslanian, and P. Unternehr (2010), A new starting point for the South and Equatorial Atlantic Ocean, *Earth Sci. Rev.*, *98*(1–2), 1–37.

Ranero, C. R., and M. Pérez-Gussinyé (2010), Sequential faulting explains the asymmetry and extension discrepancy of conjugate margins, *Nature*, *468*, 294–299.

Reston, T. J. (2007), The extension discrepancy at North Atlantic non-volcanic rifted margins: Depth-dependent stretching or unrecognised faulting?, *Geology*, *35*, 367–370.

Rowley, D. B., and D. Sahagian (1986), Depth-dependent stretching: A different approach, *Geology*, *14*, 32–35.

Sokoutis, D., G. Corti, M. Bonini, J. P. Brun, S. Cloetingh, T. Mauduit, and P. Manetti (2007), Modelling the extension of heterogeneous hot lithosphere, *Tectonophysics*, *444*(1–4), 63–79.

Stewart, J., A. B. Watts, and J. G. Bagguley (2000), Three-dimensional subsidence analysis and gravity modelling of the continental margin onshore Namibia, *Geophys. J. Int.*, *141*, 724–746.

Van der Beek, P., S. Cloetingh, and P. Andriessen (1994), Mechanisms of extensional basin formation and vertical motions at rift flanks: Constraints from tectonic modelling and fission-track thermochronology, *Earth Planet. Sci. Lett.*, *121*(3–4), 417–433.

Watts, A. B., and J. D. Fairhead (1999), A process-oriented approach to modeling the gravity signature of continental margins, *The Leading Edge 18*, *2*, 258–263.

Watts, A. B., and W. B. F. Ryan (1976), Flexure of the lithosphere and continental margin basins, *Tectonophysics*, *36*, 25–44.

Watts, A. B., and M. S. Steckler (1979), Subsidence and eustacy at the continental margin of eastern North America, *Deep Drilling Results in the Atlantic Ocean: Continental Margins and Paleoenvironments*, Maurice Ewing Series 3, edited by M. Talwani, W. Hay, and W. B. F. Ryan, pp. 218–234, AGU, Washington, D. C.

Watts, A. B., and M. Torné (1992), Subsidence history, crustal structure and thermal evolution of the Valencia through: A young extensional basin in the western Mediterranean, *J. Geophys. Res.*, *97*, 20,021–20,041.

Wyer, P., and A. B. Watts (2006), Gravity anomalies and segmentation at the East Coast, USA continental margin, *Geophys. J. Int.*, *166*(3), 1015–1038.

Ziegler, P. A., and S. Cloetingh (2004), Dynamic processes controlling evolution of rifted basins, *Earth Sci. Rev.*, *64*, 1–50.

3

Strain rate dependent lithosphere rifting and necking architectures in analogue experiments

Under Review for
Journal of Geophysical Research-Solid Earth
Manuscript # 2014JB010994

Strain rate dependent lithosphere rifting and necking architectures in analogue experiments.

Yago Nestola, Fabrizio Storti, and Cristian Cavozzi.

NEXT - Natural and Experimental Tectonics Research Group, Department of Physics and Earth Sciences "Macedonio Melloni", Università di Parma, Parco Area delle Scienze 157/A, 43121, Parma, Italy.

Key points

- Evolution of necking profiles is strongly influenced by plate divergence rate.
- Thinning factor maps are produced for the experimental lithosphere layers.
- Thinning factor patterns strongly depend on the plate divergence rate.

Keywords: Analog modeling; Rifting; Necking; Strain rate.

ABSTRACT

Analogue models provide a useful tool to investigate on the three – dimensional evolution of geodynamic processes. In this contribution, we describe the results of an experimental programme designed for studying the progression through time of lithosphere thinning and necking. In particular, by exploiting the three-dimensional real time information on surface topography and base lithosphere geometry provided by paired top and bottom laser scanning, we studied the evolution of lithosphere necking at low and fast asymmetric plate divergence. Our results indicate that this parameter plays a fundamental control on the incremental and finite slope of the lithosphere necking. Influences are discussed on the application of experimental data to natural rift system.

1. Introduction

Rifting is a fundamental geodynamic process shaping the earth surface and, hence, governing the distribution of water in continental and oceanic basins, thus exerting a control on global climate changes. Important energy resources are associated with rifting and this has being contributing to incentivate geological and geophysical research on lithosphere thinning.

The rheological layering of the lithosphere, thermal perturbations, inherited discontinuities, and the mode, amount, and velocity of extension, are parameters exerting a fundamental control on the structural style of rifts [*Buck*, 1991; *van der Beek et al.*, 1994; *Bassi*, 1995; *Brun*, 1999; *Ziegler and Cloetingh*, 2004]. Rheological layering is primary controlled by the thermal state of the lithosphere, which plays a decisive role on extension localisation [*Ranalli and Murphy*, 1987; *Buck*, 1991; *Brun*, 1999; *Sokoutis et al.*, 2007]. When the Moho temperature is lower than 500-600 °C, a brittle upper mantle layer exists [*Davy and Cobbold*, 1991], which is the site where the highest strength is located in the so-called "cold and strong" lithosphere multilayer. Boudinage of a sub-Moho high strength layer favours the development of lithosphere necking, leading to extreme crustal thinning, which facilitates mantle exhumation up to the surface [*Brun and Beslier*, 1996]. Different deformation partitioning assumptions between crust and mantle gave rise to alternative lithosphere stretching models [*McKenzie*, 1978; *Wernicke*, 1985; *Rowley and Sahagian*, 1986; *Hopper and Buck*, 1998; *Kusznir and Karner*, 2007].

Significant uncertainty is intrinsic in the scale of the processes governing rifting, which does not allow direct observations of the entire rift architecture. Geophysical information at depth is commonly fragmentary, particularly when the whole lithosphere is considered. Laboratory models provide effective complement to direct and indirect data for a better understanding of rifting evolution in space and time [e.g. *Corti*, 2012]. Analogue experiments illustrated the dependence of lithosphere necking modes on plate divergence rate [*Brun*, 1999]. We performed further research on this subject by exploiting the improved monitoring capability provided by coupled top and basal laser scanning of models, implemented in our apparatus (Fig. 1a). Such a device allows the evolution of lithosphere necking to be quantitatively analysed through time [*Nestola et al.*, 2013].

2. Analogue modelling

2.1 Experimental apparatus, scaling and materials.

The experimental apparatus consists of a plexiglass box (80 x 30 x 15 cm) subdivided in two halves by a U-shaped mobile wall with 20cm long lateral arms, which provide the orthogonal velocity discontinuity in the model (Fig. 1a). The motor-side half of the box is the compensation reservoir, while the other one hosts the experimental lithosphere multilayer floating on the viscous analogue asthenosphere material. To ensure asthenosphere free-flow between the two halves, the mobile wall does not reach the bottom of the box. The mobile wall is pulled apart at selected constant velocity, extending the model-side of the box at the expense of the reservoir-side. This experimental configuration simulates asymmetric rifting, which commonly occurs in nature [e.g. *Doglioni et al.*, 2003; *Aslanian et al.*, 2009; *Ranero and Pérez-Gussinyé*, 2010]. Two paired laser-scanner devices contemporary acquire at 0,25mm resolution the topographic surface of the model and the base of the lithosphere geometry through the experimental asthenosphere every 5mm of side divergence. Model evolution is also monitored by time lapse photographing the experiment top. At the end of deformation, the experimental crust is carefully removed and the 3D geometry of the model Moho surface and the base of the lithosphere are acquired by laser scanning. The same procedure is repeated after removing the experimental brittle mantle. To facilitate model description, we refer to the multilayer region between the mobile wall and the necking area as the "mobile side"; conversely the multilayer region confined between the necking area and the fixed wall is the "fixed side" (Fig. 1a).

Scaling models to their natural prototypes requires similarity in geometry, kinematics, dynamics, and rheology [*Ramberg*, 1981]. Stresses scale down according to:

$$\sigma^* = \rho^* g^* L^* \qquad (1)$$

where the starred symbols are the dimensionless ratios between model and natural prototype for the following parame-

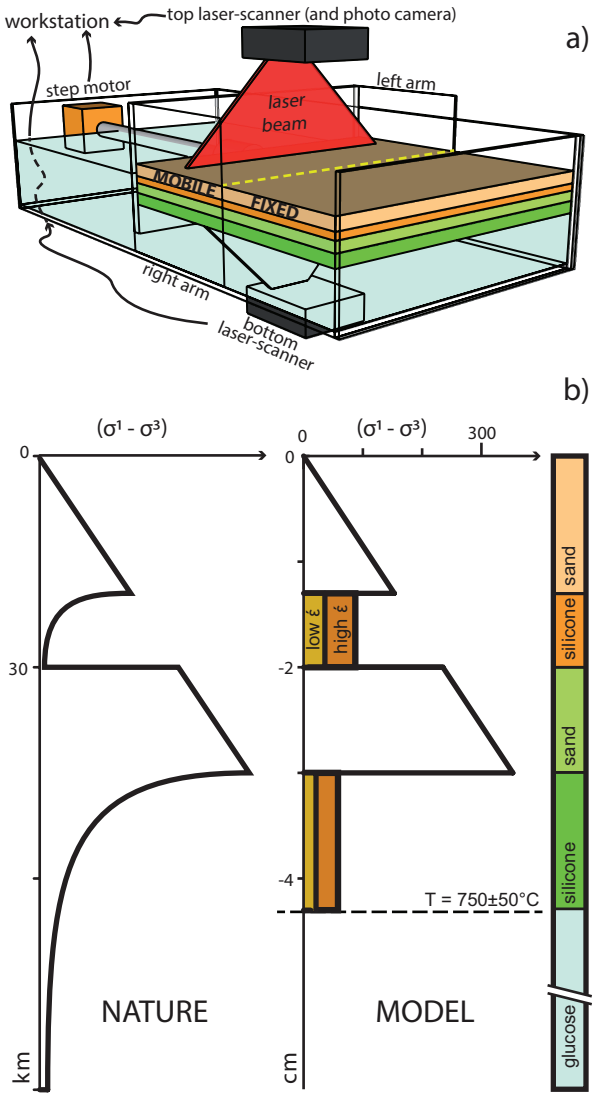

Figure 1| (a) Sketch illustrating the basic technical architecture of our experimental apparatus. Details are provided in the text. (b) Comparison between the strength profile of the lithosphere (left) and the corresponding experimental multilayer (right) [after *Nestola et al.*, 2013].

TABLE 1.

	lengths	densities	gravity	stresses	viscosities	strain-rates	NECK-05		NECK-50	
	[m]	*[kg/m³]*	*[m/s²]*	*[N/m²]*	*[Pa.s]*	*[1/s]*	Rm	Sm	Rm	Sm
Model(s)	0,007	1200	9,81	8,24E+01	4,00E+04	2,06E-03	1,04E-03	1,28	1,04E-04	1,28
Nature	10500	2850	9,81	2,94E+08	5,00E+21	5,87E-14	1,04E-03	1,24	1,04E-04	1,24
scale (M/N)	6,67E-07	4,21E-01	1	2,81E-07	8,00E-18	3,51E+10	1	1,03	1	1,03

ters: σ^* is stress, ρ* is density, g* is gravity, and L^* is the length scale-factor. In our experiments, L* = 6.66 x 10^{-7}, that is 10mm correspond to15km in nature. Scaling of time for the viscous materials is achieved by

$$t^* = \eta^*/\sigma^* \quad (2)$$

where t* is the dimensionless ratio of time and η^* is the dimensionless ratio for viscosity. Viscous materials in our experiments have a Newtonian rheology and their strength is provided by (e.g. Ranalli, 1995):

$$\tau = \dot{\gamma}\eta \quad (3)$$

where τ is the shear stress, $\dot{\gamma}$ is the shear strain rate, and η is viscosity . The Ramberg and Smolukowsky numbers, calculated following *Corti et al.* [2003] for the ductile and brittle layers, respectively, support the dynamic scaling of the models. The scaling factors used in our models are provided in Table 1.

The lithosphere can be effectively simulated in analogue experiments by a 4-layer strength profile, with alternating brittle and ductile layers [*Kirby*, 1983; *Davy and Cobbold*, 1991]. Brittle layers are modelled using pure quartz sand with negligible cohesion. Ductile layers are simulated using SGM36 silicone putty, which is a Newtonian viscous material widely used in normal gravity experiments [*Weijermars and Schmeling*, 1986]. In our model stratigraphy (Fig. 1b), small quantities of barite were added to the SGM36 silicone putty in order to properly scale density and viscosity. This mixing did not substantially alter the behaviour of the viscous layers since the measured rheological parameter *n* is 1.053 and 1.067 for the model lower crust and lower mantle, respectively, i.e. very close to the condition *n*=1 that describes the Newtonian rheology [e.g. *Ranalli*, 1995]. In our models stratigraphy, the upper brittle crust is a 13mm thick sand layer (ρ_C =1200kg m^{-3}, average grain-size 260μm), the lower ductile crust is a 7mm thick silicone layer (ρ_C =1200kg m^{-3}; η_C =4x10^4 Pa.s), the upper brittle mantle is a 10mm thick sand layer (ρ_L =1400kg m^{-3}, average grain-size 260μm), the lower ductile mantle layer is a 13mm thick silicone

layer with (ρ_L =1400kg m^{-3}; η_L =6x10^4 Pa.s). The lithospheric multilayer lies on glucose syrup (ρ_A =1450 kg m^{-3}; η_A =150 Pa.s) simulating the mechanical behaviour of the asthenosphere.

We investigated the response of the experimental lithosphere to 50mm of total extension over one-order magnitude range of side divergence rate. In particular, in this paper we describe results from models extended at 5mm/h (NECK-05) and 50mm/h (NECK-50). Experimental rifting produced at 10mm/h of side divergence rate, with the same model configuration, is described in *Nestola et al.*[2013]. According to eq.3, this range of experimental velocities is representative of prototype velocities varying between 2mm/y and 20mm/y, for a lower crustal viscosity of 5x10^{21} Pa.s. The corresponding natural average strain-rate values are 5,65x10^{-15} s^{-1} and 5,65x10^{-14} s^{-1} respectively. These values are appropriate for narrow rifting [*Buck*, 1991]. To ensure reproducibility of model results, our experiments were repeated three times. Only two representative ones for the low and the fast side divergence rate, respectively, are described in this paper.

2.2 Model results

Comparison between model evolutions indicates that side divergence rate exerted a strong control on experimental rifting since the very early stages of deformation (Figs 2, 3). Fault zones were not evident in the slow model during the first 5mm of side divergence and started to develop after about 10mm (Fig. 2b). Conversely, evidence of deformation structures was well visible in the fast model very soon after the onset of side motion and tectonic depressions developed after few mm of divergence (Fig. 2d). The quite different behaviour of the two models since the early extension is illustrated also in their cross-sectional evolution. The geometry of the bottom of the lithosphere after 10mm of divergence shows a well developed gentle antiformal shape located in the boundary region between the fixed side and the rifted area of model NECK-05. On the other hand, NECK-50 is characterized by a very broad, very low amplitude convexity underneath the rifted area (Fig.3a,b).

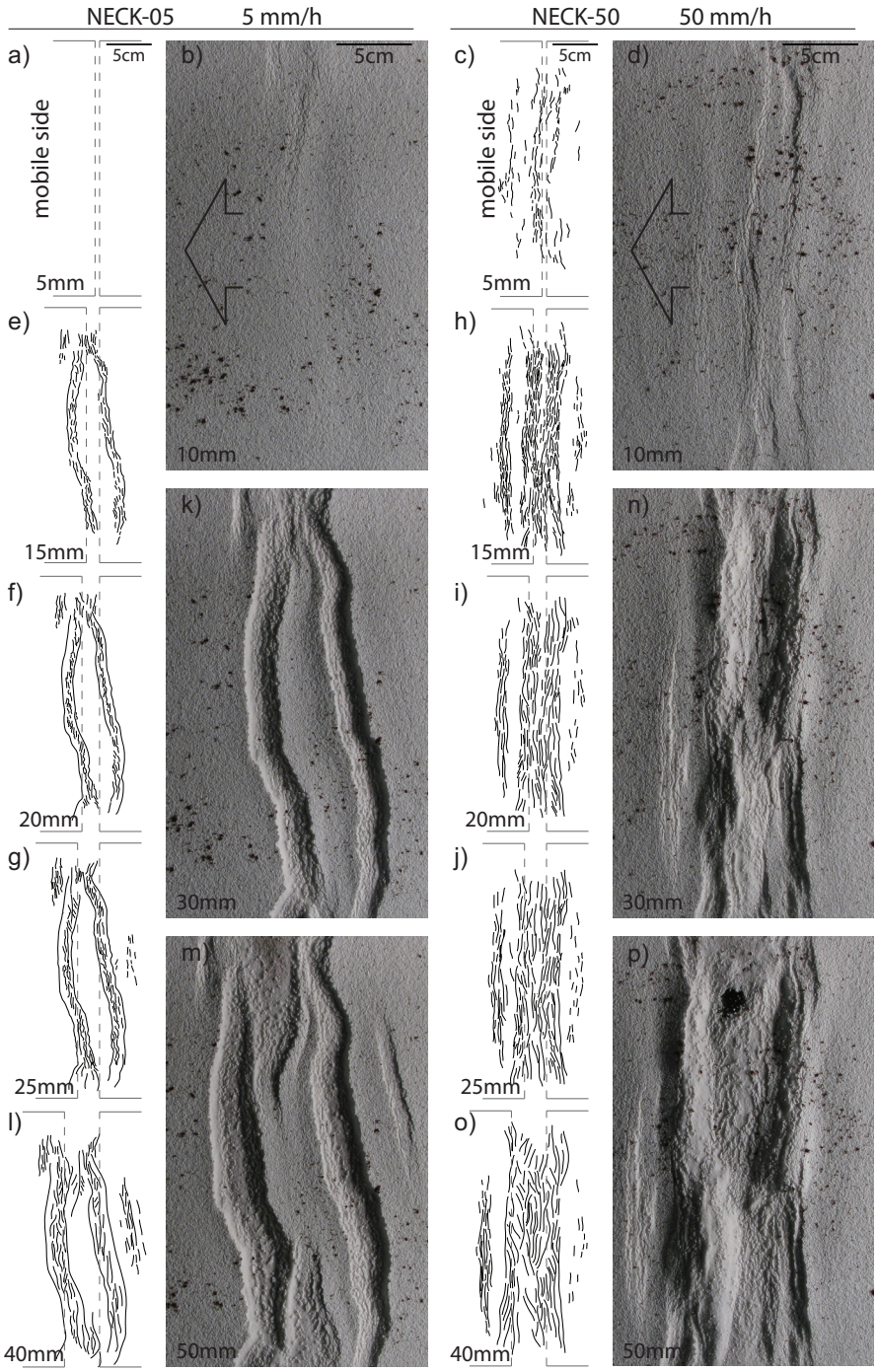

Figure 2| Top views of model NECK-05 (left) and NECK-50 (right). (a) Line drawing of neck-05 after 5mm of extension: no deformation features are evident. (b) Photograph of model topography after 10mm of extension (the arrow indicates the direction of lateral motion of the mobile plate).

(c) Line drawing of main deformation features of model NECK-50 after 5mm of extension. (d) Photograph of model topography after 10mm of extension. (e, f, g) Line drawings of main deformation features after 15, 20, and 25mm of extension, respectively, for the slow divergence rate model. (h, I, j) Line drawings of main deformation features after 15, 20, and 25mm of extension, respectively, for the fast divergence rate model. (k, n) Photograph of the model after 30mm of extension of models NECK-05 and NECK-50, respectively. (l, o) Line drawing of the model after 40mm of extension for the slow and the fast model, respectively. (m) Neck-05 topography photograph at the end of deformation. (p) Neck-50 topography photograph at the end of deformation.

With increasing the outward translation of the moving side, two narrow basins separated by a wide unfaulted region formed in the slow model, while fault zones were much more abundant and diffuse over a broad area in the fast model (Figs. 2e-j). These faults delineated a major basin in the central region of the rift system, preserving a narrow central high. Another basin formed at the boundary of the area undergoing stretching on the mobile side and an incipient tectonic depression grew on the fixed side. The necking profile of the bottom of the lithosphere in model NECK-05 evolved by the rapid vertical growth of the asthenosphere antiform at the boundary between the rifted region and the fixed side, which maintained a well rounded, bell shaped crestal area up to about 25mm of side divergence. At the fold inflection points, the limb dip suddenly changed to much shallower values that asymptotically attained the flat-lying attitude of the undeformed state (Fig. 3a). The cross-sectional shape of the extending lithosphere was strongly asymmetric at this stage, with the locus of major mantle thinning located underneath the inner basin, and the outer basin overlying only slightly stretched mantle. In model NECK-50, at about 15mm of side divergence the necking profile of the bottom of the lithosphere started to develop three antiformal corrugations that became more accentuated with increasing deformation (Fig.3b). The central fold was located below the shoulder of the inner basin on the fixed side, which underwent significant uplift. The more external antiform was located below the outer basin and the less developed, third fold grew well inside the fixed side. Like in

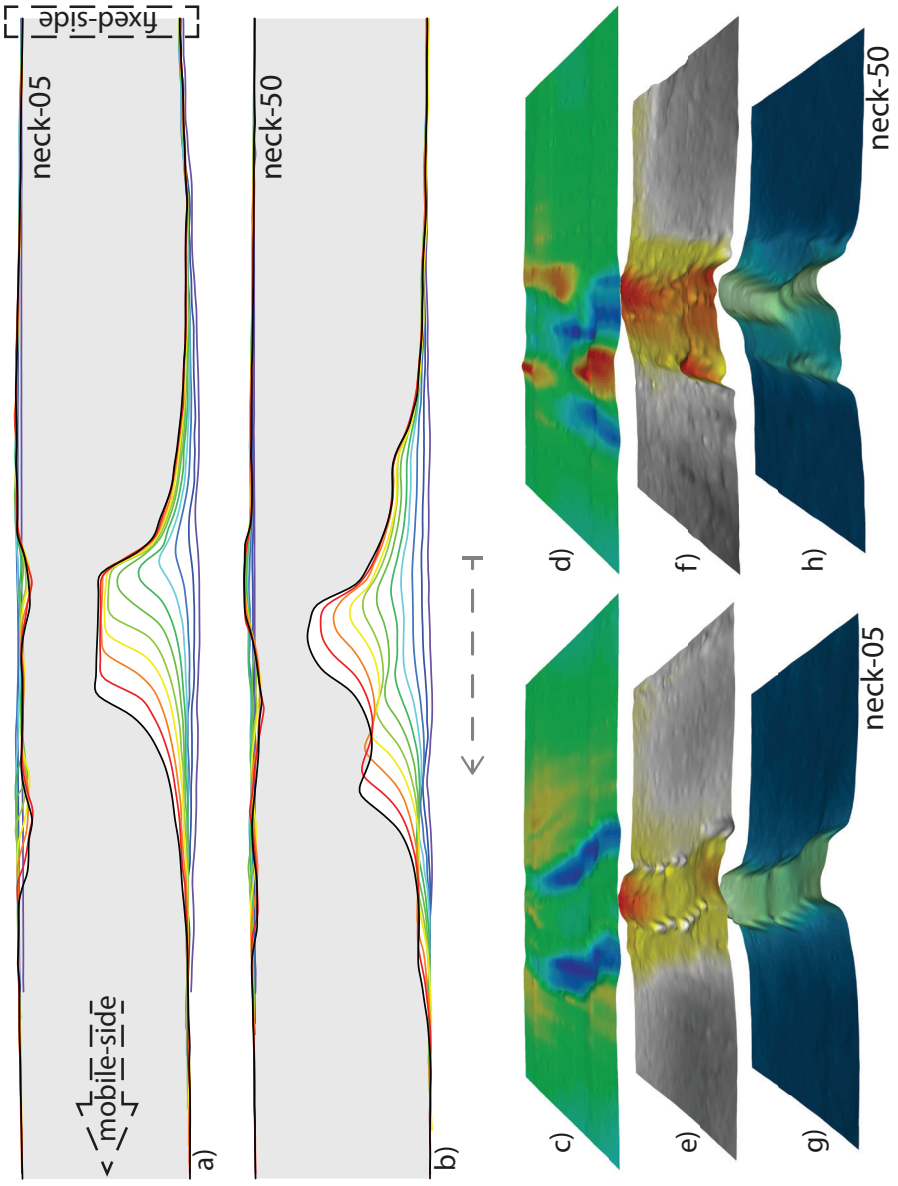

Figure 3| (a) Cross-sectional incremental shapes of model NECK-05 during progressive extension (see Fig. 5e for localization). The undeformed state is in purple and the final one is in black. (b) Cross-sectional incremental shapes of model NECK-50 during progressive extension. Colour codes as above. (c, d) Three-dimensional view of model topography at the end of model NECK-05 and NECK-50, respectively. (e, f) Three-dimensional view of the corresponding model Moho surface. (g, h) Three-dimensional view of the corresponding bottom of lithosphere. Note that the separation among the three layers is exaggerated to facilitate the visualization.

the slow model, the limbs of the anticlinorium asymptotically attained the flat lying attitude of the undeformed lithosphere bottom.

The second half of model evolution, in both cases, was characterized by the preservation of the overall rift architecture. In model NECK-05, the two basins widened and a subordered tectonic depression formed on the fixed side (Figs. 2k-m). In model NECK-50, the central high within the inner basin was progressively dismembered and, eventually, almost disappeared (Figs. 2n-p). The late-stage necking profiles of the lithosphere base are very different. In the slow model, fast uplift of the major bulge abruptly switched to upward stoping and lateral migration accommodating the outward motion of the mobile side (Fig. 3a). Conversely, the main central bulge in the fast model underwent an increased upward migration, with the fold hinge following an almost vertical trajectory. On the other hand, the lateral bulge on the mobile side was characterized by minor uplift and dominant sideward migration of the fold hinge, which followed a trajectory asymptotic toward the horizontal (Fig. 3b). The subordered bulge on the fixed side underwent negligible growth.

At the end of deformation, the surface expression of lithosphere stretching and thinning reached a comparable cross-sectional width in both experiments, despite the structural architecture of the two rift-systems was different. In model NECK-05, crustal thinning is accommodated in two well-defined grabens separated by a wide almost unfaulted central region (Figs. 2m, 3c). Model NECK-50 shows a more distributed deformation, with a large central depression symmetrically bounded by two uplifted shoulders in half of the rift system. The remaining half model is characterized by two composite grabens separated by a strongly uplifted central block (Figs.2p, 3d). The shape of the experimental Moho in the slow

Figure 4| (a) Evolution of the asthenosphere bulge height (H) during the evolution of models NECK-05, NECK-10 and NECK-50. (b) Evolution of the asthenosphere bulge basal amplitude (L) in the same models. (c) Evolution of the corresponding aspect ratio (H/L). See text for details.

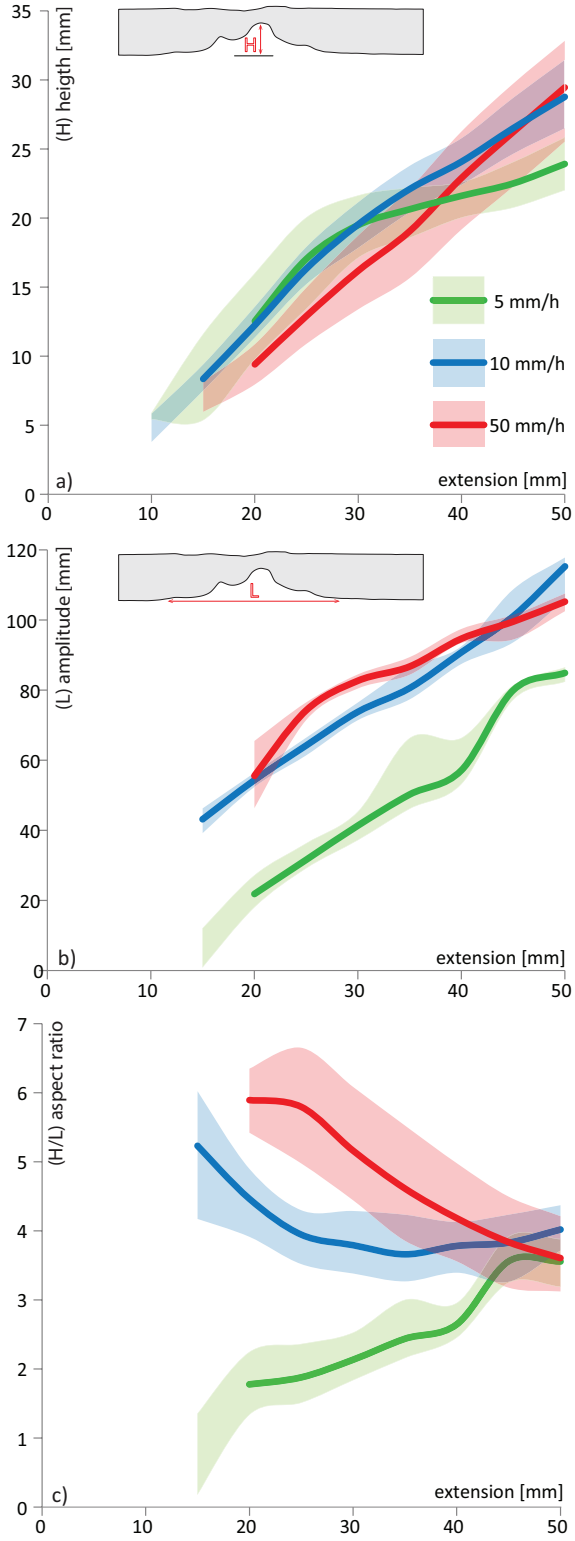
(H) heigth [mm]
H
5 mm/h
10 mm/h
50 mm/h
a)
extension [mm]
(L) amplitude [mm]
L
b)
extension [mm]
(H/L) aspect ratio
c)
extension [mm]

model shows a central high localized below the large horst separating the two basins at the surface. Two narrow throughs bound the central high on both sides (Fig. 3e). The fast model has a broader uplifted central area in the Moho underlying the rifted region, with a maximum localized below the uplifted central block (Fig. 3f). A near cylindrical strongly uplifted belt mimicking that in the overlying Moho (Fig. 3g) characterizes the base of the lithosphere in model NECK-05. A comparable behaviour occurs in model NECK-50 lithosphere base, which has a much more emphasized elevation compared to the Moho, but a similar overall geometry (Fig. 3h).

Quantitative analysis of the base lithosphere necking profile provides instructive information on the influence of plate divergence rate on rifting. The height of the main bulge has comparable growth trends regardless of the mobile side outward migration velocity. Only after about 30mm of extension, the slowest model shows a significant decrease of the bulge upward growth (Fig. 4a). The behaviour of the necking amplitude shows a very similar linear growth for intermediate and fast velocity. On the other hand, the slow model has a similar trend but systematically smaller amplitude values (Fig. 4b). Interestingly, the ratio between necking height and amplitude shows quite different values in the early evolutionary stages, which progressively decrease and converge towards a value of about 3.5 (Fig. 4c)

3. Finite deformation analysis

The experimental evolution is quantitatively analysed using the 3D distribution of the thinning factor ($TF = 1-1/\beta$ [e.g. *Reston*, 2009]), calculated according to *Nestola et al.*[2013]. The crustal pattern of this parameter is quite different in the two experiments (Fig.5). In the slow model, a wide belt of TF_C in the 0,25-0,50 range characterizes the rifted region; a localized area that includes much higher values occurs in the central sector. The fast model shows a central belt of very high TF_C values localized in the new space created by the outward translation of the mobile side. At the mantle level, high TF_M

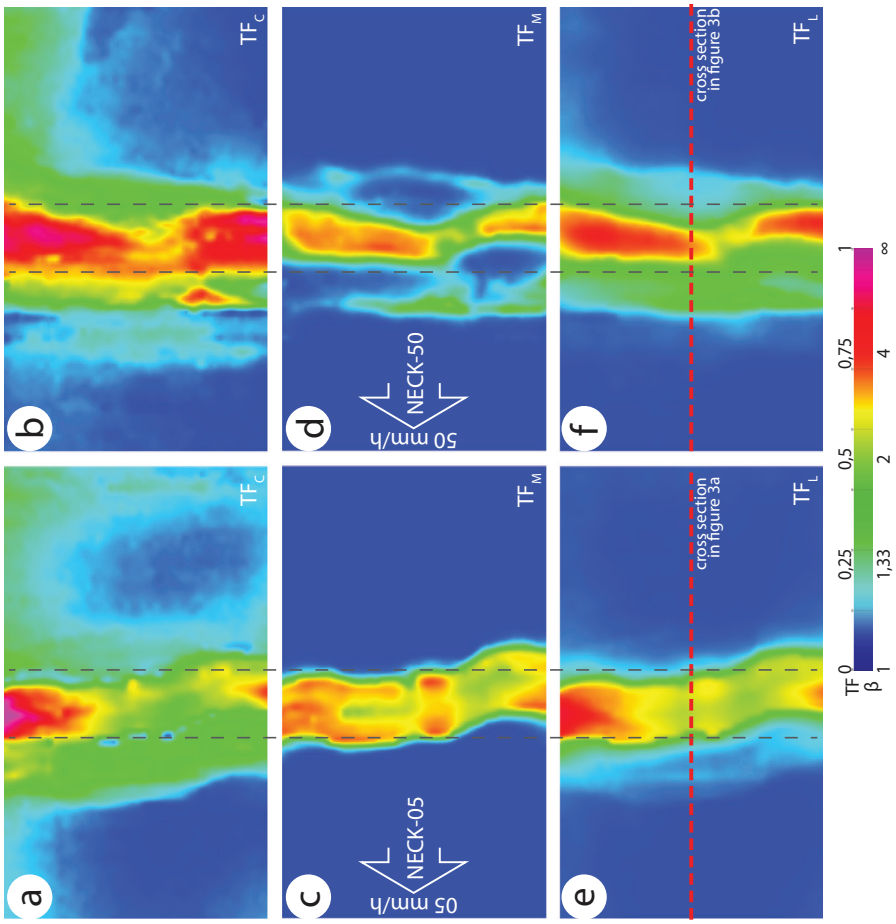

Figure 5| Map view of the thinning factor pattern calculated for the crust (a,b) the mantle (c,d), and the whole lithosphere (e,f) from models NECK-05 and NECK-50, respectively. See text for details. The black dashed lines indicate the initial and final position of the velocity discontinuity.

values are comparable in both models but in NECK-05 they occupy almost the entire central region of the rift system, and has the highest TF_M values underneath the large rift basin. On the other hand, the intensely stretched belt is narrower and discontinuous in NECK-50 (Fig. 5c,d). In the latter case, positive values of TF_M occurs also outside in the central belt, particularly on the mobile side, and they isolate areas of undeformed brittle mantle. The pattern of the thinning factor calculated for the entire lithosphere (TF_L> 0,25) is wider in the fast model, but the central belt of very high values is narrower. In the slow model this belt is wider and, apart from a localized sector

adjacent to the lateral side wall, is characterized by TF_L values that typically do not exceed 0,6.

4. Discussion

Using analogue models to investigate on geodynamic processes at the lithosphere scale requires accepting severe limitations. Among them, there is the impossibility to include in the simulations fundamental parameters like pore fluid pressure, heat flow, and mineral phase changes. Despite this, physical experiments are widely used because they provide a simple tool for reproducing at the laboratory scale in a convenient time scale, the 4D progression of complex geologic systems that in nature have an evolution time spanning from millions to hundreds millions years [*Faccenna et al.*, 1996; *Brun*, 1999; *Corti et al.*, 2003; *Sokoutis et al.*, 2007]. The impact of experimental limitations is minimized when models are used for relative comparisons rather than being directly contrasted against nature. In our case, very simple models show first-order differences in the rift architecture as a function of plate divergence rate. This is further supported when the intermediate velocity case [*Nestola et al.*, 2013] is also considered. The aspect ratio evolution during lithosphere necking well illustrates such differences (Fig. 4c). The evidence that the three cases tend to reach similar values suggests that differences in rift system architectures can be imprinted in the very early evolutionary stages and that diagnostic first-order signatures of plate divergence rate on neck geometry may be hidden in natural rifts, particularly when trying to reconstruct rift architectures from conjugate passive margins separated by long-living drift histories.

In our experiments, availability of the incremental evolution of the base lithosphere geometry allows us to make inferences on the behaviour of parameters related to lithosphere thickness, like heat flow. The very localized thinning in the slow model, up to half of its evolution, and the rapid asthenosphere rise, suggest significant increase of heat flow values only in the inner basin and its main shoulder. Conversely, in

the fast model the broad thinned area may imply a lower heat flow increase in most of the rifted region and its main shoulder on the fixed side. Further with this reasoning, we may expect a strong thermal pulse in the early stage of slow plate separation, which then decreases up to near constant values because of the stabilization of the necking depth (Fig. 3a). On the other hand, fast plate divergence may imply a progressive increase of the thermal anomaly associated with rifting and lithosphere necking (Fig. 3b). Speculations on possible magmatic activity triggered by heat flow increase suggest that at slow divergence rate magmatism is expected to be incentivised in the inner basin since the onset of rifting. At fast divergence rate, magmatism is expected a wider distribution, and a delay between the age of rift initiation and the magmatic rock emplacement may occur.

The combined analysis of the lithosphere base geometry and surface topography, may suggest that plate divergence rate can play an important role on rift dynamics. Experiments at slow divergence rate do not show significant uplift accompanying faulting in the early evolutionary stages; this is a typical features of passive rifting. Conversely, strong rift shoulder uplift occurs coevally with faulting in the fast experiments, thus resembling a mantle plume-dominated process, i.e. active rifting [e.g. *Ruppel*, 1995]. Since magmatism is not included in our models, experimental results indicate that fast plate divergence may add, or even be an alternative factor, to mantle plume activity for producing diagnostic features of active rifting.

Analysis of the thinning factor distribution for the entire lithosphere (Fig. 5e,f) indicates that the necking area as a whole is more localized in the slow models, in agreement with previous experiments [*Brun*, 1999]. However, the width of the strongly thinned central belt is narrower in fast experiments, as expected from the dependence of strength on strain rate in viscous materials [e.g. *Ranalli*, 1995]. This evidence contributes to solve the apparent contrast between experimental and numerical results [e.g. *Bassi*, 1995].

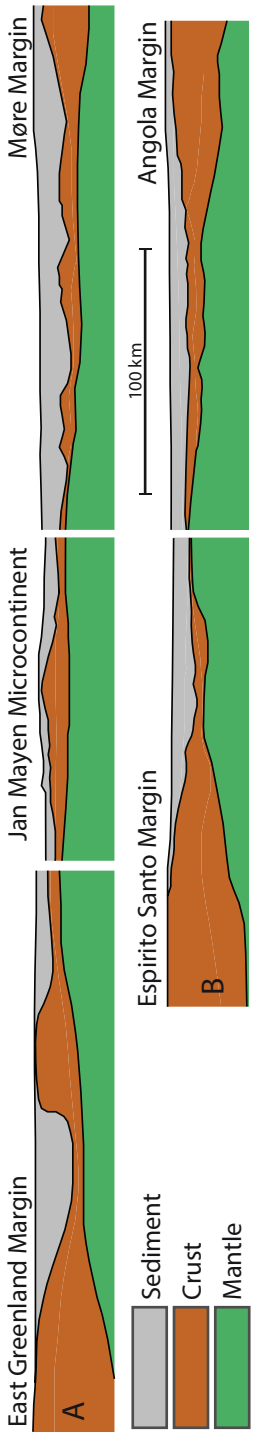

Figure 5 | Schematic, composite, lithospheric sections across the (A) conjugates "East Greenland – Jan Mayen – Møre" margins in the North Atlantic, and the (B) conjugates "Espirito Santo – Angola" margins in the South Atlantic, as reconstructed by *Peron-Pinvidic et al.* [2013]. Note the difference in width, in sediment distribution, and in necking shape between the two sections. The section in (A) resembles the features of the slow divergence rate model, whilst in (B) resembles the features of fast divergence rate model. Horizontal and vertical scales are equal.

Finally, comparison of experimental results with first-order features of rift systems supports their applicability to nature. In slow divergence rate models, development of two deep and narrow basins separated by an unfaulted wide crustal block, resembles the crustal structure of the Jan Mayen 'micro-continent' between Greenland and Norway in North Atlantic (Fig. 6a) [*Peron-Pinvidic and Manatschal*, 2010], thus supporting long-lasting slow rifting preceding continental breakup. On the other hand, distributed faulting over a wide area and the smoothed experimental Moho in the fast models have similarities with the crustal structure reconstructed along the Brazil-Kwanza conjugate margins in the South Atlantic Ocean [*Aslanian et al.*, 2009; *Peron-Pinvidic et al.*, 2013] (Fig. 6b).

6. Conclusion

We studied the rifting and necking response of the lithosphere to plate divergence velocity in analogue models. The geometry of lithosphere necking and the surface deformation were monitored during model evolution by paired top and bottom laser scanning, which provides an effective tool to comprehensively describe the evolution of model rift systems.

The experimental asymmetric kinematics, where a mobile side moves apart from a fixed one, imparts an asymmetry to the cross-sectional geometry of the extensional system, with the major asthenosphere bulge located below the basin and rift shoulder on the fixed plate side, while the basins on the opposite rift shoulder rest over an almost unstretched lithosphere.

Plate divergence rate in our experiments strongly affects the shape of lithosphere necking. At low divergence rates, a sharp cusp develops at the base of the lithosphere on the fixed plate side and only after reaching the lower crust it widens sideward towards the mobile plate. At fast divergence rate, the necking area in the mantle is wider and two subsidiary bulges develop aside the central major one, thus favouring isolation of unstretched blocks.

Analysis of the aspect ratio of the base lithosphere necking profile indicates that slow plate divergence produces slightly increasing values with progressing extension, while fast divergence results in strongly decreasing values. Regardless of the plate divergence rate, the aspect ratios reach very similar values when approaching continental breakup, thus suggesting that this parameter is controlled by the rheological layering of the lithosphere.

The significant differences and evolution produced by plate divergence rate on the lithosphere necking profile suggest that this parameter can exert a fundamental control on the time and space distribution of heat flow during rifting. Following up on this we can speculate on the location and timing of syn-rift magmatism, which is expected to be preferentially produced on one shoulder for slow plate divergence rate, and more widely distributed and delayed at fast divergence rates.

Acknowledgment

We acknowledge financial support to our laboratory by Eni S.p.A. We are grateful to Midland Valley for providing Academic licenses of MOVE® to our department. We are also grateful to C. Faccenna and F. Funicello for the rheological characterization of our viscous materials in the Laboratory of Experimental Tectonics at "Roma Tre" University.

Reference

Aslanian, D. et al. (2009), Brazilian and African passive margins of the Central Segment of the South Atlantic Ocean: Kinematic constraints, *Tectonophysics*, *468*(1-4), 98–112, doi:10.1016/j.tecto.2008.12.016.

Bassi, G. (1995), Relative importance of strain rate and rheology for the mode of continental extension, *Geophys. J. Int.*, *122*(1), 195–210, doi:10.1111/j.1365-246X.1995.tb03547.x.

Van der Beek, P., S. Cloetingh, and P. Andriessen (1994), Mechanisms of extensional basin formation and vertical motions at rift flanks: Constraints from tectonic modelling and fission-track thermochronology, *Earth Planet. Sci. Lett.*, *121*(3-4), 417–433.

Brun, J. P., and M. O. Beslier (1996), Mantle exhumation at passive margins, *Earth Planet. Sci. Lett.*, *142*(1-2), 161–173, doi:10.1016/0012-821X(96)00080-5.

Brun, J.-P. (1999), Narrow rifts versus wide rifts: Inferences for the mechanics of rifting from laboratory experiments, *Philos. Trans. R. Soc. A Math. Phys. Eng. Sci.*, *357*(1753), 695–712.

Buck, W. R. (1991), Modes of continental lithospheric extension, *J. Geophys. Res.*, *96*(12), 20–178, doi:10.1029/91JB01485.

Corti, G. (2012), Evolution and characteristics of continental rifting: Analog modeling-inspired view and comparison with examples from the East African Rift System, *Tectonophysics*, *522-523*, 1–33, doi:10.1016/j.tecto.2011.06.010.

Corti, G., M. Bonini, S. Conticelli, F. Innocenti, P. Manetti, and D. Sokoutis (2003), Analogue modelling of continental extension: a review focused on the relations between the patterns of deformation and the presence of magma, *Earth-Science Rev.*, *63*(3-4), 169–247, doi:10.1016/S0012-8252(03)00035-7.

Davy, P., and P. R. Cobbold (1991), Experiments on shortening of a 4-layer model of the continental lithosphere, *Tectonophysics*, *188*(1-2), 1–25.

Doglioni, C., E. Carminati, and E. Bonatti (2003), Rift asymmetry and continental uplift, *Tectonics*, *22*(3), n/a–n/a, doi:10.1029/2002TC001459.

Faccenna, C., P. Davy, J. P. Brun, R. Funiciello, D. Giardini, M. Mattei, and T. Nalpas (1996), The dynamics of back-arc extension: An experimental approach to the opening of the Tyrrhenian Sea, *Geophys. J. Int.*, *126*(3), 781–795.

Hopper, J. R., and W. R. Buck (1998), Styles of extensional decoupling, , doi:10.1130/0091-7613(1998)026<0699.

Kirby, S. H. (1983), Rheology of the lithosphere, *Rev. Geophys.*, *21*(6), 1458, doi:10.1029/RG021i006p01458.

Kusznir, N. J., and G. D. Karner (2007), Continental lithospheric thinning and breakup in response to upwelling divergent mantle flow: application to the Woodlark, Newfoundland and Iberia margins, *Geol. Soc. London, Spec. Publ.*, *282*(1), 389–419, doi:10.1144/SP282.16.

McKenzie, D. (1978), Some remarks on the development of sedimentary basins, *Earth Planet. Sci. Lett.*, *40*(1), 25–32.

Nestola, Y., F. Storti, E. Bedogni, and C. Cavozzi (2013), Shape evolution and finite deformation pattern in analog experiments of lithosphere necking, *Geophys. Res. Lett.*, *40*(19), 5052–5057, doi:10.1002/grl.50978.

Peron-Pinvidic, G., and G. Manatschal (2010), From microcontinents to extensional allochthons: witnesses of how continents rift and break apart?, *Pet. Geosci.*, *16*(3), 189–197, doi:10.1144/1354-079309-903.

Peron-Pinvidic, G., G. Manatschal, and P. T. Osmundsen (2013), Structural comparison of archetypal Atlantic rifted margins: A review of observations and concepts, *Mar. Pet. Geol.*, *43*, 21–47, doi:10.1016/j.marpetgeo.2013.02.002.

Ramberg, H. (1981), *Gravity, Deformation and the Earth's Crust in Theory, Experiments and Geologic Application*, Second., Academic Press, London.

Ranalli, G. (1995), *Rheology of the Earth,*, 2nd ed., London, Glasgow, Weinheim, New York, Tokyo, Melbourne, Madras: Chapman & Hall.

Ranalli, G., and D. C. Murphy (1987), Rheological stratification of the lithosphere, *Tectonophysics*, *132*(4), 281–295.

Ranero, C. R., and M. Pérez-Gussinyé (2010), Sequential faulting explains the asymmetry and extension discrepancy of conjugate margins., *Nature*, *468*(7321), 294–9, doi:10.1038/nature09520.

Reston, T. J. (2009), The structure, evolution and symmetry of the magma-poor rifted margins of the North and Central Atlantic: A synthesis, *Tectonophysics*, *468*(1-4), 6–27, doi:10.1016/j.tecto.2008.09.002.

Rowley, D. B., and D. Sahagian (1986), Depth-dependent stretching: A different approach, *Geology*, *14*(1), 32–35, doi:10.1130/0091-7613(1986)14.

Ruppel, C. (1995), Extensional processes in continental lithosphere, *J. Geophys.*

Res., *100*(B12), 24187, doi:10.1029/95JB02955.
Sokoutis, D., G. Corti, M. Bonini, J. Pierre Brun, S. Cloetingh, T. Mauduit, and P. Manetti (2007), Modelling the extension of heterogeneous hot lithosphere, *Tectonophysics*, *444*(1-4), 63–79, doi:10.1016/j.tecto.2007.08.012.
Weijermars, R., and H. Schmeling (1986), Scaling of Newtonian and non-Newtonian fluid dynamics without inertia for quantitative modelling of rock flow due to gravity (including the concept of rheological similarity), *Phys. Earth Planet. Inter.*, *43*(4), 316–330.
Wernicke, B. (1985), *Uniform-sense normal simple shear of the continental lithosphere.*
Ziegler, P. a., and S. Cloetingh (2004), Dynamic processes controlling evolution of rifted basins, *Earth-Science Rev.*, *64*(1-2), 1–50, doi:10.1016/S0012-8252(03)00041-2.

4

Impact of lithospheric heterogeneities on continental rifting evolution: Constraints from analogue modelling on South Atlantic margins

Published in
Tectonophysics (2013)
vol. 608, pp. 30-50.

Tectonophysics 608 (2013) 30–50

Contents lists available at ScienceDirect

Tectonophysics

journal homepage: www.elsevier.com/locate/tecto

Review Article

Impact of lithospheric heterogeneities on continental rifting evolution: Constraints from analogue modelling on South Atlantic margins

A. Cappelletti [a,b,*], F. Tsikalas [a,c,1], Y. Nestola [d], C. Cavozzi [d], A. Argnani [e], M. Meda [a], F. Salvi [a]

[a] Eni E&P, Via Emilia 1, I-20097 San Donato Milanese, MI, Italy
[b] Eni Us Operating Co. Inc., 1200 Smith St., Suite 1700, Houston, TX 77002, USA
[c] Eni Norge AS, P.O. Box 101 Forus, NO 4064 Stavanger, Norway
[d] NEXT — Natural and Experimental Tectonics Research Group, Department of Physics and Earth Sciences "Macedonio Melloni", University of Parma, Via G. Usberti 157/A, I-43100 Parma, Italy
[e] ISMAR-CNR, Via Gobetti 101, I-40129 Bologna, Italy

ARTICLE INFO

Article history:
Received 3 September 2012
Received in revised form 12 September 2013
Accepted 20 September 2013
Available online 3 October 2013

Keywords:
Lithospheric-scale analogue modelling
Structural inheritance
Lithospheric inhomogeneities
Crustal extension
Continental breakup
South Atlantic

ABSTRACT

Lithospheric-scale experiments integrated with restored crustal transects are used to study the evolution of the Central Segment (confined between the Rio Grande Fracture Zone to the south and the Chain Fracture Zone to the north) of the South Atlantic margin. The presence of crustal inhomogeneities, located within the Brazilian Santos and Campos basins, have been analysed and modelled in order to better understand their effects on the rift evolution and resulting structural architecture of the conjugate rifted margins. The results show that heterogeneities located within the lower crust can have a remarkable impact on the along-margin segmentation promoting articulated basins with horsts and grabens in response to a relative "strong" rheology, and focused and deeper basins related to a relatively "weak" rheology on the equivalent parts of the conjugate pairs. In particular, at the early-stage rift evolution the deformation is concentrated at the inner margin where, in the presence of a weak lower crust rheology, a main deep listric half-graben fault and associated thick and wedge-shaped syn-rift basin sequences are developed. A strong lower crust rheology, instead, gives rise to more planar, rotated, domino-type faulted basins with thinner sequences directly controlled by the individual fault-blocks. At the late-stage rift evolution, once the effects of the initial crustal rheology inhomogeneities are reduced due to the lithosperic thinning process, the outer margin records a late syn-rift sequence which shows comparable thicknesses for both cases of lower crust rheologies. This tectono-stratigraphic evolution of the rifting process gives rise to along-margin alterations in symmetry versus asymmetry of the width and structural architecture. The performed analogue modelling experiments also indicate that during the rifting evolution pieces of brittle mantle are preserved and could be elevated beneath the developed upper crustal structures, giving rise to complicated predictions for the along-margin heat-flow.

Contents

* Corresponding author at: Eni Us Operating Co. Inc., 1200 Smith St., Suite 1700, Houston, TX 77002, USA.
E-mail addresses: alessio.cappelletti@enipetroleum.com (A. Cappelletti), filippos.tsikalas@eninorge.com (F. Tsikalas), yago.nestola@unipr.it (Y. Nestola), cristian.cavozzi@unipr.it (C. Cavozzi), andrea.argnani@bo.ismar.cnr.it (A. Argnani), marco.meda@eni.com (M. Meda), francesca.salvi@eni.com (F. Salvi).
[1] Also at: Department of Geosciences, University of Oslo, P.O. Box 1047 Blindern, NO-0316 Oslo, Norway.

0040-1951/$ – see front matter © 2013 Elsevier B.V. All rights reserved.
http://dx.doi.org/10.1016/j.tecto.2013.09.026

1. Introduction

The rifting processes and the mechanism with which the continental crust is, through stretching and thinning processes, eventually broken are still far away to be completely understood (e.g. Ebinger, 2005; Reston and Pérez-Gussinyé, 2007; Rosenbaum et al., 2008; Rosendahl et al., 2005; Sawyer et al., 2007). Several generic models describing the above processes have been proposed during the end of the last century (e.g. Barbier et al., 1986; Lister et al., 1986; McKenzie, 1978; Wernicke, 1981), and have defined the complex interaction of structural and magmatic relationships during the continental rifting and breakup. This interaction results in a wide variety of margin styles, ranging, among others, from narrow to wide, and from "magma-poor" to "magma-dominated" conjugate-pair rifted margins (e.g. Blaich et al., 2011; Menzies et al., 2002; Péron-Pinvidic et al., 2013; Sawyer et al., 2007). "Magma-poor" rifted margins are those where volcanic products are sporadically distributed along the margin while the crust is affected by highly intensive, faulting of the brittle rheology (e.g. Iberia–Newfoundland margins, Péron-Pindivic and Manatschal, 2009; Australian–East Antarctic margins, Close et al., 2009; Direen et al., 2007). On the other hand, "magma-dominated" rifted margins are those where magma products are very well diffused and recognised along the rifted margins, and are characterised by seaward dipping reflector (SDR) sequences close to the continent–ocean boundary (COB), large igneous provinces both onshore and offshore, and voluminous along-margin crustal igneous intrusions (e.g. Namibia margin, Gladczenko et al.,

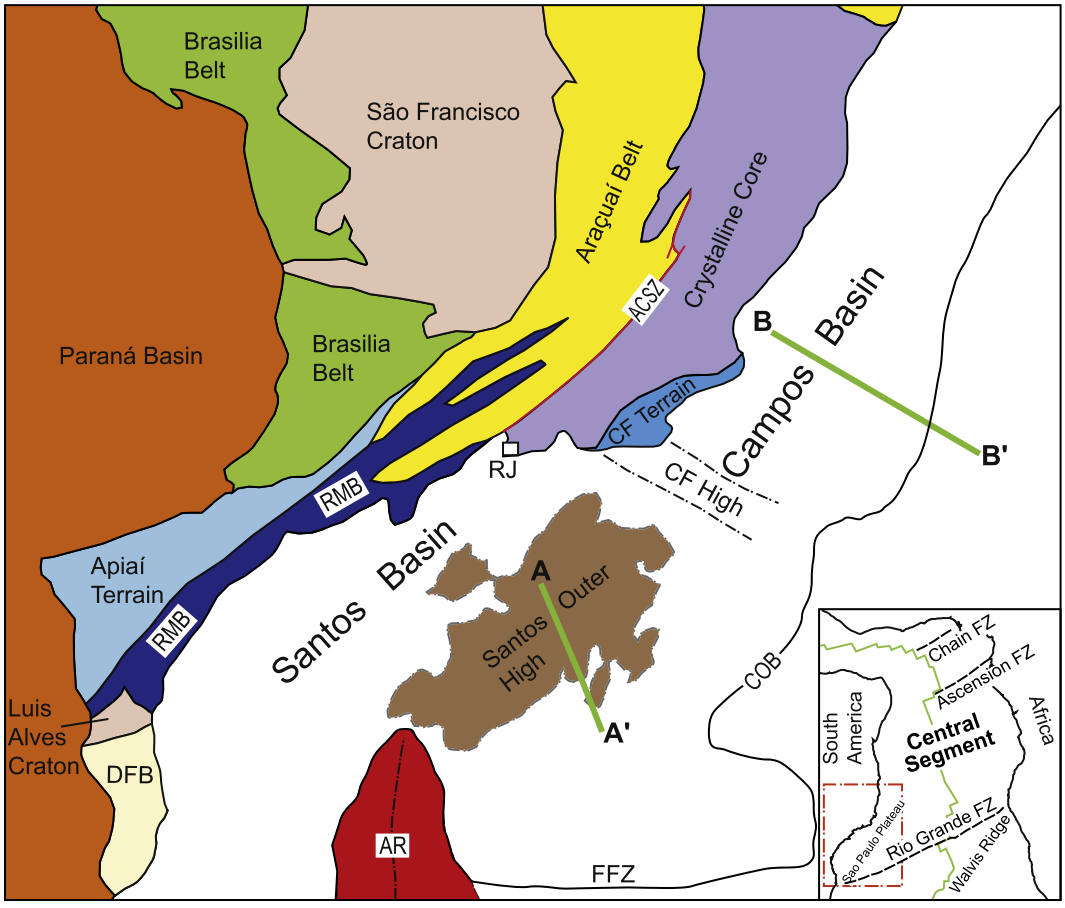

Fig. 1. Simplified geological map of southeastern Brazil (modified from Peres et al., 2004; Heilbron et al., 2008) depicting the main geological provinces and the location of the two restored seismic transects in Santos and Campos basins. ACSZ, Abre Campo shear zone; AR, Abimael Ridge; CF, Cabo Frio; COB, continent–ocean boundary; DFB, Dom Feliciano Belt; FZ, Fracture Zone; FFZ, Florianopolis Fracture Zone; RMB, Ribeira Mobile Belt; RJ, Rio de Janeiro.

1998; Lofoten-Vesterålen margin, Tsikalas et al., 2001; North-West Australia margin, Sawyer et al., 2007; East Greenland margin, Tsikalas et al., 2012).

Along the South Atlantic margins there is evidence of both magma-dominated and magma-poor margin types. In this study, we focus on the conjugate margin pairs along the Central Segment (confined between the Rio Grande Fracture Zone to the south and the Chain Fracture Zone to the north) of South Atlantic (Fig. 1) that have been proposed to have a magma-poor margin affinity as no major volcanic products are evidenced along the margin (e.g. Blaich et al., 2011; Contrucci et al., 2004; Moulin et al., 2005; Reston, 2009). The existing rifting models only partially explain the geophysical and geological observations along the Central Segment of the South Atlantic. In particular, the hyper-extended crust cannot be simply accounted by applying the McKenzie- or Wernicke-type models, thus, several other models were proposed to resolve the structural kinematic and extensional discrepancies that arise. The proposed models include, among other variants, considerations on depth-depending stretching (Kusznir and Karner, 2007), mantle exhumation (Blaich et al., 2010; Boillot et al., 1987; Manatschal and Bernoulli, 1999; Unternehr et al., 2010; Zalán et al., 2011), and polyphase faulting evolution (Reston, 2007, 2009). In this context, during the last decade complex lithospheric-scale analogue modelling rifting experiments of both magma-poor (Autin et al., 2010; Brun, 1999) and magma-dominated extension (Bonini et al., 2001; Corti et al., 2003a) have been performed and have provided a valuable tool to address and analyse several of the issues dealing with the rifting processes. These include: the relationships between the rift kinematic and deformation patterns, the influence of lithospheric rheological structure on rift architecture, the mode of extension and the faulting evolution during the rifting process, and the rifting relations with inherited structures (e.g. Agostini et al., 2009; Bonini et al., 2007; Callot et al., 2002; Corti, 2012; Sokoutis et al., 2007).

In this study of the Central Segment of the South Atlantic, we utilise an integrated approach of structural restoration on regional crustal transects and lithospheric-scale analogue modelling in order to address the impact of lithospheric heterogeneities on continental rifting evolution. In particular, we concentrate on the Santos and Campos basins offshore Brazil, but extrapolate the observations and considerations on the West African conjugate margin, in order to better understand the generation, architecture and evolution of rift-basins in terms of subsidence and structural style, spanning from the initial phase of continental rifting to the breakup stage. Moreover, the applied integrated analysis provides insights on the observed along-margin segmentation and its relationship to pre-existing lithospheric weaknesses, the symmetry versus asymmetry of the conjugate rifted margin pairs, and the nature of the crust on the outer margin close to the continent–ocean boundary with related heat-flow considerations.

2. Data and methodology

2.1. Structural restoration

In order to constrain several of the input parameters to be used in the lithospheric-scale analogue modelling, structural restoration was performed on selected regional transects. Construction of the transects is based on a regional set of seismic reflection profiles, combined with structural trend interpretation on available potential field data. The dataset in our disposal included a compilation of industrial seismic reflection profiles, published seismic reflection and wide-angle refraction profiles, and potential field data on both conjugate margins of the Central Segment of South Atlantic (Fig. 1). In particular, the industrial seismic dataset has been licensed by Eni E&P and comprises several 2D multi-client post-stack depth migrated (PSDM) seismic sections acquired by TGS-Nopec on the Brazilian side and by ION-GXT (CongoSPAN) on the conjugate Kwanza and Lower Congo basins. Published vertical incidence reflection and wide-angle refraction profiles along both sides of the Central Segment (e.g. Contrucci et al., 2004; Péron-Pinvidic et al., 2009; Unternehr et al., 2010; Zalán et al., 2011) were also analysed and incorporated in our interpretations. In addition, we had in our disposal potential field data that were used to map and constrain structural trends within the study area. The datasets consist of the publicly available satellite radar-altimeter gravity anomaly grid (Sandwell and Smith, 1997; version 18.1) and the aeromagnetic anomaly map grid (World Digital Magnetic Anomaly Map, WDMAM, 2007). Moreover, published elaborations of gravity and magnetic anomalies in the Santos and Campos basins (Carminatti et al., 2008; Gomes et al., 2009) were used to better define the structural trends and the presence of pre-rift inherited structures along the Brazilian margin. Finally, several gravity modelled transects both along the Brazilian and West African margins (Blaich et al., 2008, 2009, 2010, 2011) were analysed and compared with our constructed regional transects.

Two crustal transects along the Brazilian margin (Figs. 2 and 3) and three transects along the West African margin were constructed and structurally restored. Structural restoration was performed utilising the 2D-Move software (Midland Valley) that uses analytical and geometrical procedures to build balanced cross sections. The restoration technique provides indications on the original depositional geometry of the sedimentary sequences and, eventually, it gives an overview on the structural style of a particular geological system at different time-steps, progressively removing the effects of the deformation (Gibbs, 1983; Groshong, 2006). The restoration in this study was performed using a vertical shear, algorithm which was applied to the post-breakup sequences in order to remove the effects of the post-rift thermal subsidence affecting the Brazilian rifted margin. Insights deriving from restored sections were extremely useful to understand the pre-salt basin architecture of the Santos and Campos basins (Figs. 2 and 3). Furthermore, structural restoration provided us some of the parameters to be tested and compared with the analogue modelling results, such as the amount of brittle crust extension, the geometry of the sedimentary sequences, and the structural style of the faults for both the early and late syn-rift phases. In order to restore the interpreted seismic horizons to their most probable depth and paleo-depositional environment, at the time of their deposition, paleo-bathymetries were extracted along the constructed transects (Figs. 2 and 3) from various regional paleo-bathymetry sections (e.g. Contreras et al., 2010).

2.2. Lithospheric-scale analogue modelling

The analogue models were performed at the Physics and Earth Sciences Department of Parma University ("Elisabetta Costa Analogue Modelling Laboratory") (Fig. 4a–b). The models were built to reproduce a four-layer lithosphere rheology (Fig. 4b), which is assumed to represent a strength profile for a stable and young continent before rifting (Afonso and Ranalli, 2004; Corti et al., 2003a; Davy and Cobbold, 1991; Michon and Merle, 2003). The four-layer models are set so as to float above a glucose solution that represents the viscous asthenosphere rheology, and aims to reproduce the isostatic response of the deeper layers to the lithosphere thinning processes (Fig. 5a–d). In general terms, this technique is a forward modelling that allows to reproduce, through the building of 3D physical models, the tectono-stratigraphic events that occurred during the evolution of a geological system and to verify the hypothesis at the basis of the inferred geological model. Analogue models can be compared to the natural counterparts when the densities, rheologies and stresses of the two systems are similar (Brun, 1999; Corti, 2012; Corti et al., 2003a; Hubbert, 1937; Vendeville et al., 1987).

The modelled four-layer lithosphere was set to comprise an upper brittle crust (BC), a lower ductile crust (DC), an upper brittle mantle (UM), and a lower ductile mantle (LM), that are made of loose sand for the brittle rheologies and silicone putty with barite addition in order to have different densities and viscosities for the ductile rheologies

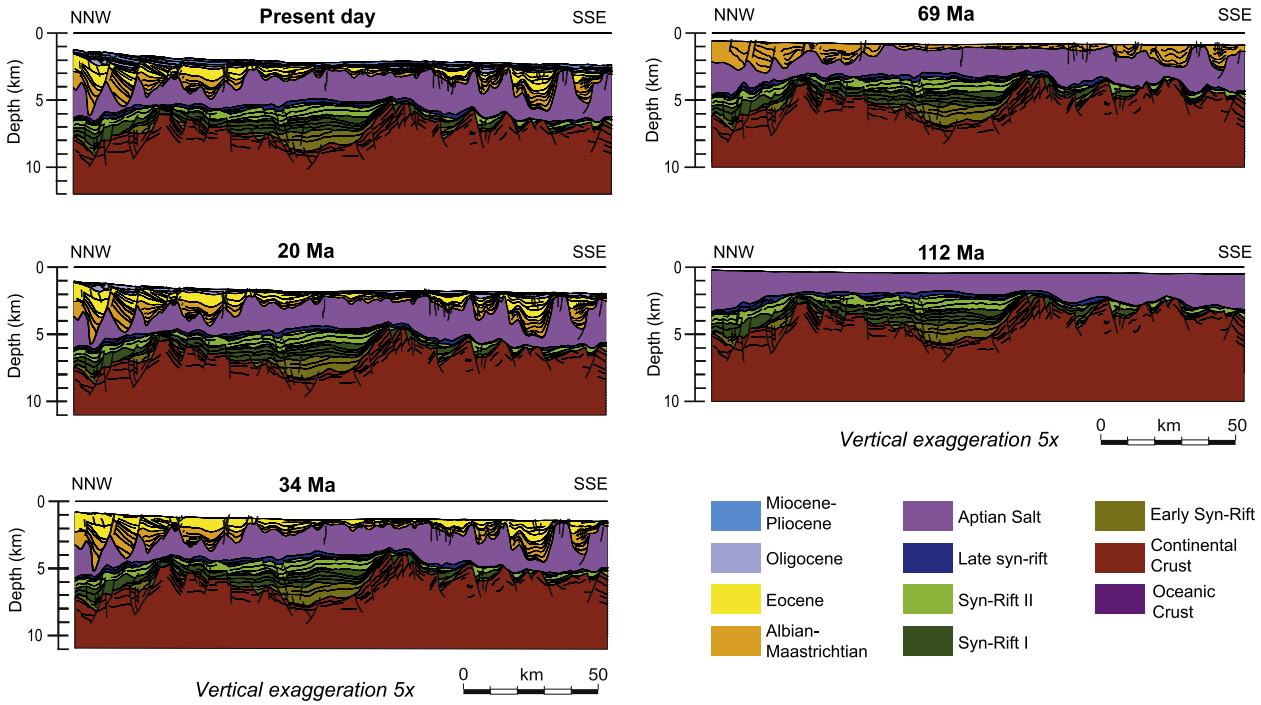

Fig. 2. Restoration of the Santos Basin geological cross-section A–A′ (location in Fig. 1), crossing the Santos Outer High region, at five different time steps starting from the present day situation and ending at the Aptian salt deposition (112 Ma). Regional paleo-bathymetries from Contreras et al. (2010).

(Table 1, Fig. 4b). The modelled lithosphere strength profiles were designed to reproduce a 40-km-thick crust and a 56-to-80-km-thick mantle (Table 1). In this way, the analogue experiments simulated a total lithosphere thickness ranging from 95 to 120 km, which are typical values for the continental lithosphere (Corti et al., 2003a; Fadaie and Ranalli, 1990). Considering a scale-ratio for the models of 1 to 7.14×10^{-7} in nature, a 120-km-thick lithosphere is thus scaled to a thickness of 8.5 cm, while a 95-km-thick lithosphere is scaled to a thickness of 6.5 cm (1 cm = 14 km) (Table 2, Figs. 4b and 5a–d). The modelling materials represent a good analogue of the natural strength profile for brittle rheologies, whereas the viscous layers differ from the natural counterparts (lower crust and lower mantle) in that the silicon putty shows a uniform strength profile with depth. On the contrary, the lower crust and lower mantle strengths in nature are believed to decrease non-linearly with depth (Fig. 4b) (e.g. Davy and Cobbold, 1991). Scaling of the analogue models into their natural prototypes ensures fulfilment of similarity in geometry, kinematics, dynamics and rheology (e.g. Hubbert, 1937; Ramberg, 1981). Given the lower crust viscosity of 40,000 Pa s, the imposed extension velocity of the model of 3 cm/h scales down to about 1 cm/yr

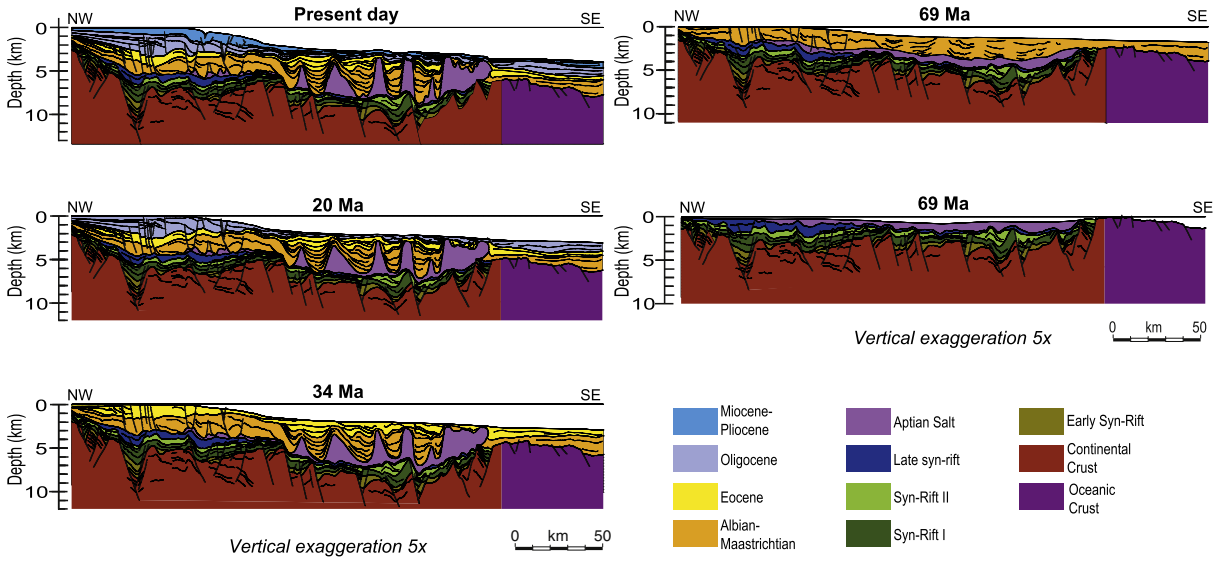

Fig. 3. Restoration of the Campos Basin geological cross-section B–B′ (location in Fig. 1), crossing the continent–ocean boundary on its eastern part, at five different time steps starting from the present day situation and ending at the Aptian salt deposition (112 Ma). Regional paleo-bathymetries from Contreras et al. (2010).

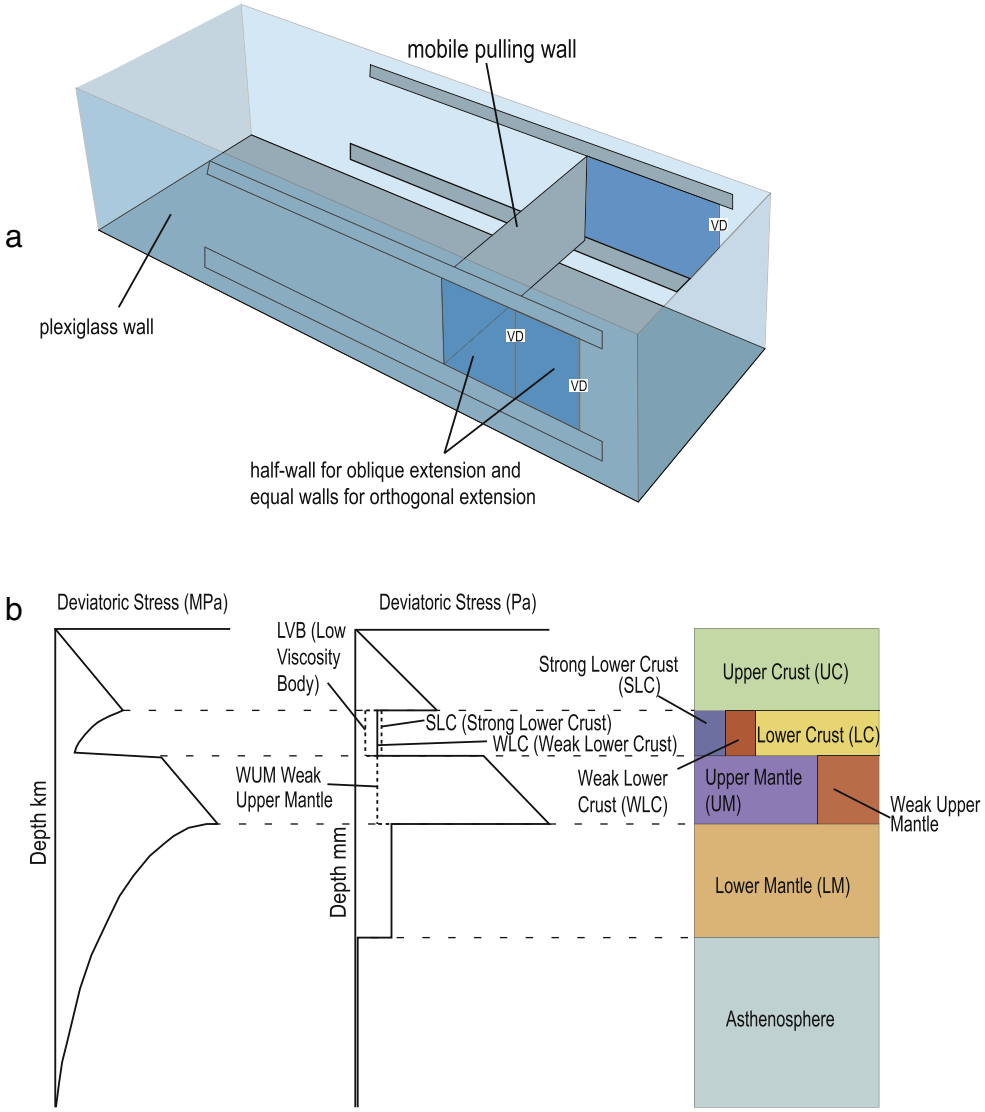

Fig. 4. Model set-up. (a) 3D view of the sandbox used. (b) Strength profile of a continental lithosphere with a normal thermal gradient (left side) and its experimental counterpart (centre) used in this study. VD, velocity discontinuities.

if a natural viscosity of 5×10^{21} is assumed; in the same conditions the experimental velocity of 1.5 cm/h scales to 5 mm/yr. In Table 2 we list the values of dimensionless ratios, referred to the lower crust values, which are used to scale the model.

The sandbox device (Fig. 4a) is made of plexiglas and has width and length of 30 cm and 40–50 cm, respectively. One of the short walls of the sandbox device, attached to the sand/silicone layer-cake, was pulled using a computer-controlled motor at a velocity of 1.5 to 3 cm/h. Some of the models were extended to a middle stage of lithosphere thinning, whereas extension on other models was completed once the breakup stage was reached, when the glucose was flowing out of the uppermost sand layer. During extension, coloured sand layers were uniformly and constantly deposited on the top surface of the models, in order to completely fill the syn-deformational basins reproducing syn-rift sediment accumulation. Moreover, laser scan acquisitions were taken on the top surface to obtain images of the topmost faults (upper crust fault tips) that were cutting through the surface during the rifting evolution. Complete infill of the resulting syn-deformational basin topography is clearly an approximation that precludes any comparison to the natural sedimentation rate occurring during the rifting process. Nevertheless, the sandbox models provide an objective approach that allows making inferences on the relative subsidence and thicknesses of the basins developed above different lithosphere rheologies. Therefore, any considerations on the overall basin thicknesses and on early or late syn-rift depositional sequence relationships are made only in a qualitative way. At the end of the experiments, the models were soaked in water, frozen and serially sliced from side to side. In this way, we were able to make qualitative considerations both in time and in space about the three-dimensional basin configurations and subsidence record in relation to the developed sedimentary thickness and distribution over the homogeneous or heterogeneous lithosphere.

Continental rifting is a complex process that is largely controlled by the thermo-mechanical stage of the lithosperic layering rheology. Since the analogue modelling technique is performed at an iso-thermal state, the resulting laboratory analogue counterparts of the continental rifting are greatly simplified (e.g. Corti, 2012). Moreover, boundary conditions of the sandbox models have to necessarily simplify not only the rift-related processes, but also the erosion and sedimentation that are operated in time-steps and not continuously as in nature. The extension of the natural-gravity lithospheric-scale experiments was obtained by pulling apart the models through the movement of a mobile wall that is connected to two half side-walls. The presence of these side-walls is creating lateral extensional stress velocity discontinuities (VDs) at the model edges (Fig. 4a). Although the VDs could irregularly re-orientate

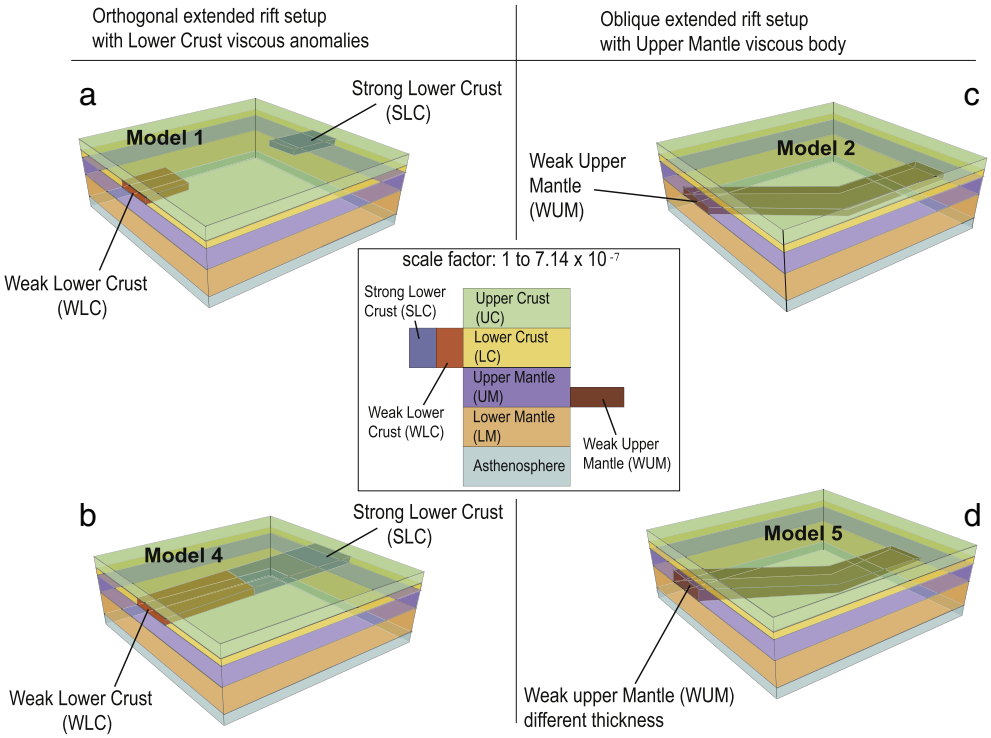

Fig. 5. Pre-extension lithospheric model setups used in the study. The orthogonal extension model setup is represented on the left side models, whereas the oblique extension model is represented on the right side. (a) Model 1: orthogonal extension model setup with lower crust (LC) inhomogeneities: weak lower crust (WLC) and strong lower crust (SLC). (b) Model 4: same orthogonal setup as Model 1 with juxtaposed inhomogeneities located in the central part of the model and along the future rift axis location. (c) Model 2: oblique extended setup with weak upper mantle (WUM) viscous body inhomogeneities that mimic inherited discontinuities or anomalous viscous material present within the mantle prior to the rift onset. (d) Model 5: same oblique setup as Model 2 with different thickness of the weak upper mantle (WUM) viscous body along the model.

local stresses within the extending lithospheric-layering portion which is close to the pulling walls (Morley, 1999a; Schreurs et al., 2006), in our experiments we do not observe any major deformation features which can be ascribed to be related to boundary effects. Furthermore, despite its limitations the sandbox analogue modelling technique has clearly demonstrated its ability to successfully reproduce some of the first-order characteristics in the rifting process evolution: the relations between rifts and inherited structures (Agostini et al., 2009; Corti et al., 2010), the role of lithosphere rheology on the rift kinematics (Brun, 1999, 2002; Corti et al., 2003a, 2011), the effects of lithospheric ductile crust or mantle heterogeneities on upper crust rifting deformation patterns (Sokoutis et al., 2007), the effects of strain localizations on upper crust continental extension (Benes and Davy, 1996), and the evolution of deformation and patterns of surface faulting in relation to the orthogonal or oblique extensional mode (Corti, 2012; McClay and White, 1995; Michon and Merle, 2003).

3. Geological framework constraining the lithosphere-setup and extension mode of the analogue modelling

3.1. Geological framework of the Central Segment of South Atlantic

The Gondwana supercontinent amalgamation occurred during the Late Proterozoic by the assembly of different fragmented cratonic nuclei (de Wit et al., 2008). The São Francisco–Congo craton is interpreted as being part of the interior and stable portion of the tectonic plates that by a series of collisions formed the western part of the Gondwana continent, thus resulting in a significant pervasive tectonic fabric affecting the lithosphere (Alkmim, 2004; Meisling et al., 2001). Within this regional context, it has been postulated that the pre-existing structural grain and major changes in the lithospheric strength have exerted a certain control on the South Atlantic Mesozoic rifting patterns (e.g. Rosendahl et al., 2005; Watts and Stewart, 1998). Distinct changes in both the onshore and offshore structural basement trends have been evoked to be the cause of the rifted margin reactivation and segmentation along the Brazilian South Atlantic Central Segment (Gray et al., 2008; Heilbron et al., 2004; Meisling et al., 2001).

In the onshore domain, along the entire South Atlantic there is distinct evidence of pre-existing orogenic remnants. In particular, the Mesozoic and Cenozoic rifting in the Central Segment developed along a pre-rift lithospheric grain that has undergone a long geologic evolution related to the Rodinia continent disarticulation (Early Neoproterozoic time, de Wit et al., 2008; Hoffman, 1991) that was subsequently sutured during the Western Gondwana assembly (Late Neoproterozoic time, Almeida, 1981; Campanha and de Brito Neves, 2004; Heilbronl et al., 2000). The West Gondwana suture comprises both the West Africa Pan-African Damara Orogen and the South America Brasiliano fold-belt. These two tectonic elements include parts of the same orogenic belt that was subsequently dissected during the South Atlantic Mesozoic rifting process (e.g. Gray et al., 2008; Ojeda, 1982; Rosendahl et al., 2005). Onshore of the Brazilian Campos and Espirito Santo basins, the Araçuaí orogen occupies the area between the São Francisco Craton (Fig. 1) and the Brazilian continental margin, and it is subdivided by the Abre Campo shear zone (ACSZ) (Haralyi and Hasui, 1982) in two major tectonic features (Fig. 1): the west vergent thrusted meta-sedimentary rocks of the Araçuaí Belt, and the coastal-located high-grade metamorphic rocks of the Crystalline Core, which is cored by older Archean and Paleoproterozoic rocks and a large volume of Neoproterozoic granites (Almeida, 1977; Pedrosa-Soares et al., 2007; Peres et al., 2004). To the south, the Araçuaí Belt is linked with a non-well defined boundary to the Ribeira mobile belt (RMB, Fig. 1) (Campanha, 1981). The transition between the two belts is marked by a slightly alteration of the structural trend, changing from a NNE–SSW to a NE–SW orientation.

Table 1
Characteristics of experimental materials and layer thickness used for the different lithospheric-scale analogue models (cf. Fig. 5). n, stress exponent; E, activation energy for creep.

	Layering and material used	Density [g/cm ^{3}]	Viscosity [Pa s]	n	E [kJ/mol]	Model 1 thickness [mm]	Model 2 thickness [mm]	Model 4 thickness [mm]	Model 5 thickness [mm]
Upper crust	Sand + fillite	1.11	–	–	–	15	18	18	18
Lower crust	Silicone + barite	1.15	40,000	1.05269	13.37916	10	10	10	10
Weak lower crust (WLC)	Silicone + barite	1.15	14,000	1.04335	13.88074	10			
Strong lower crust (SLC)	Silicone + barite + fillite	1.15	47,000	1.08531	14.95153	10			
Upper mantle	Sand + fillite	1.33	–	–	–	25	10	15	15
Weak upper mantle	Silicone + barite	1.33	42,000	1.05680	13.64847		10		5–10
Lower mantle	Silicone + barite	1.33	60,000	1.06678	13.41280	35	50	25	25
Asthenosphere	Glucose syrup	1.55	170	–	–	40	28	28	25

In the offshore domain, the presence of an aborted seafloor spreading axis, namely the Abimael Ridge (Fig. 1), within the southern edge of the Santos Basin close to the Florianopolis Fracture Zone that represents the western prolongation of the Rio Grande Fracture Zone, has been postulated by several studies (De Paula and Vidotti, 2001; Demercian, 1996; Mohriak et al., 2008). This peculiar feature, represents either a failed breakup axis generated by unsuccessful rifting due to micro-plates adjustment (Carminatti et al., 2008; Gomes et al., 2009; Moulin et al., 2012; Scotchman et al., 2010), or an abandoned seafloor spreading centre resulting from an early attempt by the incipient South Atlantic Ocean to extend its opening north of the southern edge of the Central Segment (Mohriak et al., 2010; Scotchman et al., 2006). During continental rifting the occurrence of failed sea-floor spreading axis (aulacogen) is well recognised and described in many areas worldwide (e.g. Faroes Shetland Basin, Fletcher, 2009; South China Sea, Sun et al., 2009). A ridge jump event is probably the cause of the abandonment of this tectono-magmatic process, resulting in a thinned continental crust that eventually was responsible of the resulting wide and stretched continental crust of the São Paulo Plateau (Fig. 1) (e.g. Gomes et al., 2002; Meisling et al., 2001; Scotchman et al., 2006).

3.2. Viscosity and strength alterations in the analogue models

In order to mimic the crustal/mantle inhomogeneities in lithosphere composition along the Brazilian margin described above, lower crust and upper mantle alterations of viscosity were placed within the models (Fig. 5a–d). In particular, a weak lower crust (WLC), less viscous than its surroundings, and a strong lower crust (SLC), relatively more viscous than the modelled normal lower crust were inserted.

In the analogue models, the presence of inherited structures related to the presence of old orogens within the lithosphere was reproduced by adding horizontal inhomogeneities within the layering similar to earlier performed studies (e.g. Corti et al., 2011; Sokoutis et al., 2007; Sun et al., 2009). In order to mimic the lithospheric inhomogeneity of the "cold" and high-strength rheology part of the Araçuaí Belt (Fig. 1) (Alkmim et al., 2006; Peres et al., 2004), we utilised a mixture of silicon and barite (strong lower crust, SLC; Fig. 5a, b) within the lower crust (LC) with stronger rheology in respect to the adjacent lithosphere strength profile (Fig. 4b). In this way, the analogue lithospheric strength rheology of the subsequently developing Campos Basin area was reproduced. Moreover, the meta-sedimentary belt of the western Araçuaí belt (Cunningham et al., 1998; Peres et al., 2004) that is adjacent to the São Francisco Craton (Fig. 1) was, for modelling simplicity, simulated with the normal strength lithospheric profile (Fig. 4b). Hence, the model is constructed to mimic a strong rheology affecting the immediate proximity of the rifting at the sandbox lithospheric edge, in respect to the surrounding four-layer lithosphere rheology. The strong lower crust (SLC) body has a viscosity μ that is in the order of 4.70×10^4 Pa s, whereas the surrounding ductile crust (east and west of the SLC) has a viscosity μ of 4×10^4 Pa s (Table 2).

The presence of the Abimael failed ridge (130 Ma, Cobbold et al., 2001; Contreras et al., 2010) in the southern Santos Basin (Fig. 1) represents a thinned and warmer continental crust of a weakened lithospheric strength profile (Corti et al., 2003a; Fadaie and Ranalli, 1990), that is believed to have given rise to a rheology perturbation within the São Paolo Plateau that affected the subsequently successful rifting (Scotchman et al., 2006, 2010). Analogue modelling of weaker horizontal lithospheric inhomogeneities were utilised by several studies to model and describe the relationships between weaker rheologies (within the lower crust or brittle mantle), the mode of extension (oblique or orthogonal), and the resulting structural rifting patterns (Corti, 2004; Corti et al., 2001; Sun et al., 2009). To better understand the effects of a weaker rheology on the Santos Basin rifting evolution we used a low viscosity silicone and barite mixture body (weak lower crust, WLC) within the lower crust (LC) layer. In this way, we were able to mimic the presence of a thermically "warm" discontinuity by placing a weak rheology within the four-layer lithospheric-scale models, which was assumed to be present prior to the South Atlantic Mesozoic rifting. The weak lower crust (WLC) body has a viscosity μ that is in the order of 1.4×10^4 Pa s, whereas the surrounding ductile crust (east and west of the WLC) has a viscosity μ of 4×10^4 Pa s (Table 2).

3.3. Extension mode

The opening of the Central Segment of South Atlantic is thought to have occurred with an orthogonal extension mode in the Campos Basin and an oblique extension mode in the southern Santos Basin (Cobbold et al., 2001; Meisling et al., 2001; Moulin et al., 2012; Vidal et al., 2003). In order to replicate these types of extension modes within the performed lithospheric-scale analogue models, the length of the two mobile sidewalls was adapted. Two mobile sidewalls of the same length were used to conduct orthogonal extension, whereas sidewalls with different lengths were used to conduct oblique extension (Fig. 4a) (Autin et al., 2010). In addition, the crustal/mantle rheology inhomogeneities were placed within the models in such a manner as to have an orthogonal extension affecting the "cold" rheology within the Campos Basin and an oblique extension affecting the "warm" rheology within the Santos Basin (Fig. 5c–d); i.e. the different along-margin rheologies that were assumed to be present prior to the Mesozoic rifting. Thus, the orthogonal rift analogue models are simulated by sidewalls parallel to each other that are perpendicular in respect to the discontinuities (Fig. 5a and b), whereas in the case of the oblique extension, the sandbox sidewalls were designed to have a different length in respect to eachother and to be connected to the segmented inhomogeneity within the model. In this latter case, the setup represents a 45° rift obliquity in respect to the east–west extension direction (Fig. 5c and d).

Within the range of the performed analogue models (Fig. 5a–d), the oblique extension mode with mantle inhomogeneities seems to better simulate the upper crustal pre-rift structural trend of the Santos Basin. Nevertheless, the lithospheric-scale analogue model that better

Table 2
Scaling parameters used in the analogue experiments. L, length; ρ, density; g, gravity; σ, stress (scale according to the range of lower crust viscosities); η, viscosity; ε̇, strain rate.

	L [m]	ρ [kg m^{-3}]	g [m s^{-2}]	σ [N m^{-2}]	η [Pa s]	ε̇ [s^{-1}]
Models	0.01	1200	9.81	117.72	40,000	2.94E−03
Nature	14,000	2800	9.81	3.85E+08	5.00E+21	7.69E−14
Scale ratio (M/N)	7.14E−07	4.29E−01	1	3.06E−07	8.00E−18	3.83E+10

reproduced many of the aspects and observations of the Central Segment rifted margins is the orthogonal setup-model with lower crustal inhomogeneities (Fig. 5b). In fact, the upper crustal structural evolution of the orthogonal setup models that was monitored constantly during the extension, reproduces well the upper crust observations of the Central Segment and can also be reasonably linked to the deeper levels within the lithospheric mantle. Following these results, in this paper we mainly concentrate on the outcomes of the orthogonal extension models which will be extensively described and discussed in the next paragraphs.

4. Structural inheritance and along-margin segmentation

Cross-sections through the strong lower crust (SLC) (Fig. 6a–b), at different amounts of extension, show that the presence of a hard rheology within the lower ductile crust (DC) layer promotes a general asymmetry on the rifted margin. This is achieved as deformation, at the middle stage of the rifting evolution (Fig. 6a), is avoiding and bypassing the SLC with faults soling out above it and cutting through the lithospheric crust at the SLC edge. At the mature stage of rifting, close to breakup (Fig. 6b), the SLC has been progressively and intensely affected by extensional faulting that takes place at the shallower brittle upper crustal (UC) levels (above the SLC) with regionally high-level, domino-type fault structural style (cf. also Fig. 8a–b for comparison with the weak lower crust, WLC, deformation). The same domino-type faulting style is also evidenced both in the Campos Basin restored regional transect at the end of salt deposition (Fig. 3) and in the conjugate Kwanza Basin just close to the Luanda transfer zone (Fig. 7a). This structural picture suggests a general strong behaviour of the upper and lower levels of the crust that guide the extensional deformation. On the other hand, the conjugate margin acted as a week margin, representing a main listric half-graben structure with well-focused deformation and a deep basin (Fig. 6b). Thus, a first-order control on the thinning process of the upper crust of the conjugate margins seems to be governed by the deformation that focuses on different rheologies. In particular, the deformation of the "cold" hard margin is resulting in a lesser thinned and wider margin than the conjugate side that, instead, is showing greater thinning and a narrower margin. Concerning the deeper lithospheric levels, the brittle mantle (BM) is breached apart and the deformation is mainly focused in the central area in correspondence to the SLC edge. Furthermore, as extension proceeds close to breakup, a doming developed within the asthenosphere (Fig. 6b) that at mature-rift stage resulted in narrow central focused necking. In this way, the SLC could preserve the deeper mantle from breaching the brittle mantle and from delamination of the ductile mantle.

Cross-sections through the weak lower crust (WLC), at different stages of extension (Fig. 8a–b), show that the presence of weaknesses within the lower ductile crust (DC) promotes a stronger asymmetry of the rifted margins in respect to the SLC margin (Fig. 6a–b). This behaviour is depicted by the focused upper crustal (UC) deformation in correspondence to the weak rheology, and a main upper crustal half-graben fault structure that is observed to develop in correspondence to the WLC. A similar structural style is evident during the end of salt deposition at the restored transect of the Santos Basin (Fig. 2), where a main deep basin is located in the westward vicinity and in close structural relation to the prominent outer high, and at the transition between the Lower Congo and Kwanza basins (Fig. 7b). On the other hand, the conjugate analogue model margin of Fig. 8b, is acting as the "stronger" margin and represents faulted, structurally elevated, basins. Similarly at the presence of the WLC, the same first-order control on the thinning process of the upper crust (UC) at the conjugate margins seems to be driven by the focus of deformation in respect to the different rheologies. In particular, extension of the "warm" and weaker initial lithosphere resulted in a thinner and narrower margin than at the conjugate counterpart that, instead, is thicker and wider (Fig. 8a). Concerning deformation at the deeper lithospheric levels of the middle-stage rifting, the section in Fig. 8a shows that the brittle mantle (BM) is breached apart in the central area where the deformation is initially concentrated. However as extension proceeds, the deformation is transferred to the deeper lithospheric layers where focused extension can eventually breach the brittle layer, giving rise to brittle mantle (BM) relicts (Fig. 8b).

The lithosphere thinning and the rift margin width of the analogue models are directly connected to the lower crust rheology (Figs. 6 and 8). The lithospheric-scale analogue model outcomes bear many similarities with natural rifts, where the presence of thermal and mechanical heterogeneities within the continental lithosphere causes the rifting to concentrate and propagate within ancient lithospheric structures, as for example the orogenic fabric of older plates (Lezzar et al., 2002; Michon and Sokoutis, 2005; Tommasi and Vauchez, 2001; van Wijk, 2005). Within the analogue models, the presence of lower crust (LC) discontinuities seems to control the thinning process since the inception of continental rift (Figs. 6a and 8a). In this context, narrower and highly thinned upper crust (UC) develops and gives rise to deep basins on the weaker margin side, whereas wider and less thinned upper crust (UC) is evident and exhibiting regionally elevated structures and basins in the conjugate part of the margin where hard rheologies are present. Comparable results have been also shown by Corti (2004) and Sokoutis et al. (2007) for the exerting control on the deformation of upper crust rifting patterns by lower crust rheologies. Moreover, the presence and juxtaposition of resistant (old and cold) and weaker (young and warm) lower crust (LC) within the analogue models, strongly affects the way at which rifting is initiated, propagates and evolves in terms of architecture, symmetry and structural style (Fig. 9a–e) (Corti et al., 2011; Ebinger et al., 1989). In addition, these LC domains are also affecting the way in which the deeper lithospheric mantle is evolving during the early- to middle-stage model extension. Deformation of the brittle mantle (BM) occurs beneath the weak LC (Fig. 8a), whereas in the presence of hard rheology the BM breaching occurs away from the strong lower crust (SLC) and focuses where a normal LC rheology is present (Fig. 6a).

Within the performed orthogonal lithospheric-scale models (Fig. 5a–b), the alternation along the rift axis in the upper crust structural style from half-grabens to horsts and grabens/domino-faulted blocks is developed at the transition from weak to hard lower crust rheology (Fig. 9b–c). The passage from one system to the other, results in a hard-linkage within a single system of synthetic extensional faults. The different amount of displacement accommodated between the two extensional systems, which is greater at the listric fault and partitioned at the domino-type faults, is realised with a series of breached relay-ramps which are characterised by intra-basin structural highs (Fig. 9c). The interaction of the different rift-basin border-faults has been interpreted to result in complex arrangements of the stepping, intersecting and/or parallel rift basins that give rise to a variety of accommodation or transfer zones and rift geometries (Nelson et al., 1992; Paul and Mitra, 2013; Withjack et al., 2002).

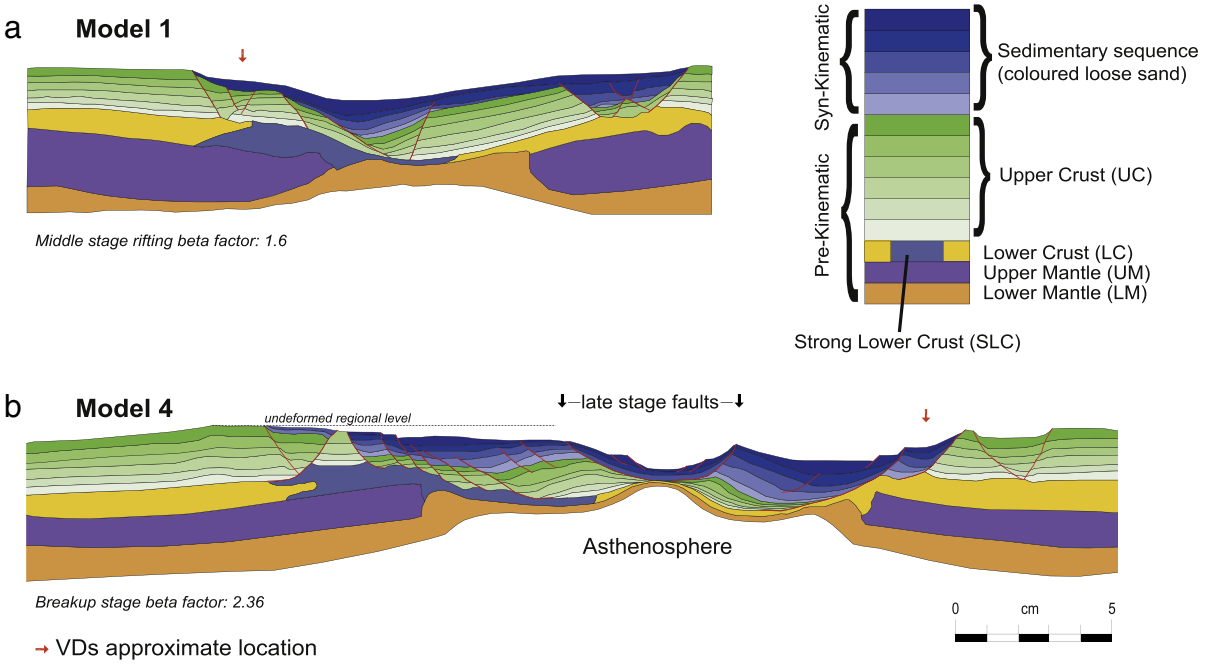

Fig. 6. Cross-sections at different amounts of extension crossing through the strong lower crust (SLC) of Model 1 and Model 4. (a) Middle stage rifting, β-stretching factor of 1.6, and (b) mature stage rifting, β-stretching factor of 2.36.

In particular, the study of natural rift examples has demonstrated that accommodation or transfer zones along the rift axis can be originated during propagation and linkage of initially-separated extensional segments (Ebinger, 1989). Along the offshore Brazilian margin, the Cabo Frio High (Fig. 1) is located at the transition between the Santos and the Campos basins (Oreiro et al., 2008). This structural

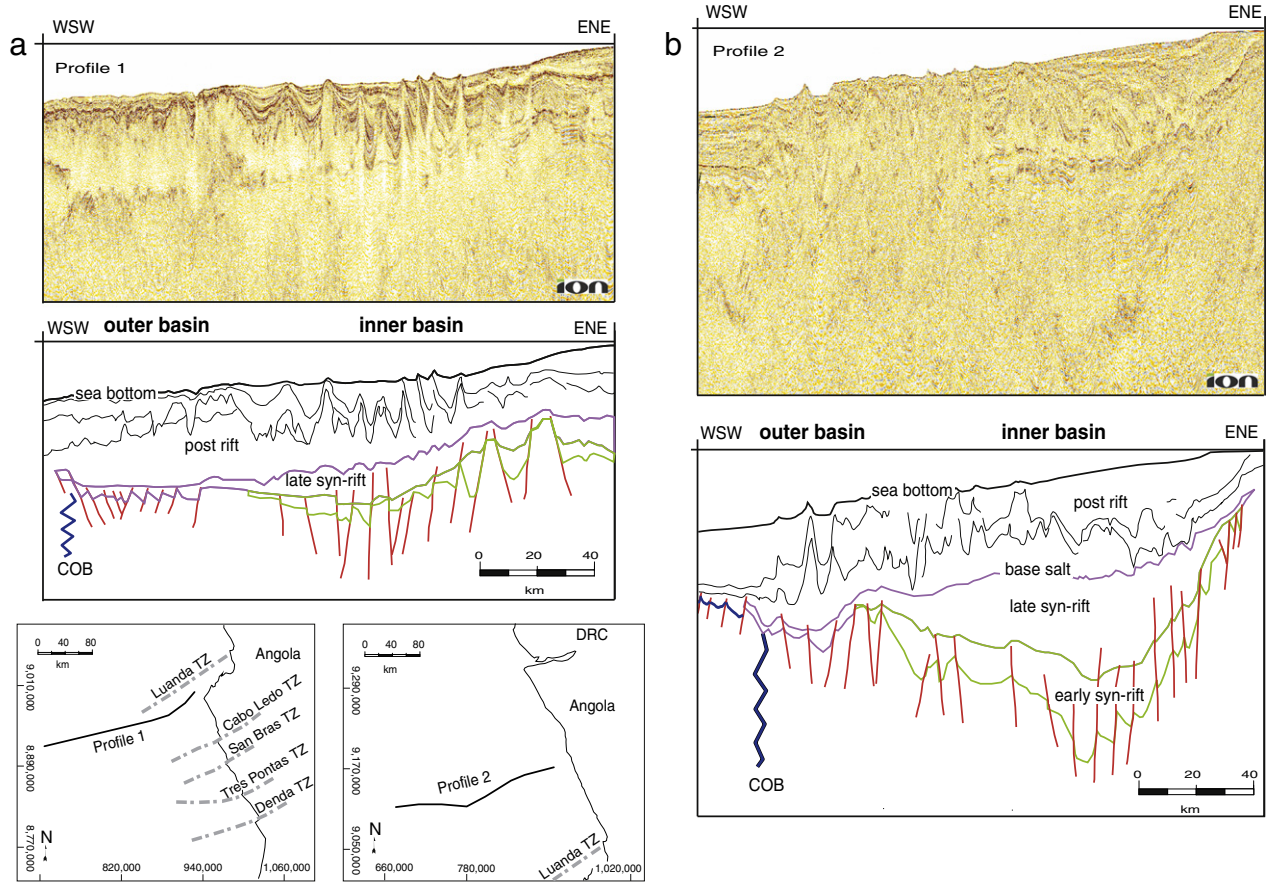

Fig. 7. Seismic examples, and interpretations (both in depth), offshore the West Africa coast: (a) in the vicinity of the Luanda Transfer Zone (GXT-ION seismic profile 1), and (b) in the vicinity to the Lower Congo–Kwanza basin transition (GXT-ION seismic profile 2). COB, continent–ocean boundary; TZ, Transfer zone.

high has been interpreted to be regionally elevated since the onset of the Neocomian rifting (Mohriak et al., 1995), thus representing an accommodation zone between the two developed rift basins. Along the entire Brazilian side of the Central Segment there is also evidence of transfer faults. In particular, within the Santos Basin, several NW–SE structural discontinuities have been interpreted as transfer faults which dissect the main gravity anomalies, and moreover are interpreted to be connected with the fossil rift transform faults (Meisling et al., 2001).

In the performed lithospheric-scale experiments, extensional basins and fault systems are separated by both soft and hard relay-ramps (Fig. 9a–e), thus suggesting a preference to develop accommodation zones in respect to strike-slip transfer zone. Similar accommodation zones have been recognised to develop in active natural continental rifts, such as the Tanganyika Lake axis of the East African Rift System. In this natural rift example the opposite dip direction asymmetric half-graben basins are separated by complex areas of fault interaction, which typically exhibit intra-rift structural highs (Morley et al., 1990; Nelson et al., 1992; Rosendahl et al., 1986). However, at a latest stage of the rift evolution these accommodation zones can be re-activated as transform fault zones, thus developing a characteristic strike-slip fault displacement separating areas at different amount of extension (Faulds and Varga, 1998). This is probably what is observed on the eastern edge of the Central Segment where several transfer zones are present within the Kwanza Basin. The major transfer fault that is evident along this margin is the Luanda transfer zone (Fig. 7a). This tectonic structure has been interpreted as a reactivation of a pre-existing basement structure during the Mesozoic rifting phase and probably acted as disjunction for the rift structures, allowing the portion of the margin located to its north and south to be extended with different amounts of extension. However apart from the Luanda transfer fault, the rift fault patterns offshore the Angolan margin, which generally trend parallel to the coastline, are only mildly dissected by these NE–SW to E–W trending strike-slip faults (Fig. 7a). This supports the presence of accommodation zones which are accommodating the rift extensional displacement between different systems. Eventually, it has been proposed that reactivation of pre-rift inherited structures (Corti, 2004; Morley et al., 2004; Younes and McClay, 2002) or syn-rift alterations in the mode of extension (Guiraud et al., 2010), can possibly originate accommodation or transfer zones.

5. Lithosphere-scale rifting

During each model experiment, laser-scanning of the top-surface has been performed at regular time intervals in order to monitor at the model surface evolution of the various fault segments and their eventual linkage, spanning from the initial stage of continental rift to the final breakup opening. Field data and seismic profiles from world-wide extensional systems have shown that both listric, low-angle normal faults and rotated planar fault blocks (domino-type faulting) are the two structural styles developed as the brittle upper crust is extended and thinned (Collettini and Barchi, 2002; Jackson and White, 1989; Schlische and Withjack, 2009). Moreover, the two different structural styles can co-exist in the same extensional system (Direen et al., 2011; Fossen, 2010; Pereira and Alves, 2011). The fault distribution, propagation and linkage and the interaction of these two types of faulting style result into different deformation patterns for the upper brittle crust. Moreover, the relationships between the two faulting styles can have a strong control on the basin architecture of extensional systems (Gawthorpe and Leeder, 2000).

5.1. Orthogonal vs oblique extension modes

In our experiments, the oblique-mode extensional models that were constructed with mantle inhomogeneities (Fig. 5c–d) are showing a broadly and diffuse “far-field” effect with oblique deformation of the upper crust and associated asymmetrical asthenospheric bulge. The upper crustal oblique deformation (Fig. 10a–e), although with possible minor edge effects, seems to be related to the extension mode-type and not to the discontinuity geometry within the mantle. In fact, as also shown by Sokoutis et al. (2007), when the oblique discontinuities are located within the mantle the upper crust fault-pattern is regularly oriented and is perpendicular to the main extension direction, ignoring the mantle discontinuity geometry. Concerning the weak upper mantle (WUM) geometry, this seems to affect only the deep asthenospheric

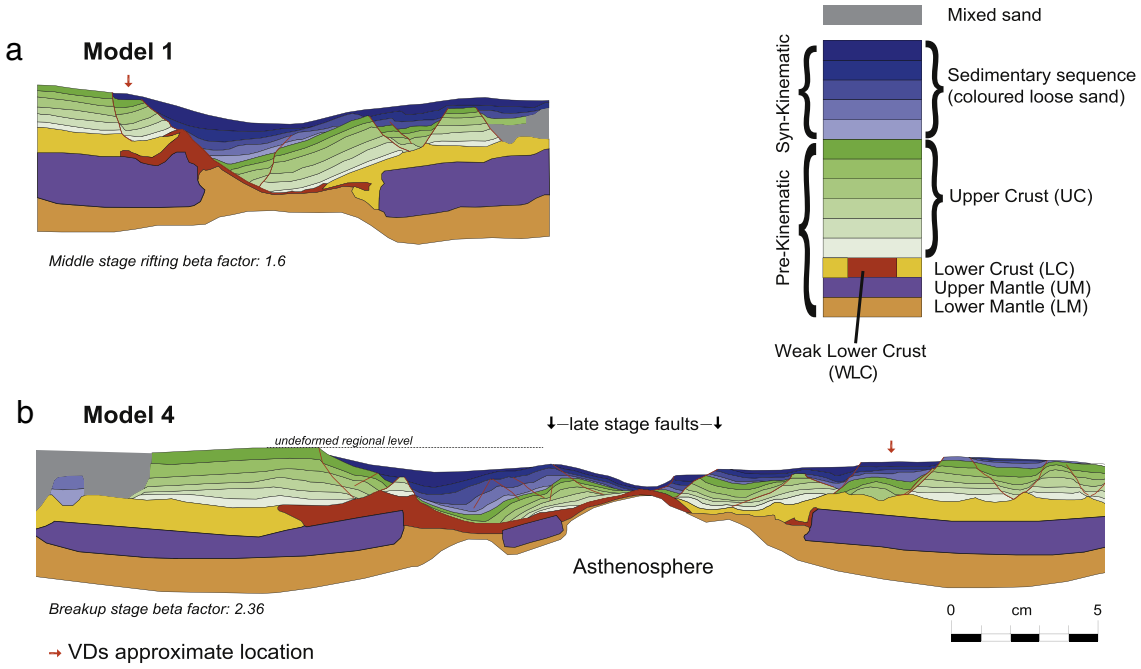

Fig. 8. Cross-sections at different amounts of extension crossing through the weak lower crust (WLC) of Model 1 and Model 4. (a) Intermediate stage rifting, β-stretching factor of 1.6, and (b) mature stage rifting, β-stretching factor of 2.36.

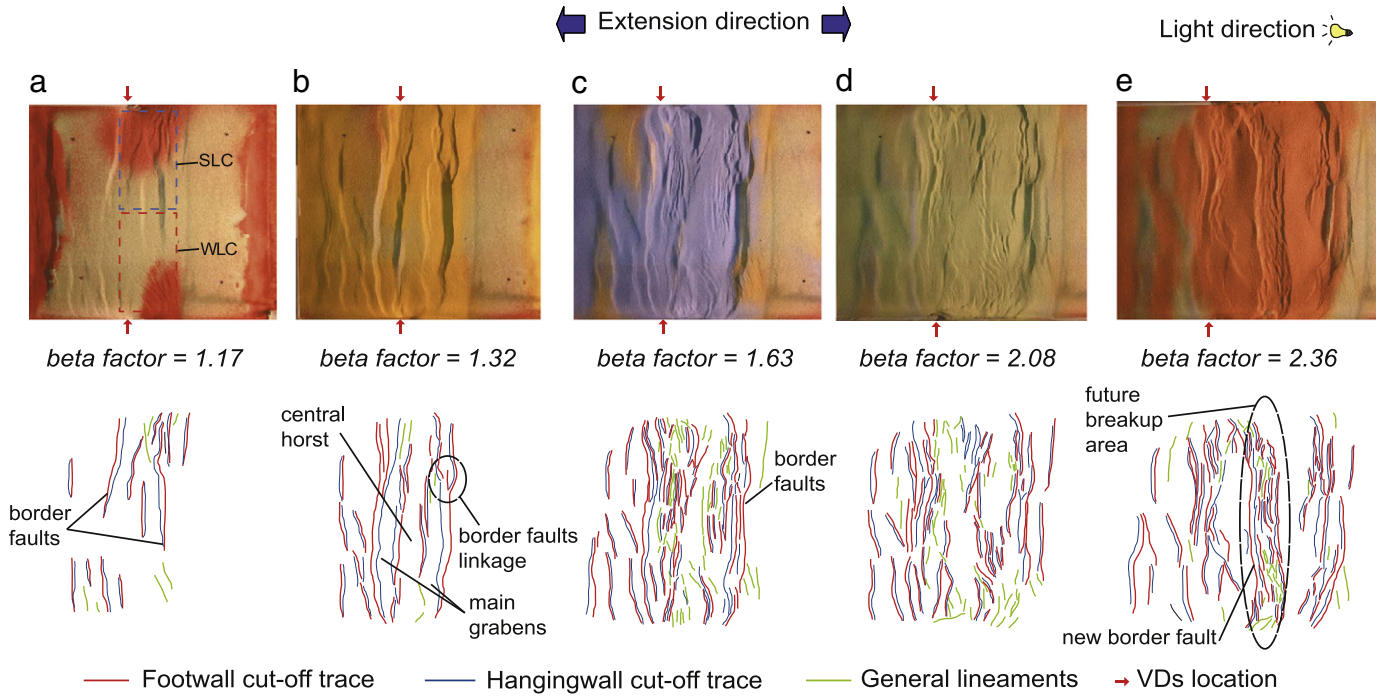

Fig. 9. Top-view photos at different amounts of extension (top panels) of the line-drawing faults of Model 4 taken during the syn-deformational loose sand deposition and their relative fault tracing (bottom panels). (a) β-Stretching factor of 1.17, (b) β-stretching factor of 1.32, (c) β-stretching factor of 1.32, (d) β-stretching factor of 2.08, and (e) β-stretching factor of 2.36. VD, velocity discontinuities.

levels, giving rise to an asymmetric asthenosphere bulge with a related asymmetric necking region. The oblique extension setup with mantle heterogeneities did not lead to breakup, demonstrating that mantle discontinuities are not effective enough to focus the rifting stresses, which are instead mainly dissipated by the ductile layers (e.g. Corti, 2012). On the contrary, the orthogonal-mode extensional models with lower crust inhomogeneities exhibit a well-focused upper crust deformation that appears to facilitate rifting which, eventually, results in the breakup of the central area (Figs. 5b and 9e). Concerning the upper crustal fault evolution, the orthogonal rift setup is mainly exhibiting faults that are parallel to the rift axis (Fig. 9a–e).

Generally, natural examples of orthogonal rifts are characterised by straight rift border-faults and intra-rift faulting that are perpendicular to the extension direction. On the contrary, several studies of oblique rifts show obliquity of the border-faults that result into en-echelon trending structures, sinuous deformed zones, and segmentation of both intra- and border-faults (Clifton and Kattenhorn, 2006; McClay and White, 1995). Nevertheless, along natural rifted margins and active continental rifting there is evidence of both orthogonal and oblique extension (e.g. mid-Atlantic Ridge: Dauteuil and Brun, 1993; East African Rift: Bosworth, 1985; Rosendahl, 1986; Red Sea: Bonatti, 1985). The transition between orthogonal and oblique extension modes often occurs where pre-existing crustal inhomogeneities create preferred ways for the rift to develop irrespective of extension direction (Morley et al., 2004; Smith and Mosley, 1993).

The modelled rifting evolution mimics well the observations from active natural continental rifts. In particular, a progressive rift evolution that could be subdivided in several stages, namely, early, mature and climax rift stages could reasonably be proposed (e.g. Autin et al., 2010; Dawers and Underhill, 2000; Prosser, 1993). In the discussion below we focus on the description of the upper crust structures that develop during these three main evolutionary stages. In particular, we concentrate on the influence of the lower crust rheology on the developing structures at every of the three different rift stages. The progressive upper crust evolution is depicted in the top-surface interpretations of Fig. 9a–e, where the orthogonal extension mode at different β-stretching factors is described.

5.2. Early-stage rift evolution

Early-stage extensional deformation (β-stretching factor up to 1.17) of the orthogonal lithospheric-scale model setup shows laterally distributed and separated border-faults that are dipping towards the central axis (Fig. 9a). Moreover, en-echelon-trending faults that are dipping towards the border-faults are present in the central rift (Fig. 9b, central part). The border-fault segments start to get aligned since the beginning of the deformation and they are linked laterally to adjacent synthetic-fault segments with a general orthogonal trend in respect to the extensional direction. A similar result has been shown by crustal-scale orthogonal extension analogue models (McClay et al., 2002). A change in the trend direction of both the hangingwall and the associated footwall cut-off traces is highlighting the points where the fault segments have been joined (Fig. 9a–e), mimicking the hard-linkage that also occurs in nature (e.g. Trudgill, 2002; Trudgill and Cartwright, 1994). In natural rifting examples, propagation of the initially separated border-faults gives rise to different rift geometries that are related to the rifting propagation (Withjack et al., 2002). In fact, it is recognised that rifts can initiate and propagate laterally from a restricted locus or by small, segmented and separated, extensional pockets that are simultaneously disseminated over the entire length of the rifting proto-axis (Morley, 1999b; Nelson et al., 1992; Schlische and Withjack, 2009). In the performed analogue models, the early-stage extensional rifting faults are initiated in correspondence to the hard lower crust rheology that is close to the lateral pulling walls and the faults propagate towards the centre of the models (Fig. 9a; SLC). In correspondence to the weaker lower crust, instead, only diffused fault segments are initially generated over the weak lower crust (WLC) area. In more detail, above the strong lower crust (SLC) more faults are present and they start to be rapidly organised and connected to each other, in contrast to the fewer and more isolated faults developing above the WLC area (Fig. 9a). This

difference in the brittle upper crust behaviour is probably related to the transmission of the extensional stresses over the lower and upper crust that, at the early-stage of rifting, is mainly absorbed by the softer WLC in respect to the SLC area. In the latter case, in fact, upper crustal faults form at lower extension values. Finally, the deformation width of the early-stage rifting model occupies only a narrow region (Fig. 9a). Similar to our results, previous analogue modelling experiments have earlier suggested that a narrow rift could be formed in a number of cases, including a lithospheric setup of high brittle/ductile layer ratio, a very strong brittle upper mantle (Corti et al., 2003a) or, eventually, in the presence of weak zones that exhibit a localised deformation over the brittle upper crust (Sokoutis et al., 2007).

5.3. Mature-stage rift evolution

Application of additional extension to the analogue models leads to structures interpreted to represent a mature-stage rift deformation at β-stretching factor values of 1.32 up to 1.63 (Fig. 9b and c). The two main border-faults which are dipping towards the central rift area are well developed at this rift stage. The curved plan-view geometry of the fault cut-offs provide evidence that the border-faults should be characterised by a listric detachment geometry at depth, soling out within the ductile crust. In the southern left side of the model and in correspondence to the weak lower crust (WLC) few, sparse and segmented faults are developed. Despite this minor deformation developing above the WLC, the main border-faults are well developed on both sides of the rift (Fig. 9b). Moreover, the rift master-fault located to the right part of the rift and above the WLC, represents higher values of displacement in the southern area in respect to the area of fringed-faults at the northern side and in correspondence to the strong lower crust (SLC). The left side master-fault, instead, represents higher values of displacement on the northern side that is progressively reduced on the southern part of the model (Fig. 9b). At a β-stretching factor of 1.63 (Fig. 9c), the increased and diffused deformation depicts a complex pattern of fault linkages. The right-side border-fault that developed above the WLC is still accommodating the majority of the displacement in the southern area. The few antithetic en-echelon trending faults, that were present since the early-stage rifting (Fig. 9a), are now bordering an elongate horst structure that occupies the central rift floor area (Fig. 9b and c). These faults show both hard- and soft-linkage relay-ramps and are accommodating the main displacement of the listric border-faults and their associated rollover anticline. The presence of such central horst is also observed on sections of earlier crustal-scale analogue modelling (Corti, 2012; Mart and Dauteuil, 2000; McClay et al., 2002).

5.4. Climax and incipient-breakup stage rift evolution

During the latest stage of extension (β-stretching factor of 2.08, Fig. 9d) even if a diffuse deformation affects the entire rifting area, faulting is mainly located close to the rift axis. It is considered that at β-stretching factors greater than 2.0 the rift extension is at its climax and eventually, if extension proceeds, breakup is then attained; for example, the model in Fig. 5b reached breakup at a β-stretching factor of 2.36 (Fig. 9e). Natural examples of active rifting climax are those where an incipient new oceanic crust is created within the rift axis, e.g. the Red Sea (Bonatti, 1985; Ligi et al., 2012) and the Ethiopian rifts (Corti, 2008). In these cases, a first phase of continental rifting that is governed by the development of the main boundary faults and only by minor diffuse volcanism is followed by faulting of the rift floor and focused magmatism close to breakup (Corti, 2008; Ebinger, 2005). The time-span of a continental rift and the time at which the rifting activity is shifting from the border faults (and associated structures) towards the central rift floor is highly variable (Ziegler and Cloetingh, 2004). In the performed lithospheric-scale models, it seems that the inward migration of the rifting activity occurs at a very late stage of deformation. This deformation took place through a narrow and rapid fault linkage, resulting to be very focused and effective in lithosphere thinning, and eventually led from the climax stage to breakup (Figs. 6b, 8b and 9e). Moreover, in Fig. 9e the rifting activity within the rift floor is bordered by a younger inner master-fault which extends between the two edges of the model and is located on the left side of the future margin. Natural rifts that are no longer active (i.e. aulacogen) apparently lack this latest stage of extension, that along the rift axis are showing only the presence of opposite dip direction asymmetric half-grabens (e.g. Luangwa Valley in Zambia, Banks et al., 1995; Withjack et al.,

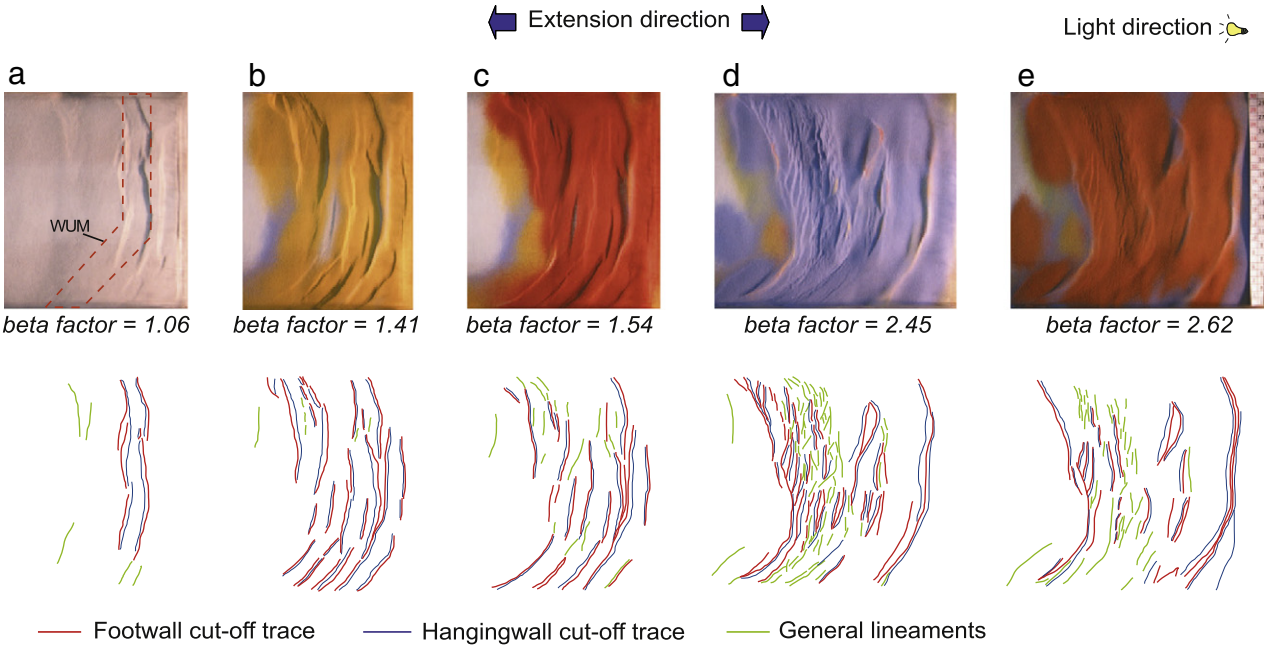

Fig. 10. Top-view photos at different amounts of extension (top panels) of the line-drawing faults of Model 5 taken during the syn-deformational loose sand deposition and their relative fault tracing (bottom panels). (a) β-Stretching factor of 1.06 with approximate location of the weak upper mantle (WUM), (b) β-stretching factor of 1.41, (c) β-stretching factor of 1.54, (d) β-stretching factor of 2.45, and (e) β-stretching factor of 2.62.

2002) or symmetric full-grabens (e.g. Euphrates Graben System, Litak et al., 1998) and associated master border-faults.

6. Basin architecture and evolution

6.1. Syn-rift faulted and unfaulted basin evolution

Analysis of model results highlights the presence of both faulted and unfaulted basins (Figs. 9a–e, 11 and 12). Since the experiments are performed at iso-thermal condition the resulting basins can be related to either faulting or isostatic re-equilibrium of the asthenosphere/lithosphere system. In the latter case, the development of late syn-rift unfaulted basins is observed (Fig. 11). On the contrary, the faulted basins result from the lithospheric stretching and can be considered to originate by tectonic-subsidence (Fig. 11b). The detailed interpretations of experiment model sections in Fig. 11a and b show that alteration of faulted and unfaulted basins is occurring during the rift time-span and, more important, that both of them can be spatially distributed along the entire margin. In particular, an early syn-rift tectonic-subsidence is mainly guiding the development of the initial basins that, at a latest stage, is followed by isostatic re-equilibrium of the lithosphere/asthenosphere system (Fig. 11b). Concerning the central rift floor area, it is mainly affected by late syn-rift faulted basins evolution (Figs. 9e, 11a and b). Considering examples of natural continental rifts it is important to notice that the time duration of each rift-related phase can be highly variable (Prosser, 1993). Moreover, it has been proposed that the main unfaulted syn-rift sequences are related to thermal subsidence and can be directly located on top of the early-rift tectonic basins, as indicated by the pure shear model, or they can be laterally shifted towards the future rift axis, as proposed by the simple shear model (e.g. Lentini et al., 2010). In addition, similar late syn-rift development of diachronous and laterally distributed, faulted (oceanward) and unfaulted (inward), basins along the rifted margins was also supported by numerical modelling (Huismans and Beaumont, 2008).

Fig. 11a shows that the late-stage subsidence seems to be focused within the area close to the continental margin, prior to breakup. In the same figure the unfaulted layers of the pre-breakup, late syn-rift, stage resemble what was described, during the rifting time-span evolution, to be a sag basin (Karner et al., 2003). Although the top-surface images of the models show that the late syn-rift fault activity, close to the inward margin, seems to be reduced in respect to the faults that develop on the central part of the rift (Fig. 9c and d), the presence of late syn-rift faults, within the entire rift-span, are active all over the entire rift area (Fig. 9e). The term “sag” was initially used to refer to slow-subsiding and unfaulted intra-cratonic or interior basins (cf. Einsele, 1992), but is recurrently used (“pre-salt sag” or “sag basin”) for the late syn-rift sedimentary sequence of the West African and Brazilian passive margins as no major seismically-resolvable faults, or only few faults, were generally recognised within these sequences (Aslanian et al., 2009; Huismans and Beaumont, 2008; Karner et al., 2003; Quirk et al., 2012; Unternehr et al., 2010). In general, a sag basin reflects a late syn-rift subsidence phase which results in unfaulted basin development just prior to breakup. Actually, evidence of late syn-rift faults affecting the Santos Basin pre-salt layers can be recognised in Figs. 2 and 3 and were also described by earlier studies (Davison, 2007; Karner and Gamboa, 2007). Therefore, a direct relationship between sag basins and absence of faults cannot be taken as the typical late-rift evolution. In fact, based on the analogue modelling results and seismic profiles (Fig. 7a–b), we prefer to use the term late syn-rift to indicate the pre-breakup sag basins within the developed syn-rift sequences.

6.2. Lower crust inhomogeneities and the development of syn-rift sequences

A detailed interpretation of syn-deformational sedimentary layers, which were deposited during model extension, can provide interesting details on both the fault development and thickness variations of the deposited sedimentary sequences. Fig. 11a shows the structures that develop at the upper crust above a weak lower crust, whereas Fig. 11b represents the upper crust structure above a hard lower crust at breakup stage. Sedimentary basins that develop on top of different lower crust (LC) rheology show a stratigraphic evolution, in terms of geometries and sediment thickness, which is strictly related to the specific location where they develop, in respect to the LC rheology. In fact, the lower crust rheology is significantly affecting the early-stage rift evolution, and the development of the resulting upper crust tectonic subsidence is directly related to the distribution of the rheology inhomogeneities along the rift. In particular, the weak lower crust promotes deep upper crustal sedimentary basins; and in the opposite sense, above the strong lower crust shallower syn-rift basins develop. Continental rifts represent well the influence of these two different subsidence drivers and in fact, they usually occur at several extensional pulses that are geometrically distinguishable within the syn-rift sediments as early-, middle- and late syn-rift pulses/stages (Driscoll et al., 1995; Karner and Driscoll, 1999; Ravnås et al., 2000).

In the presence of a weak lower crust (Fig. 11a), a full-scale sedimentary sequence that comprises early-, middle- and late syn-rift deposits is developed and the basin is showing faulted and wedge-shaped geometry. The early- to late-stage syn-rift sequence is thicker within the main basin and thinner on the outer margin basin where, however, a fairly good portion of late syn-rift is developed (Fig. 11a). On the other hand, above the stronger lower crust a similar full-scale syn-rift sedimentary sequence is deposited and the developed syn-rift sequences are thinner in comparison to the weak lower crust case (Fig. 11b). Moreover, the presence of several faults directly controls the resulting early- to middle-stage syn-rift sedimentary thicknesses at every individual fault-block. Similarly, the sequence developed at the outer margin is characterised by a good portion of late syn-rift strata (Fig. 11b). Late syn-rift stage sequences that developed on the outer margin are far away from the initial anomalous lower crust and, therefore, result in similar thicknesses for both types of lower crust rheologies (Fig. 11a–b). This means that within the performed experiments, apart from the outermost area close to the continent–ocean boundary (COB), the lateral sequence thickness variations along the margin are mainly due to variations in the tectonic subsidence that is experienced by the upper crust in relation to the lower crust rheology (Fig. 11a–b). This is obviously true in any case, natural or experimental rifting, where it is possible to demonstrate that the sedimentary input is able to keep pace with the specific tectonic/thermal subsidence rate.

In Figs. 2 and 3 the syn-rift sedimentary sequence of the Santos and Campos basins can be compared. The figures show a thicker syn-rift sequence in the Santos Basin as a result of greater accommodation space, originating from greater tectonic and thermal subsidence. Figs. 6b and 8b comprise the lithospheric-scale model sections in the simulated Santos and Campos basins and depict the final depth of the last-deposited sand layer in respect to the regional undeformed continental upper crust level at breakup stage. These figures represent well the effect of the lower crust rheology and its control on the upper crust subsidence at late syn-rift stage, showing the development of a regionally deeper basin on the Santos margin (Fig. 8b) in respect to the Campos margin (Fig. 6b). The different subsidence recorded in the two lithospheric-scale analogue model setups simulating the Brazilian margin counterparts, could in part explain the thicker salt sequence present within the Santos Basin in respect to the thinner salt sequence in the Campos Basin (Figs. 2 and 3; Quirk et al., 2012). In addition numerical models have reproduced anomalous late syn-rift subsidence developed during a late rifting stage or a major thermal subsidence phase just immediately after the breakup in the post-rift stage (Dupré, 2003; Dupré et al., 2007). The deposition of the salt layers on the South Atlantic margins is recognised to have occurred just prior to the breakup and in a very limited time-span of few million years (Garcia et al., 2012; Quirk et al., 2012;

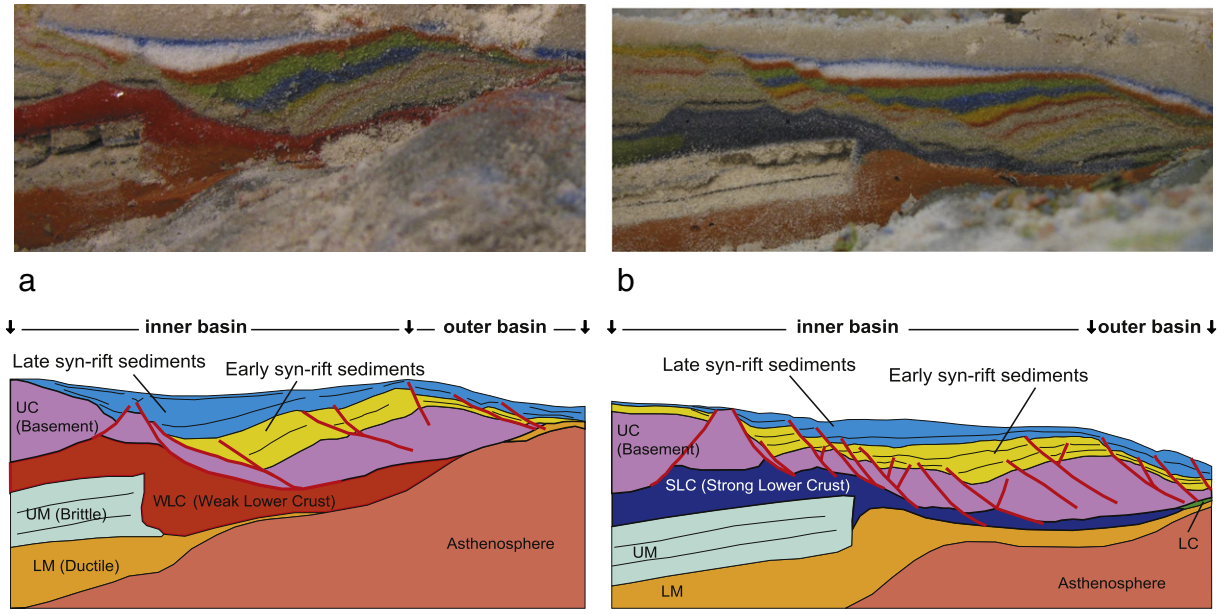

Fig. 11. Detailed interpretation of Model 4 (cf. Fig. 5) crossing through (a) a weak lower crust (WLC) within the ductile lower crust (LC), and (b) a strong lower crust (SLC) within the ductile lower crust (LC).

Torsvik et al., 2009). Thus, the thickness variations of the pre-breakup salt layers could be explained by a greater amount of subsidence experienced during the salt deposition within the Santos Basin, in respect to the Campos Basin, or by inherited differences in the depth of both basins that were present prior to the salt deposition (Figs. 2, 3, 6 and 8) or, most probably, by a combination of the two.

6.3. Along-margin basin architecture

In Fig. 12 we combine in a 3D view the top layer rendering of the lithospheric-scale model (Fig. 5b) with sections crossing the weak lower crust (WLC) and the strong lower crust (SLC) (Figs. 6b and 8b) at the breakup stage. In this way, we are able to relate the sedimentary

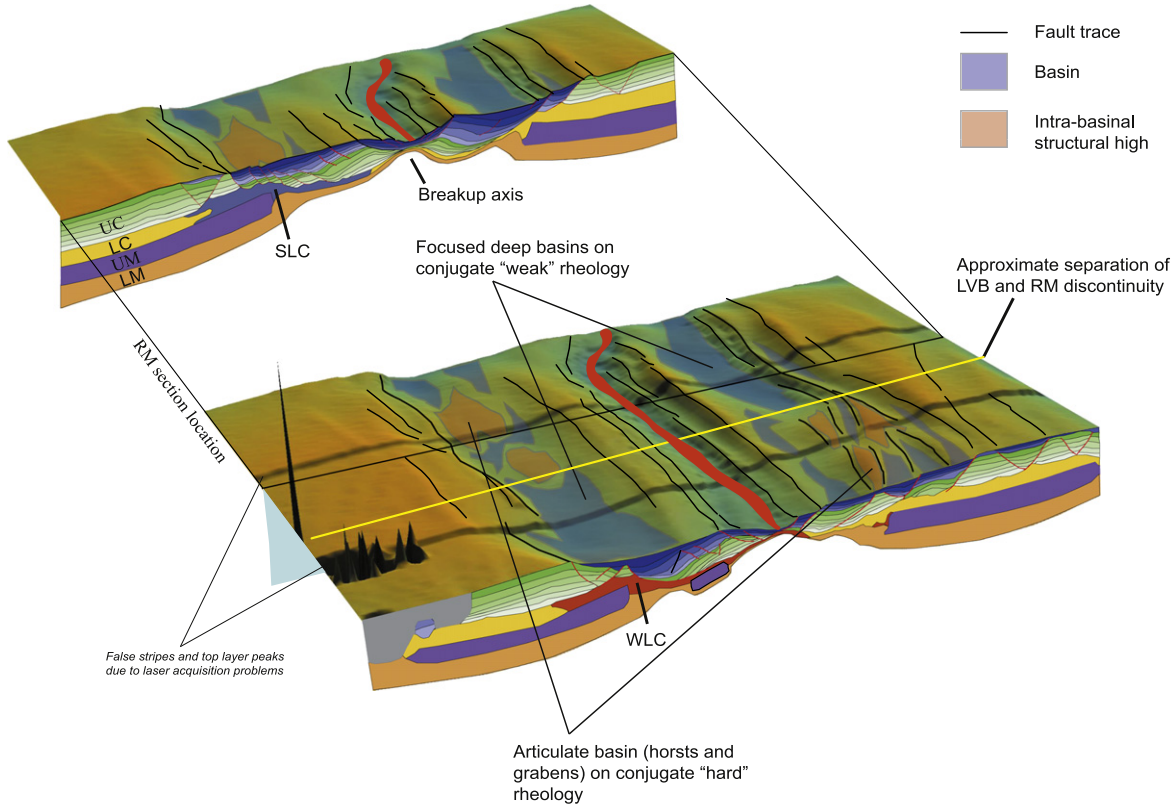

Fig. 12. 3D view of the acquired laser scanner data of the lithospheric-scale Model 4 (cf. Fig. 5) at breakup stage. The margin configuration shows intra-basins and related highs, highlighted with red and blue polygons, respectively. Fault traces are in black lines, while the yellow line indicates the approximate separation of the WLC (weak lower crust) and SLC (strong lower crust). Two interpreted sections crossing the WLC (front) and the SLC (rear) are also shown.

sequences deposited in the upper crust, with the structural architecture of the deeper lithospheric levels. The frontal section is located in correspondence to the weak lower crust (WLC) rheology, whereas the rear section is located in correspondence to the strong lower crust (SLC) rheology (Fig. 12). A decoupled early-stage deformation of the lower- and upper-crust, from the ductile- and brittle-mantle, occurs within the lithospheric model. In fact, the early extensional deformation of the deeper level is mainly guided by brittle mantle rupture (Figs. 6a and 8a). On the contrary in the upper crust, faulting is propagating in a lateral or in a diffused and separated extensional pattern, depending on whether faults develop on top of the hard or on top of the weak lower crust rheology (Fig. 9a). Application of additional extension to the lithospheric-scale model results in rupture of the brittle mantle and in the development and linkage of the main rift border-faults in the upper crust. More important, at this stage a main structural difference is taking place, which will persist through the entire rifting process. At this stage the conjugate margins are subdivided in different conjugate pairs which result in (Fig. 12): fringed fault patterns above the strong lower crust (SLC) and a main conjugate listric half-graben developing on the northern side; a listric half-graben developing on top of the weak lower crust (WLC); and a fault system of horsts and grabens developing on the opposite conjugate side of the southern model area.

Although the final phase of faulting is focused on the central rift floor, thus abandoning the inner part of the margins, the structural configuration depicted at the early stage of the rift is maintained until breakup. The crustal structure configuration of the conjugate margin pairs result in a sort of hard-to-soft and soft-to-hard architecture, thus influencing the basin evolution from the rift inception up to the ultimate central doming of the asthenosphere that will lead to the final thinning and breakup (Figs. 6b and 8b). The late syn-rift represents a renewed stage of rifting at the outer margin where new border-faults are generated. These new faults are observed both on cross-sections and on the upper crust top-layer, on photos and rendering of the laser-scanning of the lithospheric-scale model data (Fig. 9e), and in the seismic examples of the Angolan margin (Fig. 7) and in natural counterparts of active rifts (Corti, 2008). The resulting 3D tectono-stratigraphic development of the rifted margins, shows articulated basins with horsts and grabens on conjugate "hard" rheology and focused deeper basins on conjugate "weak" rheology (Fig. 12). Thus, the resulting extensional basins and their stratigraphy are affected both in subsidence and development.

7. Conjugate margin symmetry versus asymmetry

The performed lithospheric-scale analogue models provide abundant evidence that crustal inhomogeneities and discontinuities give rise to asymmetry of the rifted conjugate margins by coupling "hard-soft" or "soft-hard" rheology. Fig. 13 shows several sections of the orthogonal setup model that have been aligned along the breakup axis in order to have a comparison of the along-margin geometry of the conjugate pairs. As it was already indicated, only the first part of the modelled rifting process seems to be governed by the lower crust inhomogeneities (Fig. 13). Recent studies along the South Atlantic Central Segment support a polyphase rift margin evolution, including an early asymmetric thinning phase, characterised by detachment faulting and depth-dependent stretching, and a latest symmetric breakup phase (Blaich et al., 2011). Alternations in the conjugate margin configuration (symmetry versus asymmetry) along the performed analogue models are a common feature that appears to be related to the development of main detachments. In particular, the main detachments that developed at the early stage of the rifting demonstrate the exerting control of the lower crust inhomogeneities on the initial rift asymmetry (Figs. 6a and 8a).

It has been recognised that the later mature stage of the rift extension is focused in the central part of the rift floor, where an already thinned continental/transitional crust is present (e.g. Ethiopian rift, Corti, 2008). In nature, this later concentration of the extensional stresses within the central part of the rift could cause decompressional melting by the progressive Moho shallowing during the final phases of the rifting (e.g. Breivik et al., 2009; Nielsen and Hopper, 2004; Tsikalas et al., 2005). Eventually, an increase in the observed volcanic activity close to breakup time is believed to give rise to the abandonment of the detachment faults that can interrupt the extensional system and may also result in a failed mantle exhumation phase (Blaich et al., 2011). Since lithospheric-scale analogue modelling does not account for thermal changes during deformation, the effects of the temperature on the rheology of the lithosphere are not reproduced. Nevertheless, within the conducted models the shift and focus of the rifting strain towards the central area occurs once the initial lower crustal rheology differences are reduced enough, due to the thinning process, to become negligible for the lithosphere strength profile (Fig. 13). The final extension focus on the central rift area gives rise to oceanward rift basins, close to the COB, that are showing a general symmetry between the conjugate margin pairs.

The lithospheric-scale analogue models show that the initial rifting phase can be very asymmetric, but the evolution of the final oceanic outer basins is generally symmetric, resulting in well-defined outer basins close to the COB (Fig. 13). Such basins are well recognised in seismic sections on both the West African and Brazilian margins in the vicinity of the COB (Figs. 2, 3 and 7a, b). Moreover, these outer basins are showing a thin sedimentary sequence, in respect to the inner margin that initially was the locus of the rifting process. Some outer basins, such as those located at the outer part of the Kwanza Basin (Fig. 7a) and at the outer part of the transition of the Lower Congo to Kwanza basins (Fig. 7b), result to be highly faulted, thus reflecting a latest stage of tectonic activity which is developed at the outer margin prior to breakup. Geophysical and geological observations of rifted margin architectures were described during the last decades using conceptual, numerical or lithospheric-scale analogue modelling and a combination of two or more of them (e.g. Brun, 1999; Corti et al., 2003b; Huismans and Beaumont, 2008; Kusznir and Karner, 2007; Reston, 2007, 2009). Therefore, depending on the model adopted to explain the geophysical and the drilling information and observations, the resulting tectono-stratigraphic picture of the rifted margins can be extremely different (Fraser et al., 2007). In particular concerning the rifted margin geometry, the resulting conjugate rifted margin pairs can be generally characterised as: symmetric, if the pure shear model of McKenzie (1978) is applied; asymmetric, if the simple shear model of Wernicke (1981) is applied; combined symmetric or asymmetric if a combination of non-unique pure or simple shear models is eventually applied (Barbier et al., 1986; Lister et al., 1986).

Recent studies and proposed models account for polyphase evolution of the rifting process. These models have highlighted the possibility to have changes, from rift inception to breakup stage, spanning from: early asymmetry of the basins to a final symmetric conjugate pair character of the margins (Blaich et al., 2011); or, in the opposite sense, from symmetric basins to an asymmetric conjugate pair character of the margins (Huismans and Beaumont, 2008; Reston, 2009, 2010). Nevertheless, since natural rift systems include several thermal and mechanical processes, that in some cases can be very peculiar to a specific rift, it has been proposed that pre-existing structures can eventually interfere with the final locus of the rift breakup, giving rise to symmetry of the conjugate pairs (Direen et al., 2012). Concerning the geometry of the Central Segment of the South Atlantic, the existing extension models are not yet converging to a common idea of conjugate symmetry (Reston, 2009, 2010; Reston and Pérez-Gussinyé, 2007) or asymmetry (Blaich et al., 2011; Davison, 1997; Unternehr et al., 2010). The performed orthogonal lithospheric-scale analogue models (Fig. 5a–b) suggest a rift evolution that: (1) initiates by developing a main asymmetric character due to a main detachment developed on the weaker margin rheology, and (2) terminates with symmetric conjugate rift structures on the outer margin at breakup stage (Fig. 13).

8. Nature of the crust and heat-flow considerations

The lithospheric-scale modelling (Fig. 4b) provides interesting insights into the nature of the crust at magma-poor rifted margins. In fact, cross-sections of the models at the breakup stage show the presence of brittle upper mantle relicts along the rifted margins (Fig. 14). The presence of such relicts along the rifted margin may resemble what was interpreted to be a pre-rift or breakup-related high-velocity body along the deeper crustal part of the Angolan margin (e.g. Contrucci et al., 2004; Guiraud et al., 2010). In other areas such as the Norwegian margin, the presence of deeper high-velocity inhomogeneities observed along the margin was described to be of lower crust/upper mantle origin (Lundin and Doré, 2011; Reynisson et al., 2010; Tsikalas et al., 2008, 2012). Within the majority of the models the pristine brittle upper mantle was broken in pieces. These upper mantle pieces ended to be "trapped" in between the ductile lower mantle and the ductile lower crust during extension. Detailed analysis of the evolution of the lithospheric-scale model sections (Fig. 14) show that once the upper mantle pieces are breached they are passively floating during the entire rifting process without any evidence that they are subjected to internal deformation. Thus, the presence of a lower crustal detachment that allows decoupling of the brittle mantle from the upper crustal levels is inferred (Fig. 14). Furthermore, if the brittle mantle is breached during the lithospheric extension some pieces can eventually be exhumed through the same lower crustal detachment. Earlier lithospheric-scale analogue modelling studies, that have been conducted using similar lithospheric strength profiles, have attained comparable results (Autin et al., 2010; Brun and Beslier, 1996). The detached upper mantle bodies can potentially give rise to a ompletely different depleted magma in the case of future magmatism in the area. The depleted magma produced by these bodies can readily be mistaken as magma produced by a heterogeneous mantle source.

The cross-sections through the performed analogue models of Fig. 14 suggest that rift models which consider a brittle mantle should also take into consideration the possibility to have isolated exhumed upper mantle pieces. Furthermore, since there is strong evidence of mantle exhumation along magma-poor rifted margins (e.g. Iberia–Newfoundland margins, Lavier and Manatschal, 2006; Péron-Pinvidic et al., 2007; Reston, 2009; Reston et al., 2007; Sibuet et al., 2007) a similar process was also proposed for the outer area of the Angolan and the Brazilian margins (Unternehr et al., 2010; Zalán et al., 2011). It is generally considered that between the clearly recognisable continental crust and the clear oceanic crust the nature of the crust can be of different nature, possibly including: (1) a highly extended and intruded continental crust (Whitmarsh and Miles, 1995; Whitmarsh et al., 1996); (2) an oceanic crust derived by ultra-slow or slow seafloor spreading (Srivastava et al., 2000; Whitmarsh and Sawyer, 1996); and (3) exhumed mantle through continental rifting by shear tectonics (Lavier and Manatschal, 2006; Péron-Pinvidic et al., 2007; Reston, 2009; Reston et al., 2007; Sibuet et al., 2007). Concerning the magma-poor South Atlantic margins, the different type of crusts were described as: "proto-oceanic crust", defined as possible anomalous crust emplaced prior to normal oceanic crust formation (Mohriak and Rosendahl, 2003; Rosendahl et al., 2005); and "transitional domain crust", that

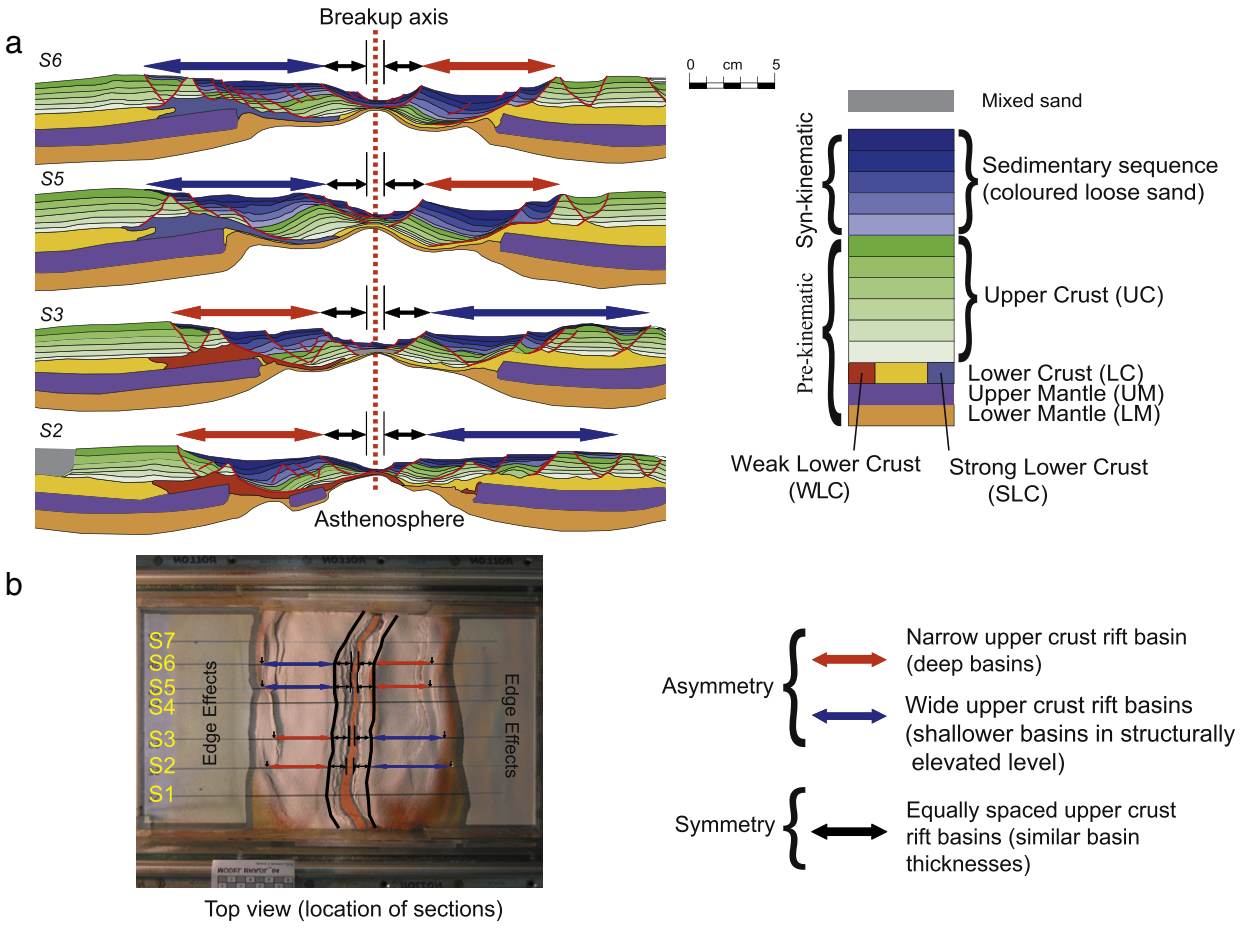

Fig. 13. (a) Serially sliced cross-sections of the orthogonal lithospheric-scale Model 4 (cf. Fig. 5) aligned along the breakup axis. The width of the conjugate pairs is represented with different coloured arrows; red for narrower margins and blue for wider margins, showing the early-stage rifting basin evolution. Black arrows, instead, represent the width of the late-stage rifted basin evolution at the incipient-breakup time. (b) Plane view of the lithospheric-scale Model 4 at breakup stage with section location and top interpretation of the margin width.

is described as the portion of the lithosphere which is located between the clearly identifiable stretched crystalline crust domain, and the first appearance of fully oceanic crust (Blaich et al., 2010).

The fact that so many different models have been proposed in order to better define the along-margin nature of the crust and its evolution, reflects that the answer is still ambiguous. In our experiments, in addition to the crustal attenuation, there are mechanical processes that affect the brittle mantle and result in a breached lithosphere (Fig. 14). However, beyond the mechanical implications, the presence of these brittle mantle relicts along the rifted margins may have a remarkable impact on the heat-flow affecting the upper crustal sedimentary basins. The upper crustal heat-flow input is directly influenced by the configuration of the underlying asthenosphere and lithosphere, therefore the resulting heat-flow can be strongly influenced from the different types of crust present along the margin. At an upper crust basin scale it has been recognised that a typical undepleted mantle shows by far less heat contribution in respect to the same amount of crystalline crust (Allen and Allen, 2005; Turcotte and Schubert, 2002). It is generally considered that the surface heat-flow represents the sum of the heat transferred from the asthenosphere to the lithosphere through conduction, and the heat produced by the radioactive decay of isotopes present within the crystalline crust (e.g. Allen and Allen, 2005; Turcotte and Schubert, 2002). Eventually, although the rifting processes of the lithosphere reduce the amount of heat-flow contribution deriving from a thinned radiogenic upper crust, rift basins usually exhibit a higher heat-flow in respect to other types of basins. Thus, the impact of a basal heat-flow at the base of the lithospheric mantle originating from a shallower asthenosphere seems to be the primary cause of a high heat-flow occurrence at rift margins that is effectively transferred to the sedimentary basins.

Even if the presence of brittle upper mantle relicts along extended rifted margins have no direct contribution to the heat-flow of the upper crustal basins, except for conduction, it may have two major indirect implications: (1) the possibility for a locally higher asthenospheric heat-flow input in regions where the brittle mantle could be absent as it is breached apart; and (2) reduction in the assumed heat-flow scenarios at the outer margin area if a semi-regional/local "isolation lid" represented by the upper mantle relicts exists. Since the brittle mantle pieces are sporadically distributed along the modelled margin sections (Figs. 12 and 14), there could be areas along the margin with locally lower, or higher, heat-flow depending whether the upper mantle is present or not. In this case, along-margin alterations in heat-flow could present a sharp transition from a locally low heat-flow area, above brittle mantle (BM) pieces, to high and atypical heat-flow in nearby areas where the BM can be absent (Fig. 14), and therefore without any direct relation to the radiogenic crystalline crust thickness. During extension in the analogue models the breached brittle mantle pieces are not affected by any late stage deformation (Figs. 12 and 14). However, as it has been already indicated for examples of natural rifted margins, pressure changes within the lithospheric mantle due to decompression can result in an important thermal component that can give rise to mantle melting (e.g. Tsikalas et al., 2005), thus resulting to important differences and deviations from the iso-thermal lithospheric-scale analogue rift models. Nevertheless, since in the current work we refer to magma-poor rifted margin these thermal aspect can be largely neglected.

9. Conclusions

An integrated analysis of lithospheric-scale analogue modelling and restored crustal transects is used to study the rifting evolution of the Central Segment of the South Atlantic. Although the study is focused on the Santos and Campos basins offshore Brazil, the resulting observations and considerations can be also extrapolated to the West African conjugate margins and to other magma-poor rifted margins worldwide. The applied analysis, combined with studies of natural examples, contribute to elucidate the effects that pre-existing lithospheric inhomogeneities have on the initiation, evolution and final architecture of rift-basins and rifted margins in terms of resulting structural style and subsidence. The study provides also insights on the along-margin segmentation, on the nature of the crust at the outer margin close to the continent–ocean boundary, and related heat-flow considerations at lithospheric-scale.

The lithospheric-scale analogue modelling has shown the important role exerted by the weak zones within the lithospheric-mantle/lower-crust on the resulting upper crust structural pattern during the rifting process. In particular, the analogue models suggest that weak zones located in the mantle have a "far-field" effect on the deformation of the brittle upper crust. Rheology heterogeneities located within the lower crust, such as a weak lower crust (WLC) and a strong lower crust (SLC) used in the experiments, have more localising effects and can have a remarkable impact on the along-margin segmentation, promoting different structural evolution in relation to their rheology. The final tectono-stratigraphic expression of the rifted margins shows articulated basins with horsts and grabens in response to a relative "hard" rheology (SLC), and focused and deeper basins related to a relatively "weak" rheology (WLC) on the equivalent parts of the conjugate pairs. The resulting extensional basins, located close or above the lithospheric rheology discontinuities, and their stratigraphic component are affected both in subsidence and development.

Interpretation of the model cross-sections provides details on the fault and the sedimentary sequence evolution, highlighting that the development of the upper crustal depocentres is a function of the lower crust rheological inhomogeneities. Lateral sequence thickness variations along the margin are mainly attributed to variations in subsidence, tectonic or thermal, that is experienced by the upper crust in relation to the lower crust rheology. A weak lower crust rheology, such as the WLC, promotes a main deep listric half-graben fault and associated wedge-shaped basin with thick syn-rift sequences. A strong lower crust rheology, represented by the (SLC), gives rise to more planar, rotated, domino-type faulted basins, with thinner sequences directly controlled by the individual fault-blocks. On the outer margin far away from the initial crust rheology inhomogeneities, the resulting late syn-rift sequences have comparable thicknesses in both the weak and the hard lower crust rheology cases.

Along-margin alterations in symmetry versus asymmetry of the width and structural architecture are common features that occur in several models and seem to be related to the main detachment (i.e. crust rheology dependant), affecting the rifting geometry. Pre-existing lithospheric inhomogeneities drive the early stage of the rifting evolution which results to be dominated by asymmetric rift-basin development. At the later stage of the rift, the differences in initial lower crustal rheology are reduced due to the thinning processes, and an additional pulse of extension focuses the deformation on the central rift area giving rise to general symmetric oceanward rift basins. Furthermore, the experiments show that during the rifting process pieces of brittle mantle are preserved and can be elevated beneath the developed upper crustal structures. The presence of these brittle upper mantle relicts along extended rifted margins may reduce the assumed internal heat-flow production at the distal/outer margin parts as they contribute less radiogenic heat production than a misinterpreted equivalent portion of crystalline crust and could act as "isolation lids", reducing the asthenospheric heat transfer at shallower levels. Finally, concerning regional exploration the detailed tectono-stratigraphic outcomes of the performed lithosperic-scale experiments at basin-scale can provide valuable insights and hints of the deep pre-salt play in the Central Segment of South Atlantic.

Acknowledgements

We thank ION for providing permission to publish the MCS examples used in this study. We acknowledge the contribution of P. Andreotti

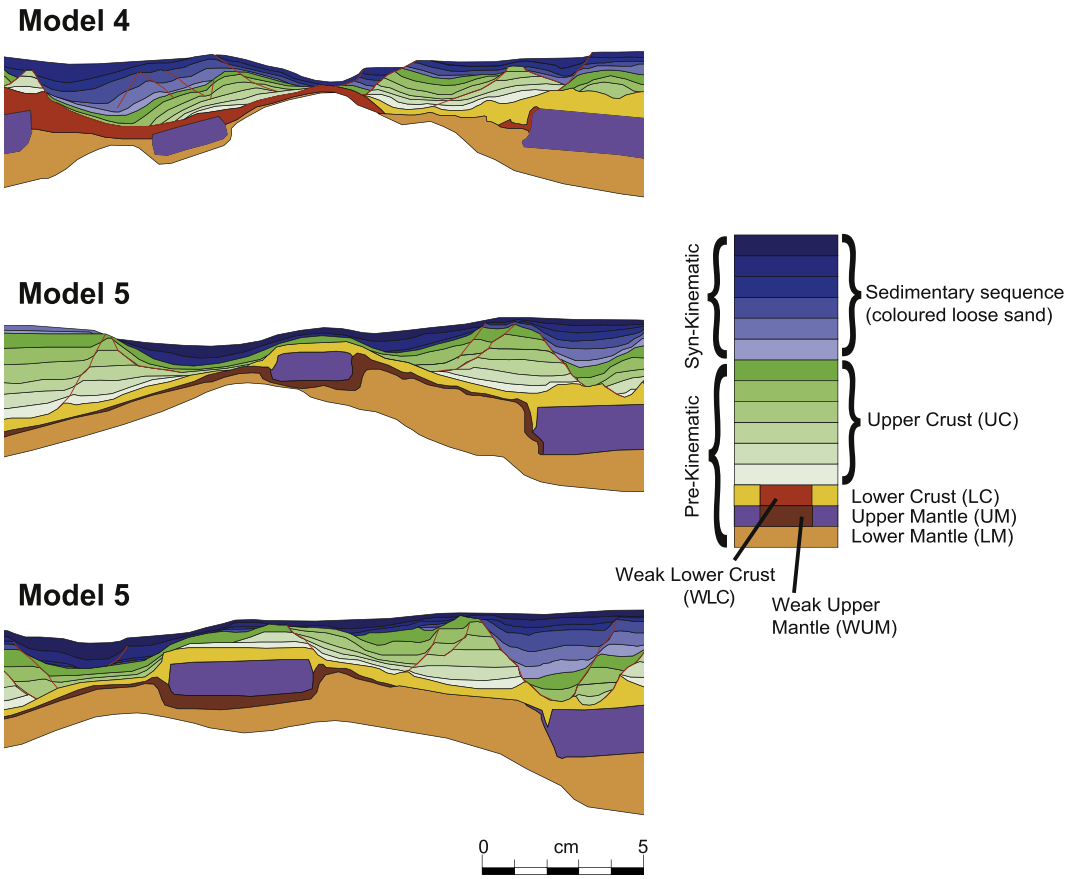

Fig. 14. Interpreted lithospheric-scale cross-sections showing the presence of brittle upper mantle (UM) pieces along the rifted margins. Model numbers refer to Fig. 5.

(Eni E&P) in the preparation of Fig. 7, and we want to thank F. Storti for his comments on the manuscript. We also thank the two reviewers, G. Corti and C. Gorini, as well as Editor L. Jolivet for their constructive comments and improvements to the manuscript. The authors want to thank Eni E&P for giving permission to publish the study.

References

Afonso, J., Ranalli, G., 2004. Crustal and mantle strengths in continental lithosphere: is the jelly sandwich model obsolete? Tectonophysics 394, 221–232. http://dx.doi.org/10.1016/j.tecto.2004.08.006.

Agostini, A., Corti, G., Zeoli, A., Mulugeta, G., 2009. Evolution, pattern and partitioning of deformation during oblique continental rifting: inferences from lithospheric-scale centrifuge models. Geochem. Geophys. Geosyst. 10, Q11015. http://dx.doi.org/10.1029/2009GC002676.

Alkmim, F.F.d, 2004. O que faz de um Cráton um Cráton? O Cráton do São Francisco e as revelações Almeidianas ao delimitá-lo. In: Neto, V.M., Bartorelli, A., Carneiro, C.D.R., Neves, B.B.d.B. (Eds.), Geologia do Continente Sul-Americano: Evolucão da Obra de Fernando Flávio Marques de Almeida. Becca, São Paulo, Brazil, pp. 17–35.

Alkmim, F.F., Marshak, S., Pedrosa-Soares, A.C., Peres, G.G., Cruz, S.C.P., Whittington, A., 2006. Kinematic evolution of the Araçuaí–West Congo orogen in Brazil and Africa: nutcracker tectonics during the Neoproterozoic assembly of Gondwana. Precambrian Res. 149 (1–2), 43–64. http://dx.doi.org/10.1016/j.precamres.2006.06.007.

Allen, P.A., Allen, J.R., 2005. Basin Analysis: Principles and Applications2nd ed. Wiley-Blackwell, Hoboken, New Jersey.

Almeida, F.F.M., 1977. O Cráton do São Francisco. Rev. Bras. Geosci. 7, 349–364.

Almeida, F.F.M., 1981. O Cráton do Paramirim e suas relações com do São Francisco. Anais Simp.Craton São Francisco e Faixas Marginais, Salvador 1–10.

Aslanian, D., Moulin, M., Olivet, J.L., Unternehr, P., Bache, F., Contrucci, I., Klingelheofer, F., Labails, C., Matias, L., Nouzé, H., Rabineau, M., 2009. Brazilian and African passive margins of the Central Segment of the South Atlantic Ocean: kinematic constraints. Tectonophysics 468, 98–112. http://dx.doi.org/10.1016/j.tecto.2008.12.016.

Autin, J., Bellahsen, N., Husson, L., Beslier, M.O., Leroy, S., d'Acremont, E., 2010. Analogue models of oblique rifting in a cold lithosphere. Tectonics 29, TC6016. http://dx.doi.org/10.1029/2010TC002671.

Banks, N.L., Bardwell, K.A., Musiwa, S., 1995. Karoo Rift basins of the Luangwa Valley, Zambia. Geol. Soc. Lond. Spec. Publ. 80 (1), 285–295. http://dx.doi.org/10.1144/GSL.SP.1995.080.01.13.

Barbier, F., Duverge, J., Xavier, L.P., 1986. Structure profonde de la marge Nord-Gascogne; implications sur le mecanisme de rifting et de formation de la marge continentale. Bull. Centres Rech. Explor.-Prod. Elf-Aquitaine 10, 105–121.

Benes, V., Davy, P., 1996. Modes of continental lithospheric extension: experimental verification of strain localization processes. Tectonophysics 254, 69–87.

Blaich, O.A., Tsikalas, F., Faleide, J.I., 2008. Northeastern Brazilian margin: regional tectonic evolution based on integrated analysis of seismic reflection and potential field data and modelling. Tectonophysics 458, 51–67. http://dx.doi.org/10.1016/j.tecto.2008.07.016.

Blaich, O.A., Faleide, J.I., Tsikalas, F., Franke, D., León, E., 2009. Crustal-scale architecture and segmentation of the Argentine margin and its conjugate off South Africa. Geophys. J. Int. 178, 85–105. http://dx.doi.org/10.1111/j.1365-246X. 2009.04171.x.

Blaich, O.A., Faleide, J.I., Tsikalas, F., Lilletveit, R., Chiossi, D., Brockbank, P., Cobbold, P., 1–17, 2010. Structural architecture and nature of the continent–ocean transitional domain at the Camamu and Almada Basins (northeastern Brazil) within a conjugate margin setting. In: Vining, B.A., Pickering, S.C. (Eds.), Petroleum Geology: From Mature Basins to New Frontiers—Proceedings of the 7th Conference. Geological Society, London, pp. 1–17. http://dx.doi.org/10.1144/070000.

Blaich, O.A., Faleide, J.I., Tsikalas, F., 2011. Crustal breakup and continent–ocean transition at South Atlantic conjugate margins. J. Geophys. Res. 116, 38. http://dx.doi.org/10.1029/2010JB007686.

Boillot, G., Recq, M., Winterer, E.L., 1987. Tectonic denudation of the upper mantle along a passive margin: a model based on drilling results (Ocean Drilling Program Leg 103, Western Galicia Margin, Spain). Tectonophysics 132, 335–342.

Bonatti, E., 1985. Punctiform initiation of seafloor spreading in the Red Sea during transition from a continental to an oceanic rift. Nature 316, 33–37.

Bonini, M., Sokoutis, D., Mulugeta, G., Boccaletti, M., Corti, G., Innocenti, F., Manetti, P., Mazzarini, F., 2001. Dynamics of magma emplacement in centrifuge models of continental extension with implications for flank volcanism. Tectonics 20, 1053–1065.

Bonini, M., Corti, G., Del Ventisette, C., Manetti, P., Mulugeta, G., Sokoutis, D., 2007. Modelling the lithospheric rheology control on the Cretaceous rifting in West Antarctica. Terra Nova 19, 360–366.

Bosworth, W., 1985. Geometry of propagating continental rifts. Nature 316, 625–627.

Breivik, A.J., Faleide, J.I., Mjelde, R., Flueh, E.R., 2009. Magma productivity and early seafloor spreading rate correlation on the northern Vøring Margin, Norway — constraints on mantle melting. Tectonophysics 468, 206–223.

Brun, J.P., 1999. Narrow rifts versus wide rifts: inferences for the mechanics of rifting from laboratory experiments. Philos. Trans. R. Soc. Lond. A 357, 695–712.

Brun, J.P., 2002. Deformation of the continental lithosphere: insights from brittle–ductile models. In: De Meer, S., Drury, S.R., De Bresser, J.H.P., Pennock, G.M. (Eds.),

Deformation Mechanism, Rheology and Tectonics: Current Status and Future Perspectives. Geological Society, London, Special Publications, 200, pp. 355–370.
Brun, J.P., Beslier, M.O., 1996. Mantle exhumation at passive margins. Earth Planet. Sci. Lett. 142, 161–173.
Callot, J.P., Geoffroy, L., Brun, J.P., 2002. Development of volcanic passive margins: three-dimensional laboratory models. Tectonics 21 (6), 2–13. http://dx.doi.org/10.1029/2001TC901019.
Campanha, G.A.C., 1981. O lineamento de Além-Paraíba na área de Três Rios (RJ). Rev. Bras. Geosci. 11, 159–171.
Campanha, G.A.C., de Brito Neves, B.B., 2004. Frontal and oblique tectonics in the Brazilian Shield. Episodes 27 (4), 255–259.
Carminatti, M., Wolff, B., Gamboa, L., 2008. New exploratory frontiers in Brazil. World Petroleum Congress, 19. Madrid, Spain, WPC Proceedings (11 f).
Clifton, A.E., Kattenhorn, S.A., 2006. Structural architecture of a highly oblique divergent plate boundary segment. Tectonophysics 419 (1–4), 27–40. http://dx.doi.org/10.1016/j.tecto.2006.03.016.
Close, D.I., Watts, A.B., Stagg, H.M.J., 2009. A marine geophysical study of the Wilkes Land rifted continental margin, Antarctica. Geophys. J. Int. 177, 430–450. http://dx.doi.org/10.1111/j.1365-246X.2008.04066.x.
Cobbold, P.R., Meisling, K.E., Mount, V.S., 2001. Reactivation of an obliquely rifted margin, Campos southeastern Brazil. AAPG Bull. 85 (11), 1925–1944.
Collettini, C., Barchi, M.R., 2002. A low-angle normal fault in the Umbria region (Central Italy): a mechanical model for the related microseismicity. Tectonophysics 359, 97–115.
Contreras, J., Zühlke, R., Bowman, S., Bechstädt, T., 2010. Seismic stratigraphy and subsidence analysis of the southern Brazilian margin (Campos, Santos and Pelotas basins). Mar. Pet. Geol. 27 (9), 1952–1980. http://dx.doi.org/10.1016/j.marpetgeo.2010.06.007.
Contrucci, I., Matias, L., Moulin, M., Géli, L., Klingelhofer, F., Nouzé, H., Aslanian, D., Olivet, J.L., Réhault, J.P., Sibuet, J.C., 2004. Deep structure of the West African continental margin (Congo, Zäire, Angola), between 50S and 80S, from reflection/refraction seismics and gravity data. Geophys. J. Int. 158, 529–553. http://dx.doi.org/10.1111/j.1365-246X.2004.02303.x.
Corti, G., 2004. Centrifuge modelling of the influence of crustal fabrics on the development of transfer zones: insights into the mechanics of continental rifting architecture. Tectonophysics 384 (1–4), 191–208. http://dx.doi.org/10.1016/j.tecto.2004.03.014.
Corti, G., 2008. Control of rift obliquity on the evolution and segmentation of the main Ethiopian rift. Nat. Geosci. 1 (4), 258–262. http://dx.doi.org/10.1038/ngeo160.
Corti, G., 2012. Evolution and characteristics of continental rifting: analog modeling-inspired view and comparison with examples from the East African Rift System. Tectonophysics 522–523, 1–33. http://dx.doi.org/10.1016/j.tecto.2011.06.010.
Corti, G., Bonini, M., Innocenti, F., Manetti, P., Mulugeta, G., 2001. Centrifuge models simulating magma emplacement during oblique rifting. J. Geodyn. 31 (5), 557–576. http://dx.doi.org/10.1016/S0264-3707(01)00032-1.
Corti, G., Bonini, M., Conticelli, S., Innocenti, F., Manetti, P., Sokoutis, D., 2003a. Analogue modelling of continental extension: a review focused on the relations between the patterns of deformation and the presence of magma. Earth-Sci. Rev. 63 (3–4), 169–247.
Corti, G., Jolante, V.W., Bonini, M., Sokoutis, D., Cloetingh, S., Innocenti, F., Manetti, P., 2003b. Transition from continental break-up to punctiform seafloor spreading: how fast, symmetric and magmatic. Geophys. Res. Lett. 30 (12), 1–4. http://dx.doi.org/10.1029/2003GL017374.
Corti, G., Ranalli, G., Mulugeta, G., Agostini, A., Sani, F., Zugu, A., 2010. Control of the rheological structure of the lithosphere on the inward migration of tectonic activity during continental rifting. Tectonophysics 490, 165–172.
Corti, G., Calignano, E., Petit, C., Sani, F., 2011. Controls of lithospheric structure and plate kinematics on rift architecture and evolution: an experimental modelling of the Baikal Rift. Tectonics 30, TC3011. http://dx.doi.org/10.1029/2011TC002871.
Cunningham, D., Alkmim, F.F., Marshak, S., 1998. A structural transect across the coastal mobile belt in the Brazilian Highlands (latitude 20°S): the roots of a Precambrian transpressional orogen. Precambrian Res. 92, 251–275.
Dauteuil, O., Brun, J.P., 1993. Oblique rifting in a low spreading ridge. Nature 361, 145–148.
Davison, I., 1997. Wide and narrow margins of the Brazilian South Atlantic. J. Geol. Soc. Lond. 154, 471–476.
Davison, I., 2007. Geology and tectonics of the South Atlantic Brazilian salt basins. In: Ries, A.C., Butler, R.W.H., Graham, R.H. (Eds.), Deformation of the Continental Crust: The legacy of Mike Coward. Geological Society, London, Special Publications, 272, pp. 345–359.
Davy, P., Cobbold, P.R., 1991. Experiments on the shortening of a 4-layer continental lithosphere. Tectonophysics 188, 1–25.
Dawers, N.H., Underhill, J.R., 2000. The role of fault interaction and linkage in controlling synrift stratigraphic sequences: Late Jurassic, Statfjord East area, northern North Sea. AAPG Bull. 84 (1), 45–64.
De Paula, O.B., Vidotti, R.M., 2001. Estimativa da Descontinuidade de Mohorovicic a partir de dados gravimétricos — Costa Leste Brasileira. VII Cong. Int. Soc. Bras. Geof., Salvador, BA. Exp. Abs., SBGf, pp. 756–758.
de Wit, M.J., de Brito Neves, B.B., Trouw, R.A.J., Pankhurst, R.J., 2008. Pre-Cenozoic correlations across the South Atlantic region: (the ties that bind). Geol. Soc. Lond. Spec. Publ. 294 (1), 1–8. http://dx.doi.org/10.1144/SP294.1.
Demercian, L.S., 1996. A halocinese na evolucão do Sul da Bacia de Santos do Aptiano ao Cretáceo Superior. (M. Sc thesis) Universidade Federal do Rio Grande do Sul, Porto Alegre, Brazil.
Direen, N.G., Borissova, I., Stagg, H.M.J., Colwell, J.B., Symonds, P.A., 2007. Nature of the continent–ocean transition zone along the southern Australian continental margin: a comparison of the Naturaliste Plateau, SW Australia, and the central Great Australian Bight sectors. In: Karner, G.D., Manatschal, G., Pinheiro, L.M. (Eds.), Imaging, Mapping and Modelling Continental Lithosphere Extension and Breakup. Geological Society, London, Special Publications, 282, pp. 235–261.
Direen, N.G., Stagg, H.M.J., Symonds, P.A., Colwell, J.B., 2011. Dominant symmetry of a conjugate southern Australian and East Antarctic magma-poor rifted margin segment. Geochem. Geophys. Geosyst. 12 (2), 1–29. http://dx.doi.org/10.1029/2010GC003306.
Direen, N.G., Stagg, H.M.J., Symonds, P.A., Norton, I.O., 2012. Variations in rift symmetry: cautionary examples from the Southern Rift System (Australia–Antarctica). Geol. Soc. Lond. Spec. Publ. 369. http://dx.doi.org/10.1144/SP369.4.
Driscoll, N.W., Hogg, J.R., Christie, N., Karner, G.D., 1995. Extensional tectonics in the Jeanne d'Arc Basin, offshore Newfoundland: implications for the timing of break-up between Grand Banks and Iberia. In: Scrutton, R.A., Stoker, M.A., Shimmield, G.B., Tudhope, A.W. (Eds.), The Tectonics, Sedimentation and Palaeoceanography of the North Atlantic Region. Geological Society, London, Special Publications, 90, pp. 1–28.
Dupré, S., 2003. Integrated tectonic study of the South Gabon Margin. Insights on the rifting style from seismic, well and gravity data analysis and numerical modelling. Netherlands Research School of Sedimentary Geology Thesis.Vrije Universiteit, Amsterdam90-9017055-3 (125 pp.).
Dupré, S., Bertotti, G., Cloetingh, S., 2007. Tectonic history along the South Gabon Basin: anomalous early post-rift subsidence. Mar. Pet. Geol. 24 (3), 151–172. http://dx.doi.org/10.1016/j.marpetgeo.2006.11.003.
Ebinger, C.J., 1989. Tectonic development of the western branch of the East African rift system. Geol. Soc. Am. Bull. 7. http://dx.doi.org/10.1130/0016-7606(1989)1010885.
Ebinger, C., 2005. Continental breakup: the East African perspective. Astron. Geophys. 46, 16–21.
Ebinger, C.J., Deino, A.L., Drake, R.E., Tesha, A.L., 1989. Chronology of volcanism and rift basin propagation: Rungwe Volcanic Province, East Africa. J. Geophys. Res. 94 (785–15,803).
Einsele, G., 1992. Sedimentary Basins Evolution, Facies, and Sediment Budget.Springer-Verlag, New York.
Fadaie, K., Ranalli, G., 1990. Rheology of the lithosphere in the East African Rift System. Geophys. J. Int. 102 (2), 445–453. http://dx.doi.org/10.1111/j.1365-246X.1990.tb04476.x.
Faulds, J.E., Varga, R.J., 1998. The role of accommodation zones and transfer zones in the regional segmentation of extended terranes. In: Faulds, J.E., Stewart, J.H. (Eds.), Accommodation Zones and Transfer Zones: The Regional Segmentation of the Basin and Range Province. Geological Society of America Special Paper, 323, pp. 1–45.
Fletcher, R.J., 2009. Mechanisms of Continental Lithosphere Thinning and Rifted Margin Formation. (PhD thesis) University of Liverpool.
Fossen, H., 2010. Structural GeologyFirst ed. Cambridge University Press978-0-521-51664-8.
Fraser, S.I., Fraser, A.J., Lentini, M.R., Gawthorpe, R.L., 2007. Return to rifts — the next wave: fresh insights into the petroleum geology of global rift basins. Pet. Geosci. 13, 99–104.
Garcia, S.F.D.M., Letouzey, J., Rudkiewicz, J.L., Danderfer Filho, A., Frizon de Lamotte, D., 2012. Structural modelling based on sequential restoration of gravitational salt deformation in the Santos Basin (Brazil). Mar. Pet. Geol. 35 (1), 337–353. http://dx.doi.org/10.1016/j.marpetgeo.2012.02.009.
Gawthorpe, R.L., Leeder, M.R., 2000. Tectono-sedimentary evolution of active extensional basins. Basin Res. 12 (3–4), 195–218. http://dx.doi.org/10.1046/j.1365-2117.2000.00121.x.
Gibbs, A.D., 1983. Balanced section construction from seismic sections in areas of extensional tectonics. J. Struct. Geol. 5, 153–160.
Gladczenko, T.P., Skogseid, J., Eldholm, O., 1998. Namibia volcanic margin. Mar. Geophys. Res. 20, 313–341. http://dx.doi.org/10.1023/A:1004746101320.
Gomes, P.O., Parry, J., Martins, W., 2002. The outer high of the Santos Basin, southern São Paulo Plateau, Brazil: Tectonic setting, relation to volcanic events and some comments on hydrocarbon potential. AAPG, Hedberg Conference "Hydrocarbon Habitat of Volcanic Rifted Passive Margins". Search and Discovery, 90022.
Gomes, P.O., Kilsdonk, B., Minken, J., Grow, T., Barragan, R., 2009. The outer high of the Santos Basin, southern São Paulo Plateau, Brazil: pre-salt exploration outbreak, paleogeographic setting, and evolution of the syn-rift structures (Search and Discovery, 10193).
Gray, D.R., Foster, D.A., Meert, J.G., Goscombe, B.D., Armstrong, R., Trouw, R.a.J, Passchier, C.W., 2008. A Damara orogen perspective on the assembly of southwestern Gondwana. Geol. Soc. Lond. Spec. Publ. 294 (1), 257–278. http://dx.doi.org/10.1144/SP294.14.
Groshong, R., 2006. Structural validation, restoration and prediction. 3-D Structural Geology: A Practical Guide to Quantitative Surface and Subsurface Map Interpretation.Birkhäuser 305–372. http://dx.doi.org/10.1007/3-540-31055-X_11.
Guiraud, M., Buta-Neto, A., Quesne, D., 2010. Segmentation and differential post-rift uplift at the Angola margin as recorded by the transform-rifted Benguela and oblique-to-orthogonal-rifted Kwanza basins. Mar. Pet. Geol. 27 (5), 1040–1068. http://dx.doi.org/10.1016/j.marpetgeo.2010.01.017.
Haralyi, N.L.E., Hasui, Y., 1982. The gravimetric information and the Archean–Proterozoic structural framework of eastern Brazil. In: ISAP, Salvador, R. (Eds.), Brasileira Geocie Paulo, 12, Nos. 1–3, pp. 160–166.
Heilbron, M., Pedrosa-Soares, A., Neto, M.D., Da Silva, L., Trouw, R., Janasi, V., 2004. Brasiliano orogens in Southeast and South Brazil. In: Weinberg, R., Trouw, R., Fuck, R., Hackspacher, P. (Eds.), The 750–550 Ma Brasiliano Event of South America. Journal of the Virtual Explorer, 17 (Paper 4).
Heilbronl, M., Mohriak, U., Valerianol, M., Milani, J., Almeida, J., Tupinambfil, M., 2000. From collision to extension: the roots of southeastern continental margin of Brazil. In: Mohriak, W., Talwani, M. (Eds.), Atlantic Rifts and Continental Margins, AGU, vol. 115, pp. 1–32.
Heilbron, M., Valeriano, C.M., Tassinari, C.C.G., Almeida, J.C.H., Tupinamba, M., SIGA, O., Trouw, R.A.J., 2008. Correlation of Neoproterozoic terranes between the Ribeira

Belt, SE Brazil and its African counterpart: comparative tectonic evolution and open questions. In: Pankhurst, R.J., Trouw, R.A.J., Brito Neves, B.B., de Wit, M.J. (Eds.), West Gondwana: Pre-Cenozoic Correlations Across the South Atlantic Region. Geological Society, London, Special Publications, 294, pp. 211–238.
Hoffman, P.F., 1991. Did the breakout of Laurentia turn Gondwanaland inside-out? Science 252 (5011), 1409–1412.
Hubbert, M.K., 1937. Theory of scale models as applied to the study of geologic structures. Geol. Soc. Am. Bull. 48, 1459–1520.
Huismans, R.S., Beaumont, C., 2008. Complex rifted continental margins explained by dynamical models of depth-dependent lithospheric extension. Geology 36, 163–166. http://dx.doi.org/10.1130/G24231A.1.
Jackson, J.A., White, N.J., 1989. Normal faulting in the upper continental crust: observation from regions of active extension. J. Struct. Geol. 11, 15–36.
Karner, G.D., Driscoll, N.W., 1999. Tectonic and stratigraphic development of the West African and eastern Brazilian margins; insights from quantitative basin modelling. In: Cameron, N.R., Bate, R.H., Clure, V.S. (Eds.), The Oil and Gas Habitats of the South Atlantic. Geological Society, London, Special Publications, 153, pp. 11–40.
Karner, G.D., Gamboa, L.A.P., 2007. Timing and origin of the South Atlantic pre-salt sag basins and their capping evaporites. In: Schreiber, B.C., Lugli, S., Babel, M. (Eds.), Evaporites Through Space and Time. Geological Society, London, Special Publications, 285, pp. 15–35.
Karner, G.D., Driscoll, N.W., Barker, D.H.N., 2003. Syn-rift region subsidence across the West African continental margin; the role of lower plate ductile extension. In: Arthur, T.J., Macgregor, D.S., Cameron, N. (Eds.), Petroleum Geology of Africa: New Themes and Developing Technologies. Geological Society, London, Special Publications, 207, pp. 105–129.
Kusznir, N., Karner, G., 2007. Continental lithospheric thinning and breakup in response to upwelling divergent mantle flow: application to the Woodlark, Newfoundland and Iberia margins. Geol. Soc. Lond. Spec. Publ. 282, 389–419.
Lavier, L.L., Manatschal, G., 2006. A mechanism to thin the continental lithosphere at magma-poor margins. Nature 440, 324–328. http://dx.doi.org/10.1038/nature04608.
Lentini, M.R., Fraser, S.I., Sumner, H.S., Davies, R.J., 2010. Geodynamics of the central South Atlantic conjugate margins: implications for hydrocarbon potential. Pet. Geosci. 16 (3), 217–229. http://dx.doi.org/10.1144/1354-079309-909.
Lezzar, K.E., Tiercelin, J.J., Le Turdu, C., Cohen, A.S., Reynolds, D.J., Le Gall, B., Scholz, C.A., 2002. Control of normal fault interaction on the distribution of major Neogene sedimentary depocenters, Lake Tanganyika, Eat African rift. Geol. Soc. Am. Bull. 86, 1027–1059.
Ligi, M., Bonatti, E., Bortoluzzi, G., Cipriani, A., Cocchi, L., Tontini, F.C., Carminati, E., Ottolini, L., Schettino, A., 2012. Birth of an ocean in the Red Sea: initial pangs. Geochem. Geophys. Geosyst. 13 (29), Q08009. http://dx.doi.org/10.1029/2012GC004155.
Lister, G.S., Etheridge, M.A., Symonds, P.A., 1986. Detachment faulting and the evolution of passive continental margins. Geology 14, 246–250.
Litak, R.K., Barazangi, M., Brew, G., Sawaf, T., Al-imam, A., 1998. Structure and evolution of the petroliferous Euphrates graben system, southeast Syria. AAPG Bull. 82 (6), 1173–1190.
Lundin, E.R., Doré, A.G., 2011. Hyperextension, serpentinization, and weakening: a new paradigm for rifted margin compressional deformation. Geology 39 (4), 347–350. http://dx.doi.org/10.1130/G31499.1.
Manatschal, G., Bernoulli, D., 1999. Architecture and tectonic evolution of non volcanic margins: present-day Galicia and ancient Adria. Tectonics 18, 1099–1199.
Mart, Y., Dauteuil, O., 2000. Analogue experiments of propagation of oblique rifts. Tectonophysics 316 (1–2), 121–132. http://dx.doi.org/10.1016/S0040-1951(99)00231-0.
McClay, K.R., White, M.J., 1995. Analogue modelling of orthogonal and oblique rifting. Mar. Pet. Geol. 12, 137–151.
McClay, K.R., Dooley, T., Whitehouse, P., Mills, M., 2002. 4-D evolution of rift systems: insights from scaled physical models. AAPG Bull. 86, 935–959.
McKenzie, D.P., 1978. Some remarks on the development of sedimentary basins. Earth Planet. Sci. Lett. 40, 25–32. http://dx.doi.org/10.1016/0012-821X(78)90071-7.
Meisling, K.E., Cobbold, P.R., Mount, V.S., 2001. Segmentation of an obliquely rifted margin, Campos and Santos basins, southeastern Brazil. AAPG Bull. 85 (11), 1903–1924.
Menzies, M.A., Klemperer, L.S., Ebinger, J.C., Baker, 2002. Characteristic of volcanic rifted margins. Geol. Soc. Am. Spec. Pap. 362, 1–14.
Michon, L., Merle, O., 2003. Mode of lithospheric extension: conceptual models from analogue modeling. Tectonics 22, 1028. http://dx.doi.org/10.1029/2002TC001435.
Michon, L., Sokoutis, D., 2005. Interaction between structural inheritance and extension direction during graben and depocentre formation: an experimental approach. Tectonophysics 409 (1–4), 125–146. http://dx.doi.org/10.1016/j.tecto.2005.08.020.
Mohriak, W.U., Rosendahl, B.R., 2003. Transform zones in the South Atlantic rifted continental margins. In: Storti, F., Holdsworth, R.E., Salvini, F. (Eds.), Intraplate Strike-slip Deformation Belts. Geological Society, London, Special Publications, 210, pp. 211–228.
Mohriak, W.U., Rabelo, J.H.L., Matos, R.D., Barros, M.C., 1995. Deep seismic reflection profiling of sedimentary basins offshore Brazil; geological objectives and preliminary results in the Sergipe Basin. J. Geodyn. 20, 515–539. http://dx.doi.org/10.1016/0264-3707(95)00024-4.
Mohriak, W.U., Nemčok, M., Enciso, G., 2008. South Atlantic divergent margin evolution: rift-border uplift and salt tectonics in basins of SE Brazil. In: Pankhurst, R.J., Trouw, R.A.J., Brito Neves, B.B., de Wit, M.J. (Eds.), West Gondwana: Pre-Cenozoic Correlations Across the South Atlantic Region. Geological Society, London, Special Publications, 294, pp. 365–398. http://dx.doi.org/10.1144/SP294.19.
Mohriak, W.U., Nobrega, M., Odegard, M.E., Gomes, B.S., Dickson, W.G., 2010. Geological and geophysical interpretation of the Rio Grande Rise, south-eastern Brazilian margin: extensional tectonics and rifting of continental and oceanic crusts. Pet. Geosci. 16 (3), 231–245. http://dx.doi.org/10.1144/1354-079309-910.
Morley, C.K., 1999a. How successful are analogue models in addressing the influence of pre-existing fabrics on rift structure? J. Struct. Geol. 21, 1267–1274.
Morley, C.K., 1999b. Patterns of displacement along large normal faults: implications for basin evolution and fault propagation, based on examples from East Africa. AAPG Bull. 83, 613–634.
Morley, C.K., Nelson, R.A., Patton, T.L., Munn, S.G., 1990. Transfer zones in the East African Rift System and their relevance to hydrocarbon exploration in rifts. Am. Assoc. Pet. Geol. Bull. 74, 1234–1253.
Morley, C., Haranya, C., Phoosongsee, W., Pongwapee, S., Kornsawan, a, Wonganan, N., 2004. Activation of rift oblique and rift parallel pre-existing fabrics during extension and their effect on deformation style: examples from the rifts of Thailand. J. Struct. Geol. 26 (10), 1803–1829. http://dx.doi.org/10.1016/j.jsg.2004.02.014.
Moulin, M., Aslanian, D., Olivet, J.L., Contrucci, I., Matias, L., Géli, L., Klingelhoefer, F., Nouzé, H., Réhault, J.P., Unternehr, P., 2005. Geological constraints on the evolution of the Angolan margin based on reflection and refraction seismic data (ZaïAngo project). Geophys. J. Int. 162, 793–810. http://dx.doi.org/10.1111/j.1365-246X.2004.02303.x.
Moulin, M., Aslanian, D., Rabineau, M., Matias, L., Moulin, M., Aslanian, D., Rabineau, M., 2012. Kinematic keys of the Santos–Namibe basins. Geol. Soc. Lond. Spec. Publ. 369. http://dx.doi.org/10.1144/SP369.3.
Nelson, R.A., Patton, T.L., Morley, C.K., 1992. Rift–segment interaction and its relation to hydrocarbon exploration in continental rift systems. AAPG Bull. 76, 1153–1169.
Nielsen, T.K., Hopper, J.R., 2004. From rift to drift: mantle melting during continental breakup. Geochem. Geophys. Geosyst. 5, Q07003. http://dx.doi.org/10.1029/2003GC000662.
Ojeda, H.A.O., 1982. Structural framework, stratigraphy, and evolution of Brazilian marginal basins. AAPG Bull. 66 (6), 732–749. http://dx.doi.org/10.1306/03B5A309-16D1-11D7-8645000102C1865D.
Oreiro, S., Cupertino, J., Szatmari, P., Filho, A., 2008. Influence of pre-salt alignments in post-Aptian magmatism in the Cabo Frio High and its surroundings, Santos and Campos basins, SE Brazil: an example of non-plume-related magmatism. J. S. Am. Earth Sci. 25 (1), 116–131. http://dx.doi.org/10.1016/j.jsames.2007.08.006.
Paul, D., Mitra, S., 2013. Experimental models of transfer zones in rift systems. AAPG Bull. 97, 759–780. http://dx.doi.org/10.1306/10161212105.
Pedrosa-Soares, A.C., Noce, C.M., Alkmim, F.F.D., Carlos, L., Babinski, M., Cordani, U., Castañeda, C., 2007. Orógeno Araçuaí: Síntese Do Conhecimento 30 Anos Após Almeida 1977. Geonomos 15 (1), 1–16.
Pereira, R., Alves, T.M., 2011. Margin segmentation prior to continental breakup: a seismic–stratigraphic record of multiphased rifting in the North Atlantic (Southwest Iberia). Tectonophysics 505 (1–4), 17–34. http://dx.doi.org/10.1016/j.tecto.2011.03.011.
Peres, G.G., Alkmim, F.F., Jordt-evangelista, H., 2004. The southern Araçuaí belt and the Dom Silvério Group: geologic architecture and tectonic significance. An. Acad. Bras. Cienc. 76, 771–790.
Péron-Pindivic, G., Manatschal, G., 2009. The final rifting evolution at deep magma-poor passive margins from Iberia–Newfoundland: a new point of view. Int. J. Earth Sci. 98, 1581–1597. http://dx.doi.org/10.1007/s00531-008-0337-9.
Péron-Pindivic, G., Manatschal, G., Minshull, T.A., Sawyer, D.S., 2007. Tectonosedimentary evolution of the deep Iberia–Newfoundland margins: evidence for a complex breakup history. Tectonics 26 (2). http://dx.doi.org/10.1029/2006TC001970.
Péron-Pindivic, G., Van Wijk, J., Shillington, D.J., Gernigon, L., 2009. An introduction to the Tectonophysics Special Issue "Role of magmatism in continental lithosphere extension". Tectonophysics 468, 1–5.
Péron-Pindivic, G., Manatschal, G., Osmundsen, P.T., 2013. Structural comparison of archetypal Atlantic rifted margins: a review of observations and concepts. Mar. Pet. Geol. 43, 21–47. http://dx.doi.org/10.1016/j.marpetgeo.2013.02.002.
Prosser, S., 1993. Rift-related linked depositional systems and their seismic expression. Geol. Soc. Lond. Spec. Publ. 71 (1), 35–66. http://dx.doi.org/10.1144/GSL.SP.1993.071.01.03.
Quirk, D.G., Schodt, N., Lassen, B., Ings, S.J., Hsu, D., Hirsch, K.K., Von Nicolai, C., 2012. Salt tectonics on passive margins: examples from Santos, Campos and Kwanza basins. Geol. Soc. Lond. Spec. Publ. 363 (1), 207–244. http://dx.doi.org/10.1144/SP363.10.
Ramberg, H., 1981. Gravity, Deformation and the Earth's Crust in Theory, Experiments and Geologic ApplicationSecond ed. Academic Press, London (452 pp.).
Ravnås, R., Nottvedt, A., Steel, R.J., Windelstad, J., 2000. Syn-rift sedimentary architectures in the Northern North Sea. Geol. Soc. Lond. Spec. Publ. 167, 133–177. http://dx.doi.org/10.1144/GSL.SP.2000.167.01.07.
Reston, T.J., 2007. Extension discrepancy at North Atlantic nonvolcanic rifted margins: depth-dependent stretching or unrecognized faulting? Geology 7, 367–370. http://dx.doi.org/10.1130/G23213A.1.
Reston, T.J., 2009. The structure, evolution and symmetry of the magma-poor rifted margins of the North and Central Atlantic: a synthesis. Tectonophysics 468, 6–27. http://dx.doi.org/10.1016/j.tecto.2008.09.002.
Reston, T.J., 2010. The opening of the central segment of the South Atlantic: symmetry and the extension discrepancy. Pet. Geosci. 16 (3), 199–206. http://dx.doi.org/10.1144/1354-079309-907.
Reston, T.J., Pérez-Gussinyé, M., 2007. Lithospheric extension from rifting to continental breakup at magma-poor margins: rheology, serpentinisation and symmetry. Int. J. Earth Sci. 96, 1033–1046. http://dx.doi.org/10.1007/s00531-006-0161-z.
Reston, T.J., Leythaeuser, T., Booth-Rea, G., Sawyer, D., Klaeschen, D., Long, C., 2007. Movement along a low-angle normal fault. The S reflector west of Spain. Geochem. Geophys. Geosyst. 8, Q06002. http://dx.doi.org/10.1029/2006GC001437.
Reynisson, R.F., Ebbing, J., Lundin, E., Osmundsen, P.T., 2010. Properties and distribution of lower crustal bodies on the mid-Norwegian margin. In: Vining, B.A., Pickering, S.C. (Eds.), Petroleum Geology: From Mature Basins to New Frontiers: Proceedings of the 7th Petroleum Geology Conference. Geological Society of London Petroleum Geology Conference Series, 7, pp. 843–854. http://dx.doi.org/10.1144/0070843.
Rosenbaum, G., Weinberg, R.F., Regenauer-Lieb, K., 2008. The geodynamics of lithospheric extension. Tectonophysics 458, 1–8. http://dx.doi.org/10.1016/j.tecto.2008.07.016.

Rosendahl, B.R., 1986. Architecture of continental rifts with special reference to east Africa. Annu. Rev. Earth Planet. Sci. 15, 445–503.
Rosendahl, B.R., Mohriak, W.U., Odegard, M.E., Turner, J.P., Dickson, W.G., 2005. West African and Brazilian conjugate margins: crustal types, architecture, and plate configurations. In: Post, P., Rosen, N., Olson, D., Palmes, S.L., Lyons, K.T., Newton, G.B. (Eds.), Petroleum Systems of Divergent Continental Margin Basins. 25th Gulf Coast Section, SEPM Research Conference, CD-ROM.
Rosendahl, B.R., Reynolds, D.J., Lorber, P.M., Burgess, C.F., McGill, J., Scott, D., Lambiase, J.J., Derksen, S.J., 1986. Structural expressions of rifting: lessons from Lake Tanganyika, Africa. In: Frostick, L.E., Renaut, R.W., Freid, I., Tiercelin, J.J. (Eds.), Sedimentation in the African Rifts. Geological Society, London, Special Publications, 25, pp. 29–43.
Sandwell, D.T., Smith, W.H.F., 1997. Marine gravity anomaly from Geosat and ERS 1 satellite altimetry. J. Geophys. Res. 102, 10039–10054. http://dx.doi.org/10.1029/96JB03223.
Sawyer, D.S., Coffin, M.F., Reston, T.J., Stock, J.M., Hopper, J.R., 2007. COBBOOM: the continental breakup and birth of oceans mission. Sci. Drill. 5. http://dx.doi.org/10.2204/iodp.sd.5.02.2007 (September 2007).
Schlische, R.W., Withjack, M.O., 2009. Origin of fault domains and fault-domain boundaries (transfer zones and accommodation zones) in extensional provinces: result of random nucleation and self-organized fault growth. J. Struct. Geol. 31 (9), 910–925. http://dx.doi.org/10.1016/j.jsg.2008.09.005.
Schreurs, G., Buiter, S.J.H., Boutelier, D., Corti, G., Costa, E., Cruden, A.R., Daniel, J.M., Hoth, S., Koyi, H.A., Kukowski, N., Lohrmann, J., Ravaglia, A., Schlische, R.W., Withjack, M.O., Yamada, Y., Cavozzi, C., Delventisette, C., Brady, J.A.E., Hoffmann-Rothe, A., Mengus, J.M., Montanari, D., Nilforoushan, F., 2006. Analogue benchmarks of shortening and extension experiments. In: Buiter, S.J.H., Schreurs, G. (Eds.), Analogue and Numerical Modelling of Crustal-scale Processes. Geological Society, London, Special Publications, 253, pp. 1–27.
Scotchman, I.C., Marais-gilchrist, G., Souza, F.G.D., Chaves, F.F., Atterton, L.A., Roberts, A., Nick, J., 2006. A Failed Sea-floor Spreading Centre, Santos Basin, Brasil, Rio Oil and Gás Conference. IBP, Rio de Janeiro, pp. 1–9.
Scotchman, I.C., Gilchrist, G., Kuznir, N.J., Roberts, A.M., Fletcher, R., 2010. The breakup of the South Atlantic Ocean: formation of failed spreading axis and blocks of thinned continental crust in the Santos basin, Brazil, and its consequences for petroleum system development. In: Vining, B.A., Pickering, S.C. (Eds.), Petroleum Geology: From Mature Basin to New Frontiers. Proceedings of the 7th Petroleum Geology Conference. Geological Society, London, pp. 855–866. http://dx.doi.org/10.1144/0070855.
Sibuet, J., Sibuet, J.-claude, Srivastava, S., Manatschal, G., 2007. Exhumed mantle-forming transitional crust in the Newfoundland–Iberia rift and associated magnetic anomalies. J. Geophys. Res. 112, 1–23. http://dx.doi.org/10.1029/2005JB003856.
Smith, M., Mosley, P., 1993. Crustal heterogeneity and basement influence on the development of the Kenya rift, East Africa. Tectonics 12, 591–606.
Sokoutis, D., Corti, G., Bonini, M., Brun, J.P., Cloetingh, S., Mauduit, T., Manetti, P., 2007. Modelling the extension of heterogeneous hot lithosphere. Tectonophysics 444, 63–79.
Srivastava, S.P., Sibuet, J.C., Cande, S., Roest, W.R., Reid, I.D., 2000. Magnetic evidence for slow seafloor spreading during the formation of the Newfoundland and Iberian margins. Earth Planet. Sci. Lett. 182 (1), 61–76.
Sun, Z., Zhong, Z., Keep, M., Zhou, D., Cai, D., Li, X., Wu, S., Jiang, J., 2009. 3D analogue modeling of the South China Sea: a discussion on breakup pattern. J. Asian Earth Sci. 34, 544–556.
Tommasi, A., Vauchez, A., 2001. Continental rifting parallel to ancient collisional belts: an effect of the mechanical anisotropy of the lithospheric mantle. Earth Planet. Sci. Lett. 185, 199–210.
Torsvik, T.H., Rousse, S., Labails, C., Smethurst, M.A., 2009. A new scheme for the opening of the South Atlantic Ocean and the dissection of an Aptian salt basin. Geophys. J. Int. 177, 1315–1333.
Trudgill, B.D., 2002. Structural controls on drainage development in the Canyonlands grabens of southeast Utah. AAPG Bull. 86 (6), 1095–1112.
Trudgill, B., Cartwright, J., 1994. Relay-ramp forms and normal-fault linkages, Canyonlands National Park, Utah. Geol. Soc. Am. Bull. 106, 1143–1157. http://dx.doi.org/10.1130/0016-7606(1994)1061143.
Tsikalas, F., Faleide, J.I., Eldholm, O., 2001. Lateral variations in tectono-magmatic style along the Lofoten–Vesteralen volcanic margin off Norway. Mar. Petrol. Geol. 18, 807–832.
Tsikalas, F., Eldholm, O., Faleide, J.I., 2005. Crustal structure of the Lofoten–Vesteralen margin, off Norway. Tectonophysics 404, 151–174.
Tsikalas, F., Faleide, J.I., Kusznir, N.J., 2008. Along-strike variations in rifted margin crustal architecture and lithosphere thinning between northern Vøring and Lofoten margin segments off mid-Norway. Tectonophysics 458 (1–4), 68–81. http://dx.doi.org/10.1016/j.tecto.2008.03.001.
Tsikalas, F., Faleide, J.I., Eldholm, O., Blaich, O.A., 2012. The NE Atlantic conjugate margins. In: Roberts, D.G., Bally, A.W. (Eds.), Phanerozoic Passive Margins, Cratonic Basins and Global Tectonic Maps. http://dx.doi.org/10.1016/B978-0-444-56357-6.00004-4.
Turcotte, D.L., Schubert, G., 2002. Geodynamics2nd ed. Cambridge University Press, Cambridge, New York, Melbourne.
Unternehr, P., Péron-Pinvidic, G., Manatschal, G., Sutra, E., 2010. Hyper-extended crust in the South Atlantic: in search of a model. Pet. Geosci. 16, 207–215. http://dx.doi.org/10.1144/1354-079309-904.
van Wijk, J.W., 2005. Role of weak zone orientation in continental lithosphere extension. Geophys. Res. Lett. 32 (2), 1–4. http://dx.doi.org/10.1029/2004GL022192.
Vendeville, B., Cobbold, P., Davy, P.R., Brun, J.P., Choukroune, P., 1987. Physical models of extensional tectonics at various scales. In: Coward, M.P., Dewey, J.F., Hancock, P.L. (Eds.), Continental Extensional Tectonics. Geological Society, London, Special Publications, 28, pp. 95–107.
Vidal, A.C., Kiang, C.H., Correa, F.S., Fernandes, F.L., de Castro, J.C., Tinen, J.S., Koike, L., Assine, M.L., Rostirolla, S.P., 2003. Interpretação e Mapeamento dos Sistemas Petrolíferos da Bacia de Santos.ANP/UNESP/LEBAC.
Watts, A.B., Stewart, J., 1998. Gravity anomalies and segmentation of the continental margin offshore West Africa. Earth Planet. Sci. Lett. 56, 239–252. http://dx.doi.org/10.1016/S0012-821X(98)00018-1.
Wernicke, B., 1981. Low-angle normal faults in the Basin and Range province: nappe tectonics in an extending orogen. Nature 291, 645–648. http://dx.doi.org/10.1038/291645a0.
Whitmarsh, R.B., Miles, P.R., 1995. Models of the development of the West Iberia rifted continental margin at 40°30′N deduced from surface and deep-tow magnetic anomalies. J. Geophys. Res. 100, 3789–3806. http://dx.doi.org/10.1029/94JB02877.
Whitmarsh, R.B., Sawyer, D.S., 1996. The ocean/continent transition beneath the Iberia Abyssal Plain and continental-rifting to seafloor-spreading processes. Proceedings of the Ocean Drilling Program Scientific Results, 149, pp. 713–733.
Whitmarsh, R.B., White, R.S., Horsefield, S.J., Sibuet, J.C., Recq, M., Louvel, V., 1996. The ocean continent boundary off the western continental margin of Iberia: crustal structure west of Galicia Bank. J. Geophys. Res. 101, 28291–28314. http://dx.doi.org/10.1029/96JB02579.
Withjack, M.O., Schlische, R.W., Olsen, P.E., 2002. Rift-basin structure and its influence on sedimentary systems. Sedimentation in continental rifts. SEPM Spec. Publ. 73, 57–81.
World Digital Magnetic Anomaly Map (WDMAM), 2007. IAGA, International Association of Geomagnetism and Aeronomy.IUGG, Perugia, Italy.
Younes, A.I., Mcclay, K., 2002. Development of accomodation zones in the Gulf of Suez–Red Sea rift Egypt. AAPG Bull. 86, 1003–1026.
Zalán, P.V., Severino, M.C.G., Rigoti, C.A., Magnavita, L.P., de Oliveira, J.A.B., Viana, A.R., 2011. An entirely new 3D-view of the crustal and mantle structure of a South Atlantic passive margin — Santos, Campos and Espírito Santo Basins, Brazil. AAPG Annual Conference and Exhibition. Making the Next Giant Leap in Geosciences. April 10–13, 2011, Houston, Texas (AAPG, Search and Discovery Article, 90124. World Wide Web Address: http://www.searchanddiscovery.com/abstracts/html/2011/annual/abstracts/Zalan.html).
Ziegler, P.A., Cloetingh, S., 2004. Dynamic processes controlling evolution of rifted basins. Earth Sci. Rev. 64 (1–2), 1–50. http://dx.doi.org/10.1016/S0012-8252(03)00041-2.

5

Intraplate deformation in NE Brazil induced by repeated post-rift shear reversal along the Pernambuco Fracture Zone

Submitted to
Nature Geoscience
Manuscript # NGS-2014-02-00210

Intraplate deformation in NE Brazil induced by repeated post-rift shear reversal along the Pernambuco Fracture Zone

Fabrizio Balsamo[1], Yago Nestola[1], Fabrizio Storti[1], F. Cézar C. Nogueira[2] and Francisco H.R. Bezerra[3]

1: NEXT – Natural and Experimental Tectonic Research Group, Department of Physic and Earth Sciences, Parma University, Parma, Parco Area delle Scienze 157/A, Campus Universitario, 43124, Italy. **2:** Universidade Federal de Campina Grande, Brazil. **3:** Universidade Federal do Rio Grande do Norte, Brazil.

Plate tectonics assumes that transform faults at mid-oceanic ridges are tectonically active brittle shear zones linking adjacent ridge segments to accommodate opposite seafloor spreading directions (Wilson, 1965). This postulate has been recently questioned by geological and geophysical evidence from the Antarctic Plate, showing that oceanic fracture zones can transfer shear into plate interior (Storti et al., 2007). In the NE Brazilian continental margin, historical and recent seismic activity is clustered along a few major continental-scale, long-lived inherited shear-zones striking near parallel to the oceanic fracture zones. The origin of such unexpected seismicity pattern in a stable continental margin is not yet fully understood. Here we show that, in the last ~83 Ma, the oceanic seafloor on the opposite sides of the ~E-W Pernambuco Fracture Zone grew with different and non-uniform spreading rates, thus indicating that the two adjacent lithospheric lanes are cinematically independent. The resulting differential spreading rate along the Pernambuco Fracture Zone, calculated in 8 age provinces from late Cretaceous to Present, varies between 1.5 and 8.8 mm/yr and switched from right-lateral to left-lateral excess shear, with at least 5 major reversals. In particular, the Tortonian reversal from right-lateral to left-lateral excess shear is consistent with structural data acquired in coeval sediments of the Pernambuco Basin. Our results indicate that the Pernambuco Fracture Zone systematically transferred excess shear from the mid-oceanic ridge, at the plate boundary, into the plate interior thus providing the remote trigger for post-rift intraplate seismicity and tectonic activity along the inherited Pernambuco shear zone. These findings add the concept of periodic shear reversal to the notion of post-rift activity of fracture zones, thus further contributing to release the postulate of rigid tectonic plates and stable continental margin inactivity.

In the plate tectonics conceptual framework, oceanic transform faults are strike-slip brittle shear-zones that connect two adjacent offset spreading axes at mid ocean ridges (Wilson, 1965). Their prosecution into the plate interiors is provided by fracture zones, which are thousand km-long narrow belts decorating oceanic seafloors like fossil scars of plate divergence. Tectonic activity is not expected along fracture zones, apart from minor dip-slip motions and uplift induced by differential thermal contraction of juxtaposed crustal sectors having different ages (Collette et al., 1979), and/or small changes in the spreading directions (Bonatti, 1978). However, since 1978 Sykes (1978) proposed that fracture zones are weakness belts that play an important role in intraplate seismicity along the continental margins of the South Atlantic. More recently, geological and geophysical evidence from the Ross Sea Region, on the Antarctic passive margin of the Southern Ocean, indicate that strike-slip shear can be transferred from transform faults to fracture zones and, eventually, to their collinear prosecution within the Antarctic continent (Salvini et al., 1997; Storti et al., 2007). Assessing whether this geodynamic setting is peculiar of the Antarctic Plate region facing Australia or it is suitable to be acquired as a new general scenario that adds to the paradigms of plate tectonics, has the potential to significantly modify

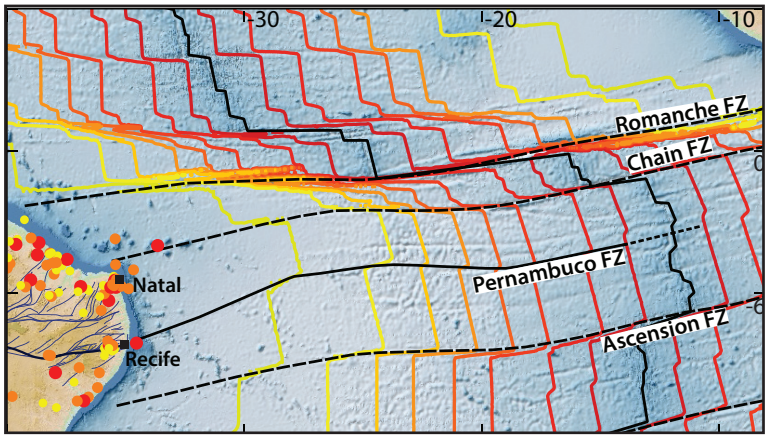

Figure 1| Seafloor bathymetry and NE Brazil topography ("The GEBCO_08 Grid, version 20100927, http://www.gebco.net"), showing the position of major fracture zones in the central-south Atlantic ocean and the continental Pernambuco shear zone. Dots indicate earthquake epicenters from (Ferreira et al., 2008) (red dots=m_b ~ 5, orange dots=m_b ~ 4, yellow dots=m_b ~ 3).

our current knowledge of the kinematics of the lithosphere in our planet. Furthermore, understanding whether the oceanic crust at plate passive margins can be segmented into fracture zone corridors undergoing slow differential strike-slip motions that can be transferred into the interior of the continents, dramatically impacts current seismogenic reference models and, hence, earthquake and tsunami risk assessment. Finally, passive plate margins are sites of huge unrenewable energy reserves, as in the Brazil offshore and in North Sea (Szatmari, 2000); their possible shearing along fracture zone continental prosecutions is expected to exert a significant influence on hydrocarbon migration and accumulations and, consequently, on the future reservoir exploration and production strategies.

The Precambrian continental lithosphere of the NE Brazil, where the link between oceanic fracture zones and intraplate seismicity was first proposed (Sykes, 1978), preserves a network of continental-scale shear zones that imprinted development of the collinear huge fracture zones characterizing the South Atlantic Ocean (Bezerra et al., 2011). Among the major ~E-W-trending continental shear zones of the NE Brazil, the Pernambuco shear zone (Fig. 1) provides the proper case to investigate on the possible ocean-continent post-rift kinematic connection because it is one of the most seismically active intraplate areas in South America (Ferreira et al., 2008; Lima Neto et al., 2013; Lopes et al., 2010), where the correlation between inherited structural grain and earthquakes has been observed. To this end, we have integrated offshore spreading rate data calculated for 8 age provinces of lithospheric lanes juxtaposed across the Pernambuco Fracture Zone, with onshore structural data collected in post-rift sediments along its continental prolongation near the town of Recife (Fig. 2).

The ~1-5 km wide Pernambuco shear zone (Fig. 1) extends for more than 700 km into the Brazilian intraplate area. It formed during the Brasiliano Orogeny (750-540 Ma) and was reactivated as rift basin-boundary fault system during the Cretaceous breakup between Africa and South America (Lima Filho et al., 2006; Matos, 1992). In the coastal sector, faults related to

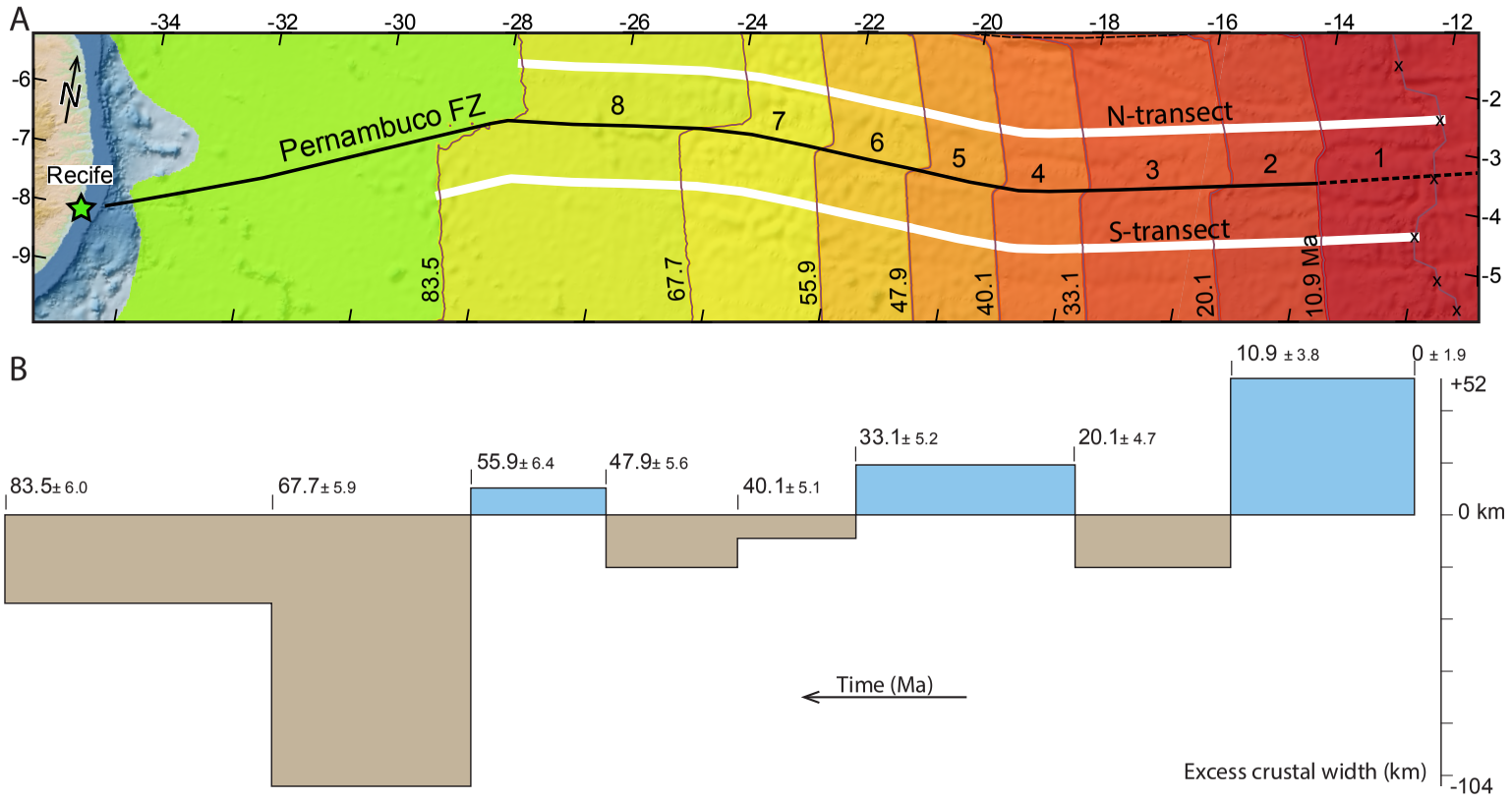
A
-34
-32
-30
-28
-26
-24
-22
-20
-18
-16
-14
-12
-6
-7
-8
-9
-2
-3
-4
-5
N
Recife
Pernambuco FZ
8
7
6
5
4
3
2
1
N-transect
S-transect
83.5
67.7
55.9
47.9
40.1
33.1
20.1
10.9 Ma
B
83.5± 6.0
67.7± 5.9
55.9± 6.4
47.9± 5.6
40.1± 5.1
33.1± 5.2
20.1± 4.7
10.9 ± 3.8
0 ± 1.9
+52
0 km
-104
Time (Ma)
Excess crustal width (km)

the brittle reactivation of the Pernambuco shear zone cross cuts post-rift Miocene marine deposits of the Barreiras Formation, which yielded Ar/Ar and U–Th/He ages at 17-25 Ma (Lima, 2008; Rossetti et al., 2013). They also cut across Quaternary fluvial, marine, aeolian, and colluvial sediments, which yielded optically stimulated luminescence (SAR protocol) ages mainly from ~230 to ~2 ka (Bezerra et al., 2008; Nogueira et al., 2010; Rossetti et al., 2011; Suguio et al., 2011). Offshore, the Pernambuco Fracture Zone lies in between the Chain and Ascension Fracture Zones (Fig. 1). From 12° to 20° W and from 28° to 35° W, the Pernambuco Fracture Zone strikes N80°, whereas in the central sector, between 20° and 28° W, it strikes E-W (Fig. 2A). Analysis of the width of eight age provinces, from Cretaceous to the Present, on the two adjacent lithospheric lanes separated by the Pernambuco Fracture Zone, provides different values from the corresponding provinces, alternatively higher to the south and to the north, respectively (Fig. 2B). The difference in width of each age province (Δwi) is listed in Table 1 and broadly ranges between 8.9 km in province 4, and 104.1 km in province 7. This result indicates that, during the last 83 Ma, there was a cyclical differential production of oceanic lithosphere to the north and south of Pernambuco Fracture Zone. In particular, during age provinces 1, 3, and 6, more lithosphere was produced in the northern lane compared to the southern one, while the opposite occurred during the formation of age provinces 2, 4, 5, 7, and 8. The wavelength of such oscillations in lithosphere production rate varies between ~27 and ~8 My (Fig. 2B). Age province width variations across

Figure 2 | a, Detail of the oceanic seafloor age map along the Pernambuco Fracture Zone, which brings into contact lithospheric lanes characterized by N-S trending isochrones. Isochrone positions are derived from (Müller et al., 2008) and subdivide the lithospheric seafloor into 8 age provinces, each one encompassing approximately 8-12 Ma time intervals and with ages spanning between ~83.5±6 and ~67.7±5.9 Ma (western age province 8), up to ~10.9±3.8 Ma and present (eastern age province 1, close to the ridge). In the proximity of the E-W trending Pernambuco Fracture Zone, all the isochrones are shifted with an apparent right-stepping offset. Numbers on the northern lane indicate age provinces. **B**, Graph showing the distribution of the excess crustal width in the two lithospheric lanes along the Pernambuco Fracture Zone. Positive values and pale blue color refer to the northern lane; negative values and grey color refer to the southern lane.

fracture zones were not previously recognized in the Central-South Atlantic Ocean and are unexpected from the plate tectonic theory, which postulates that adjacent lanes grow at the same uniform rate. Conversely to theoretical predictions, our data indicates for the first time that accretion of new crust at divergent plate boundaries can occur non-uniformly along the Mid-oceanic ridge. This is well illustrated by the pattern of the average spreading rates calculated for each age province in the two lithospheric lanes to the south and north of the Pernambuco Fracture Zone (Table 1, Fig. 3A). Corresponding values on the opposite sides of the Pernambuco Fracture Zone never coincide and have an oscillatory behavior, where maxima alternatively locate to the north or to the south.

Occurrence of differential spreading rates on the two adjacent lithospheric lanes implies induction of strike-slip motions along the Pernambuco Fracture Zone. In particular, for a given age province, higher spreading rates on the northern lane result in a left-lateral excess transform shear (Storti et al., 2007), while the opposite occurs when faster production of new crust occurs on the southern lane. The distribution of excess transform shear along the Pernambuco Fracture Zone is provided in Fig. 3B; right-lateral strike-slip motions, which reach a rate of ~9mm/y between ~ 68 and ~ 56 Ma, dominate the early spreading history. They are followed by 7-10 My excess transform shear domains that periodically reverse. The last reversal, from right- to left-lateral shear, occurred at about 11 Ma (Fig. 3B).

The geological setting in the coastal tip region of the Pernambuco shear zone, where sediments coeval with the oceanic age province 1 unconformably overly sediments coeval with age provinces 2 and 3, allows investigating whether excess transform shear along the Pernambuco Fracture Zone is dissipated in the oceanic domain or it is partially accommodated along its continental prosecution. Structural data collected in quarries along the Pernambuco shear zone area shows that the deformation pattern in the Barreiras Formation sandstone mostly consists of NE-SW reverse faults and ~NW-SE extensio-

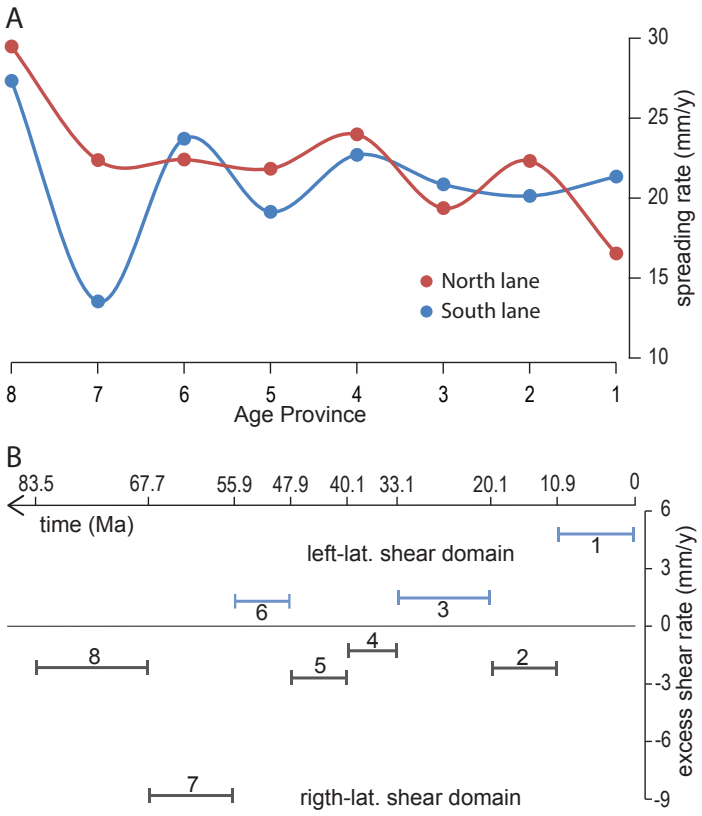

Figure 3| a, Spreading rates calculated for the 8 age provinces along the northern and southern lithospheric lanes, respectively, bounded by the Pernambuco Fracture Zone. **b**, Distribution of differential spreading rates for the eight age provinces on both sides of the Pernambuco Fracture Zone. Positive and negative values of differential spreading rates result in left-lateral and right-lateral excess transform shear, respectively.

nal faults, both overprinted by NNE-SSW extensional faults. On the other hand, the deformation pattern in the overlying post-Barreiras deposits consists of NNE-SSW extensional faults (Fig. 4A). Quaternary sediments in the Recife urban area are also affected by NNE-SSW-trending extensional fault zones (Fig. 4B), which are also associated with paleo-fluidization structures likely induced by coseismic rupture propagation along the Pernambuco shear zone (Fig. 4C). Given the 80°E average strike of the Pernambuco shear zone in this area, faulting in Barreiras sediments, which are coeval with Age Province 2 and 3, is consistent with right-lateral strike-slip shearing.

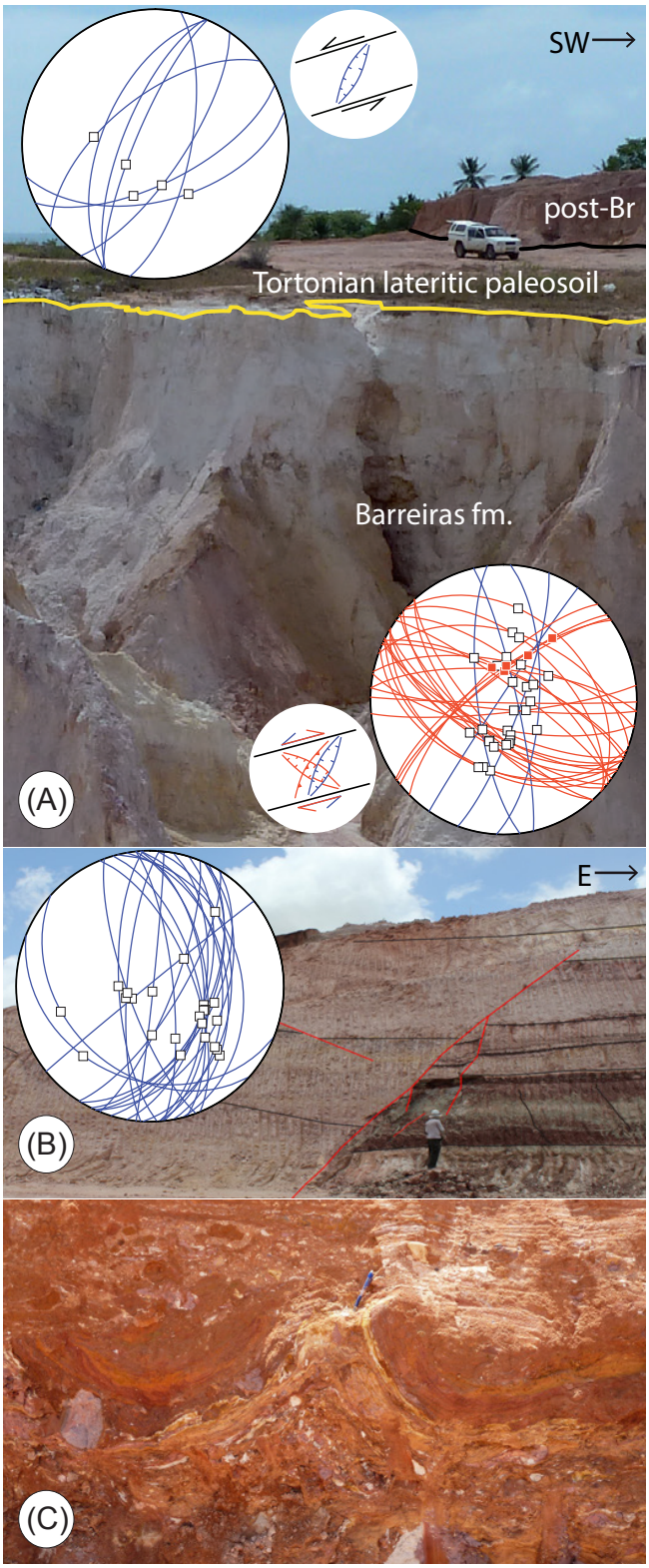
SW⟶
post-Br
Tortonian lateritic paleosoil
Barreiras fm.
(A)
E⟶
(B)
(C)

Figure 4| a, Deformation patterns recorded in a coastal field site ~ 15 km north of Recife. NW-SE extensional (slickenline orientation provided by white squares in the lower hemisphere stereographic projections) and NE-SW reverse (slickenline orientation provided by red squares in the stereographic projections) faults in the Miocene Barreiras Formation sandstones support right-lateral strike-slip motions along the Pernambuco shear zone (red great circles in the stereographic projection and related kinematic cartoon), overprinted by NNE-SSW extensional faults that support left lateral strike-slip faulting (blue great circles in the stereographic projection and related kinematic cartoon). Faults affecting the Quaternary post-Barreiras sediments strike-NNE-SSW and have extensional kinematics, supporting left lateral strike-slip faulting. Structural evidence for both right-lateral and left-lateral strike-slip faulting in the Barreiras Formation, and only left-lateral faulting in the post-Barreiras sediments, support right-lateral shearing along the Pernambuco shear zone at the time of the oceanic age province 2, and of left-lateral shearing at the time of the oceanic age province 1. **b**,NNE-SSW striking extensional fault zone cutting through Quaternary sediments, exposed in a quarry site in the hinterland of Recife. Major fault segments in the picture are highlighted in red. Analogously to the previous site, this fault attitude and kinematics supports left-lateral shearing along the Pernambuco shear zone at the time of the oceanic age province 1. **c**, Detail of paleofluidization structures exposed at the same site, supporting coseismic faulting in Quaternary time along the coastal segment of the Pernambuco shear zone.

On the other hand, faulting in the overlying Quaternary sediments is consistent with left-lateral strike-slip shear, which overprinted the previous deformation pattern.

Onshore confirmation of kinematic predictions made from the oceanic seafloor spreading pattern, provides robust evidence for the transfer of excess transform shear from the mid-ocean ridge, along the Pernambuco Fracture Zone, up to the continental area of NE Brazil, where it reactivates the inherited structural fabric of the Pernambuco shear zone. This result led to the following two-fold conclusion. (1) Passive margin asymmetry by excess transform shearing along oceanic fracture zones is a general concept that has to be added to the conceptual background of the plate tectonics theory, contemporary releasing the notion of rigid plates. A consequence of this point is the non-uniqueness of plate tectonic reconstructions by Eulerian pole best-fitting and, consequently, of deformation pattern predictions from the associated misfits. (2) Accommodation of excess transform shear provides an additional trigger of seismicity in stable continental margins, such as NE Brazil. The evidence of periodic reversal of the

Table 1 | Age and width of oceanic seafloor age provinces

Age Province	Age interval (Ma)	Time	Width North (km)	Width South (km)	Δ width (km)	ε North (mm/y)	ε South (mm/y)	Δ ε (mm/y)
1	0 - 10,9	10,9	232,61	180,21	52,40	21,34	16,53	4,81
2	10,9 - 20,1	9,2	185,24	205,33	-20,09	20,14	22,32	-2,18
3	20,1 - 33,1	13	271,04	251,78	19,26	20,85	19,37	1,48
4	33,1 - 40,1	7	158,93	167,83	-8,90	22,70	23,98	-1,27
5	40,1 - 47,9	7,8	149,29	170,33	-21,04	19,14	21,84	-2,70
6	47,9 - 55,9	8	189,68	179,27	10,41	23,71	22,41	1,30
7	55,9 - 67,7	11,8	159,79	263,89	-104,10	13,54	22,36	-8,82
8	67,7 - 83,5	15,8	431,65	465,58	-33,92	27,32	29,47	-2,15

shear sense between adjacent lithosphere lanes adds to fault zone mineralogy hydrothermal alteration (Collettini et al., 2009) to favor dramatic fault strength weakening and aseismic slip in ocean fracture zones. On the other hand, shear reversal along reactivated inherited continental weakness zones strongly increases the structural complexity of the resulting fault network, thus significantly impacting seismic hazard assessment and mitigation in continental areas facing spreading oceans.

ACKNOWLEDGEMENTS

This study was co-sponsored by the Brazilian National Research Council (CNPq) Project INCTET no. 573713/2008-1 and Project Universal no. 471950/2012-2, and by the Parma University A.D0105.STORTFIL12 project.

References

Bezerra, F.H.R., Brito Neves, B.B., Corrêa, A.C.B., Barreto, A.M.F., Suguio, K., 2008. Late Pleistocene tectonic-geomorphological development within a passive margin — The Cariatá trough, northeastern Brazil. Geomorphology 97, 555–582.

Bezerra, F.H.R., do Nascimento, A.F., Ferreira, J.M., Nogueira, F.C., Fuck, R.A., Neves, B.B.B., Sousa, M.O.L., 2011. Review of active faults in the Borborema Province, Intraplate South America — Integration of seismological and paleoseismological data. Tectonophysics 510, 269–290.

Bonatti, E., 1978. Vertical tectonism in oceanic fracture zones. Earth Planet. Sci. Lett. 37, 369–379.

Collette, B.J., Slootweg, A.P., Twigt, W., 1979. Mid-Atlantic Ridge crest topography between 12° and 15°N. Earth Planet. Sci. Lett. 42, 103–108.

Collettini, C., Niemeijer, A., Viti, C., Marone, C., 2009. Fault zone fabric and fault weakness. Nature 462, 907–10.

Ferreira, J.M., Bezerra, F.H.R., Sousa, M.O.L., do Nascimento, A.F., Sá, J.M., França, G.S., 2008. The role of Precambrian mylonitic belts and present-day stress field in the coseismic reactivation of the Pernambuco lineament, Brazil. Tectonophysics 456, 111–126.

Lima Filho, M.F.D., Barbosa, J.A., Souza, E.M., 2006. EVENTOS TECTÔNICOS E SEDIMENTARES NAS BACIAS DE PERNAMBUCO E DA PARAÍBA: IMPLICAÇÕES NO QUEBRAMENTO DO GONDWANA E CORRELAÇÃO COM A BACIA DO RIO MUNI. Geociências 25, 117–126.

Lima, M.G., 2008. The weathering history of the Oriental Borborema Province, Northeastern Brazil: Paleoclimatic and tectonic implications. (PhD Thesis). Univ. Fed. Rio Grande do Norte, Natal, Brazil.(in Portuguese).

Lima Neto, H.C., Ferreira, J.M., Bezerra, F.H.R., Assumpção, M.S., do Nascimento, A.F., Sousa, M.O.L., Menezes, E.A.S., 2013. Upper crustal earthquake swarms in São Caetano: Reactivation of the Pernambuco shear zone and trending branches in intraplate Brazil. Tectonophysics 608, 804–811.

Lopes, A.E. V., Assumpção, M., do Nascimento, A.F., Ferreira, J.M., Menezes, E. a. S., Barbosa, J.R., 2010. Intraplate earthquake swarm in Belo Jardim, NE Brazil: reactivation of a major Neoproterozoic shear zone (Pernambuco Lineament). Geophys. J. Int. 180, 1303–1312.

Matos, R.M.D. de, 1992. The Northeast Brazilian Rift System. Tectonics 11, 766–791.

Müller, R.D., Sdrolias, M., Gaina, C., Roest, W.R., 2008. Age, spreading rates, and spreading asymmetry of the world's ocean crust. Geochemistry, Geophys. Geosystems 9, n/a–n/a.

Nogueira, F.C., Bezerra, F.H.R., Fuck, R.A., 2010. Quaternary fault kinematics and chronology in intraplate northeastern Brazil. J. Geodyn. 49, 79–91.

Rossetti, D.F., Bezerra, F.H.R., Dominguez, J.M.L., 2013. Late Oligocene–Miocene transgressions along the equatorial and eastern margins of Brazil. Earth-Science Rev. 123, 87–112.

Rossetti, D.F., Bezerra, F.H.R., Góes, A.M., Valeriano, M.M., Andrades-Filho, C.O., Mittani, J.C.R., Tatumi, S.H., Brito-Neves, B.B., 2011. Late Quaternary sedimentation in the Paraíba Basin, Northeastern Brazil: Landform, sea level and tectonics in Eastern South America passive margin. Palaeogeogr. Palaeoclimatol. Palaeoecol. 300, 191–204.

Salvini, F., Brancolini, G., Busetti, M., Storti, F., Mazzarini, F., Coren, F., 1997. Cenozoic geodynamics of the Ross Sea region, Antarctica: Crustal extension, intraplate strike-slip faulting, and tectonic inheritance. J. Geophys. Res. 102, 24669.

Storti, F., Salvini, F., Rossetti, F., Phipps Morgan, J., 2007. Intraplate termination of transform faulting within the Antarctic continent. Earth Planet. Sci. Lett. 260, 115–126.

Suguio, K., Bezerra, F.H.R., Barreto, A.M.F., 2011. Luminescence dated Late Pleistocene wave-built terraces in northeastern Brazil. An. Acad. Bras. Cienc. 83, 907–920.

Sykes, L.R., 1978. Intraplate seismicity, reactivation of preexisting zones of weakness, alkaline magmatism, and other tectonism postdating continental fragmentation. Rev. Geophys. 16, 621.

Szatmari, P., 2000. Habitat of Petroleum Along the South Atlantic Margins, in: Mello, M.R., Katz, B.J. (Eds.), Petroleum Systems of South Atlantic Margins: AAPG Memoirs 73. AAPG, pp. 69–75.

The GEBCO_08 Grid, version 20100927, http://www.gebco.net [WWW Document], n.d. URL http://www.gebco.net

Wilson, J.T., 1965. A New Class of Faults and their Bearing on Continental Drift. Nature 207, 343–347.

6

Conclusions

This thesis addresses still open questions in the rifting process and the rift architecture. Specifically, we study the response of rifting to the divergence rate variation and its interaction with inherited shear zones and rheological heterogeneity. We perform these researches by using analogue modelling and field survey. The studied parameters have a general applicability, nevertheless the thesis focus on Central Segment of the South Atlantic Ocean.

A new methodology was developed that allow study lithospheric necking shape evolution and thinning factor distribution through analogue modelling. We apply this technique to characterize the influence of strain-rate on the rift architecture. The influence of rheology, and hence strength, heterogeneity in the lithosphere was address with respect to the basins localization and architecture. Finally, we investigate the possibility of a connection between the spreading in the ocean and tectonic activity in the continent in NE-Brazil.

6.1 First-order role of extensional strain-rate on rift and necking architecture.

We studied the rifting and necking response to plate divergence velocity in analogue models. The geometry of lithosphere necking and the surface deformation was monitored during model evolution by paired top and bottom laser scanning, which provides an effective tool to comprehensively describe the geometric evolution of model rift systems.

The basin architecture and distribution on the model surface shows important differences due to the velocity divergence rate. At slow divergence rate, two distinct wide and deep basins develop in the rifted area separated by a relatively unstretched sector. Conversely, at fast divergence rate several basin develops characterized by low subsidence and severe faulting. The different behaviour of the three models since the early extension is illustrated also in their cross-sectional evolution. Furthermore, plate divergence rate strongly affects the shape of lithosphere necking, too. At low divergence rates, a

sharp cusp develops at the base of the lithosphere on the fixed plate side and only after reaching the lower crust it widens sideward towards the mobile plate. At fast divergence rate, the necking area in the mantle is wider and two subsidiary bulges develop aside the central major one, thus favouring isolation of unstretched blocks.

The deformation rig, having only one mobile wall, imparts an asymmetric extensional kinematic to the models. This deformation asymmetry affects more the position of lithosphere necking with respect to the topography expression of stretched area. Indeed, the major asthenosphere bulge locates below the basin and rift shoulder on the fixed plate side, while the basins on the opposite rift shoulder rest over an almost unstretched lithosphere. The asymmetry of necking is inversely proportional to the strain-rate: necking is strongly asymmetric at slow divergence rate while at fast divergence rate the necking culmination is more centred. The difference in necking shape and asymmetry has implication about the localization (or delocalization) of isotherm upwelling, which in turn has a first-order role on the magmatism distribution.

The combined analysis of the lithosphere base geometry and surface topography, may suggest that plate divergence rate can play an important role on rift dynamics. Experiments at slow divergence rate do not show significant uplift accompanying faulting in the early evolutionary stages and this supports passive rifting. Conversely, rift shoulder strong uplift occurs coevally with faulting in the fast experiments, thus suggesting the inference of a mantle plume-dominated process, i.e. active rifting (e.g. Cruden 1995). Experimental results indicate that fast plate divergence may add, or even be an alternative parameters, to mantle plume activity for producing diagnostic features of active rifting.

Analysis of the thinning factor distribution for the whole lithosphere indicates that the necking area is more localized in the slow models. However, the width of the strongly thinned central belt is narrower in fast experiments, as expected from

the dependence of strength on strain rate in viscous materials. This evidence contributes to solve the apparent contrast between experimental and numerical results.

6.2 Impact of lithospheric heterogeneities on continental rifting evolution

We studied the effects that pre-existing lithospheric inhomogeneities have on the initiation, evolution and final architecture of rift-basins and rifted margins in terms of resulting structural style and subsidence. The experimental programme was designed in relation with the peculiar architecture of SE-Brazil margin, and its conjugate West-Africa margin. In this site the rift propagation has a direction change and the Santos and Campos basins show an very different structural architecture.

The lithospheric-scale analogue modelling has shown the important role exerted by the weak zones within the lithospheric-mantle/lower-crust on the resulting upper crust structural pattern during the rifting process. In particular, analogue models suggest that weak zones located in the mantle have a "far-field" effect on the deformation of the brittle upper crust, driving the direction of rifting propagation. Rheology heterogeneities located within the lower crust have more "local" effects and can have a remarkable impact on the along-margin segmentation, promoting different structural evolution in relation to their rheology.

The final tectono-stratigraphic expression of the experimental rifted margins shows articulated basins with horsts and grabens in response to a relative "hard" rheology, and focused and deeper basins related to a relatively "weak" rheology on the equivalent parts of the conjugate pairs. Interpretation of the model cross-sections provides details on the fault and the sedimentary sequence evolution, highlighting that the development of the upper crustal depocenters is a function of the lower crust rheological inhomogeneities. A weak lower crust rheology promotes a main deep listric half-graben fault and

associated wedge-shaped basin with thick syn-rift sequences. A strong lower crust rheology gives rise to more planar, rotated, domino-type faulted basins, with thinner sequences directly controlled by the individual fault-blocks. Preexisting lithospheric inhomogeneities drive the early stage of the rifting evolution, which results to be dominated by asymmetric rift-basin development. At the later stage of the rift, the differences in initial lower crustal rheology are reduced due to the thinning processes, and an additional pulse of extension focuses the deformation on the central rift area, giving rise to general symmetric ocean-ward rift basins.

Furthermore, the experiments show that during the rifting process sectors of brittle mantle are preserved and can be elevated beneath the developed upper crustal structures. The presence of these brittle upper mantle relicts along extended rifted margins may reduce the assumed internal heat-flow production at the distal/outer-margin parts as they contribute less radiogenic heat production than a misinterpreted equivalent portion of crystalline crust and could act as "isolation lids", reducing the asthenosphere heat transfer at shallower levels. Finally, concerning regional exploration the detailed tectono-stratigraphic outcomes of the performed lithospheric-scale experiments at basin-scale can provide valuable insights and hints of the deep pre-salt play in the Central Segment of South Atlantic.

6.3 Post-rift re-activation of inherited lineament orthogonal to the rift propagation axis.

Inherited lineaments that lie at high angle with respect to the rift propagation axis exert a segmentation of the rift, and are potential site of Transform Fault and, hence, Fracture Zone development. We studied the possibility of reactivation of these long-lived continental structures driven by their ocean prosecution, due to the differential spreading rate of the ridge segment juxtaposed to the Fracture Zone.

The magnetic anomalies show a differential spreading rate

close to the Pernambuco Fracture Zone (PeFZ): that is, in the same time range more oceanic lithosphere was produced in one ridge segment with respect to the adjacent one. The differential spreading rate is not steady-state and shows an alternation of right-lateral and left-lateral shear excess on the Fracture Zone (right-lateral if southern segment is faster than the northern, left-lateral if conversely). We measured the oceanic lithosphere production through the last 83 My , finding at least 5 major inversion on shear-excess kinematic. The last shear inversion is at the chron 5o (10,9 Ma), changing from right-lateral to left-lateral motions. The shear-excess measured as a whole in the last 83,5 My shows a major right-lateral behavior along the PeFZ.

We perform a structural field survey on the Barreiras Formation (Miocene) and post-Barreiras Formation (Quaternary) outcropping along the coast of the Pernambuco State (NE-Brazil), across the Pernambuco Lineament (PeL). Both formation recorded extensional faulting, mainly striking N300 and N040: the former congruent with a right-lateral shear along a N080 lineament, the latter congruent with a left-lateral shear along the same lineament. In details, the older formation (Barreiras-Miocene) is pervasively deformed by faults trending N300, attributable to right-lateral kinematics, conversely the younger formation (post-Barreiras-Quaternary) records only deformation attributable to left-lateral kinematics.

The structural and geophysical data Integrated approach supports the possibility of a shear-excess produced by the oceanic spreading centers, which can be transferred into the continental margin by means of the Pernambuco FZ and the Pernambuco Shear Zone. The Miocene and Quaternary deposits recorded this shear-excess both as brittle deformation and as paleo-liquefaction. Hence, the Pernambuco FZ shear-excess can be the source of the recent seismic activity recorded in the NE-Brazil margin.

References

Afonso, J.C., Ranalli, G., 2004. Crustal and mantle strengths in continental lithosphere: is the jelly sandwich model obsolete? Tectonophysics 394, 221–232.

Agostini, A., Corti, G., Zeoli, A., Mulugeta, G., 2009. Evolution, pattern, and partitioning of deformation during oblique continental rifting: Inferences from lithospheric-scale centrifuge models. Geochemistry, Geophys. Geosystems 10, n/a–n/a.

Alkmim, F.F., n.d. O que faz de um cráton um cráton? O cráton do São Francisco e as revelações almeidianas ao delimitá-lo, Geologia do continente Sul-Americano: Evolução e obra de Fernando Flávio Marques de Almeida.

Alkmim, F.F., Marshak, S., Pedrosa-Soares, A.C., Peres, G.G., Cruz, S.C.P., Whittington, A., 2006. Kinematic evolution of the Araçuaí-West Congo orogen in Brazil and Africa: Nutcracker tectonics during the Neoproterozoic assembly of Gondwana. Precambrian Res. 149, 43–64.

Allen, P.A., Allen, J.R., 2005. Basin Analysis: Principles and Applications, (2nd ed.). ed. Wiley-Blackwell, Hoboken, New Jersey.

Almeida, F.F.M., 1977. O Cráton do São Francisco. Rev. Bras. Geociências 7, 349–364.

Almeida, F.F.M., 1981. O Cráton do Paramirim e suas relações com do São Francisco, in: Anais SimpCraton São Francisco E Faixas Marginais, Salvador (1981). pp. 1 – 10.

Alsop, G.I., Holdsworth, R.E., 2004. Shear zones -- an introduction and overview. Geol. Soc. London, Spec. Publ. 224, 1–9.

Aslanian, D., Moulin, M., Olivet, J., Unternehr, P., Matias, L., Bache, F., Rabineau, M., Nouzé, H., Klingelheofer, F., Contrucci, I., Labails, C., 2009. Brazilian and African passive margins of the Central Segment of the South Atlantic Ocean: Kinematic constraints. Tectonophysics 468, 98–112.

Autin, J., Bellahsen, N., Husson, L., Beslier, M.-O., Leroy, S., D'Acremont, E., 2010. Analog models of oblique rifting in a cold lithosphere. Tectonics 29, n/a–n/a.

Banks, N.L., Bardwell, K.A., Musiwa, S., 1995. Karoo Rift Basins of the Luangwa Valley, Zambia, Hydrocarbon habitat in rift basins. Geological Society, London; Special Publication, 80.

Barbier, F., Duverge, J., Le Pichon, X., 1986. (Deep structure of the north Biscay margin. Implications on the rifting mechanism and the formation of the continental margin)., Bulletin - Centres de Recherches Exploration-Production Elf- Aquitaine.

Bassi, G., 1995. Relative importance of strain rate and rheology for the mode of continental extension. Geophys. J. Int. 122, 195–210.

Beaumont, C., Keen, C.E., Boutilier, R., 1982. On the evolution of rifted continental margins: comparison of models and observations for the Nova Scotian margin (Canada)., Geophysical Journal.

Beltrando, M., Rubatto, D., Manatschal, G., 2010. From passive margins to orogens: The link between ocean-continent transition zones and (ultra)high-pressure metamorphism. Geology 38, 559–562.

Benes, V., Davy, P., 1996. Modes of continental lithospheric extension: Experimental verification of strain localization processes. Tectonophysics 254, 69–87.

Benes, V., Davy, P., 1996. Modes of continental lithospheric extension: experimental verification of strain localization processes. Tectonophysics 254, 69–87.

Bezerra, F.H.R., Brito Neves, B.B., Corrêa, A.C.B., Barreto, A.M.F., Suguio, K., 2008. Late Pleistocene tectonic-geomorphological development within a passive margin — The Cariatá trough, northeastern Brazil. Geomorphology 97, 555–582.

Bezerra, F.H.R., do Nascimento, A.F., Ferreira, J.M., Nogueira, F.C., Fuck, R.A., Neves, B.B.B., Sousa, M.O.L., 2011. Review of active faults in the Borborema Province, Intraplate South America — Integration of seismological and paleoseismological data. Tectonophysics 510, 269–290.

Blaich, O.A., Faleide, J.I., Tsikalas, F., 2011. Crustal breakup and continent-ocean transition at South Atlantic conjugate margins. J. Geophys. Res. 116, B01402.

Blaich, O.A., Faleide, J.I., Tsikalas, F., Franke, D., León, E., 2009. Crustal-scale architecture and segmentation of the Argentine margin and its conjugate off South Africa. Geophys. J. Int. 178, 85–105.

Blaich, O.A., Faleide, J.I., Tsikalas, F., Lilletveit, R., Chiossi, D., Brockbank, P., Cobbold, P., 2010. Structural architecture and nature of the continent–ocean transitional domain at the Camamu and Almada Basins (northeastern Brazil) within a conjugate margin setting, in: Petroleum Geology: From Mature Basins to New Frontiers - Proceedings of the 7th Conference, Geological Society, London. pp. 1 – 17.

Blaich, O.A., Tsikalas, F., Faleide, J.I., 2008. Northeastern Brazilian margin: Regional tectonic evolution based on integrated analysis of seismic reflection and potential field data and modelling. Tectonophysics 458, 51–67.

Boillot, G., Recq, M., Winterer, E.L., Meyer, A.W., Applegate, J., Baltuck, M., Bergen, J.A., Comas, M.C., Davies, T.A., Dunham, K., Evans, C.A., Girardeau, J., Goldberg, G., Haggerty, J., Jansa, L.F., Johnson, J.A., Kasahara, J., Loreau, J.P., Luna-Sierra, E., Moullade, M., Ogg, J., Sarti, M., Thurow, J., Williamson, M., 1987. Tectonic denudation of the upper mantle along passive margins: a model based on drilling results (ODP leg 103, western Galicia margin, Spain). Tectonophysics 132, 335–342.

Bonatti, E., 1978. Vertical tectonism in oceanic fracture zones. Earth Planet. Sci. Lett. 37, 369–379.

Bonatti, E., 1985. Punctiform initiation of seafloor spreading in the Red Sea during transition from a continental to an oceanic rift. Nature 316, 33–37.

Bonini, M., Corti, G., Ventisette, C. Del, Manetti, P., Mulugeta, G., Sokoutis, D., 2007. Modelling the lithospheric rheology control on the Cretaceous rifting in West Antarctica. Terra Nov. 19, 360–366.

Bonini, M., Sokoutis, D., Mulugeta, G., Boccaletti, M., Corti, G., Innocenti, F., Manetti, P., Mazzarini, F., 2001. Dynamics of magma emplacement in centrifuge models of continental extension with implications for flank volcanism. Tectonics 20, 1053–1065.

Bosworth, W., 1985. Geometry of propagating continental rifts. Nature 316, 625–627.

Braun, J., Beaumont, C., 1989. A physical explanation of the relation between flank uplifts and the breakup unconformity at rifted continental margins. Geology 17, 760–764.

Breivik, A.J., Faleide, J.I., Mjelde, R., Flueh, E.R., 2009. Magma productivity and early seafloor spreading rate correlation on the northern Vøring Margin, Norway — Constraints on mantle melting. Tectonophysics 468, 206–223.

Brun, J.-P., 1999. Narrow rifts versus wide rifts: Inferences for the mechanics of

rifting from laboratory experiments. Philos. Trans. R. Soc. A Math. Phys. Eng. Sci. 357, 695–712.
Brun, J.-P., 2002. Deformation of the continental lithosphere: Insights from brittle-ductile models. Geol. Soc. London, Spec. Publ. 200, 355–370.
Brun, J.P., Beslier, M.O., 1996. Mantle exhumation at passive margins. Earth Planet. Sci. Lett. 142, 161–173.
Buck, W.R., 1991. Modes of continental lithospheric extension. J. Geophys. Res. 96, 20–178.
Callot, J.-P., Geoffroy, L., Brun, J.-P., 2002. Development of volcanic passive margins: Three-dimensional laboratory models. Tectonics 21, 2–1–2–13.
Callot, J.-P., Grigné, C., Geoffroy, L., Brun, J.-P., 2001. Development of volcanic passive margins: Two-dimensional laboratory models. Tectonics 20, 148–159.
Campanha, G.A.C., n.d. O lineamento Além Paraíba na área de Três Rios (RJ), Revista Brasileira de Geociências.
Campanha, G.A.C., de Brito Neves, B.B., 2004. Frontal and oblique tectonics in the Brazilian shield. Episodes 27, 255–259.
Carminatti, M., Wolff, B., Gamboa, L., 2008. New exploratory frontiers in Brazil, in: World Petroleum Congress, 19. Madrid, Spain, WPC Proceedings. p. 11.
Clifton, A.E., Kattenhorn, S. a., 2006. Structural architecture of a highly oblique divergent plate boundary segment. Tectonophysics 419, 27–40.
Cloetingh, S., van Wees, J.D., van der Beek, P. a., Spadini, G., 1995a. Role of pre-rift rheology in kinematics of extensional basin formation: constraints from thermomechanical models of Mediterranean and intracratonic basins. Mar. Pet. Geol. 12, 793–807.
Cloetingh, S., van Wees, J.D., van der Beek, P.A., Spadini, G., 1995b. Role of pre-rift rheology in kinematics of extensional basin formation: constraints from thermomechanical models of Mediterranean and intracratonic basins. Mar. Pet. Geol. 12, 793–807.
Close, D.I., Watts, A.B., Stagg, H.M.J., 2009. A marine geophysical study of the Wilkes Land rifted continental margin, Antarctica. Geophys. J. Int. 177, 430–450.
Cobbold, P.R., Meisling, K.E., Mount, V.S., 2001. Reactivation of an obliquely rifted margin, Campos and Santos basins, southeastern Brazil. Am. Assoc. Pet. Geol. Bull. 85, 1925–1944.
Collette, B.J., Slootweg, A.P., Twigt, W., 1979. Mid-Atlantic Ridge crest topography between 12° and 15°N. Earth Planet. Sci. Lett. 42, 103–108.
Collettini, C., Barchi, M.R., 2002. A low-angle normal fault in the Umbria region (Central Italy): a mechanical model for the related microseismicity. Tectonophysics 359, 97–115.
Collettini, C., Niemeijer, A., Viti, C., Marone, C., 2009. Fault zone fabric and fault weakness. Nature 462, 907–10.
Contreras, J., Zühlke, R., Bowman, S., Bechstädt, T., 2010. Seismic stratigraphy and subsidence analysis of the southern Brazilian margin (Campos, Santos and Pelotas basins). Mar. Pet. Geol. 27, 1952–1980.
Contrucci, I., Matias, L., Moulin, M., Géli, L., Klingelhofer, F., Nouzé, H., Aslanian, D., Olivet, J.-L., Réhault, J.-P., Sibuet, J.-C., 2004. Deep structure of the West African continental margin (Congo, Zaïre, Angola), between 5°S and 8°S, from reflection/refraction seismics and gravity data. Geophys. J. Int. 158, 529–553.
Corti, G., 2003. Transition from continental break-up to punctiform seafloor

spreading: How fast, symmetric and magmatic. Geophys. Res. Lett. 30, 1604.
Corti, G., 2004. Centrifuge modelling of the influence of crustal fabrics on the development of transfer zones: insights into the mechanics of continental rifting architecture. Tectonophysics 384, 191–208.
Corti, G., 2008. Control of rift obliquity on the evolution and segmentation of the main Ethiopian rift. Nat. Geosci. 1, 258–262.
Corti, G., 2012. Evolution and characteristics of continental rifting: Analog modeling-inspired view and comparison with examples from the East African Rift System. Tectonophysics 522-523, 1–33.
Corti, G., Bonini, M., Conticelli, S., Innocenti, F., Manetti, P., Sokoutis, D., 2003. Analogue modelling of continental extension: a review focused on the relations between the patterns of deformation and the presence of magma. Earth-Science Rev. 63, 169–247.
Corti, G., Bonini, M., Innocenti, F., Manetti, P., Mulugeta, G., 2001. Centrifuge models simulating magma emplacement during oblique rifting. J. Geodyn. 31, 557–576.
Corti, G., Calignano, E., Petit, C., Sani, F., 2011. Controls of lithospheric structure and plate kinematics on rift architecture and evolution: An experimental modeling of the Baikal rift. Tectonics 30, n/a–n/a.
Corti, G., Ranalli, G., Mulugeta, G., Agostini, A., Sani, F., Zugu, A., 2010. Control of the rheological structure of the lithosphere on the inward migration of tectonic activity during continental rifting. Tectonophysics 490, 165–172.
Cunningham, D., Alkmim, F.F., Marshak, S., 1998. A structural transect across the coastal mobile belt in the Brazilian Highlands (latitude 20°S): the roots of a Precambrian transpressional orogen. Precambrian Res. 92, 251–275.
Dauteuil, O., Brun, J.-P., 1993. Oblique rifting in a slow-spreading ridge. Nature 361, 145–148.
Davis, M., Kusznir, N., 2002. Are buoyancy forces important during the formation of rifted margins? Geophys. J. Int. 149, 524–533.
Davis, M., Kusznir, N., 2004. Depth-Dependent Lithospheric Stretching at Rifted Continental Margins, in: Karner, G.D., Al., E. (Eds.), Rheology and Deformation of the Lithosphere at Continental Margins. Columbia University Press, New York, pp. 92–137.
DAVISON, I.A.N., 1997. Wide and narrow margins of the Brazilian South Atlantic. J. Geol. Soc. London. 154, 471–476.
Davison, I.A.N., 2007. Geology and tectonics of the South Atlantic Brazilian salt basins 345–359.
Davy, P., Cobbold, P.R., 1991. Experiments on shortening of a 4-layer model of the continental lithosphere. Tectonophysics 188, 1–25.
Dawers, N.H., Underhill, J.R., 2000. The role of fault interaction and linkage in controlling synrift stratigraphic sequences: Late Jurassic, Statfjord East area, northern North Sea. Am. Assoc. Pet. Geol. Bull. 84, 45–64.
De Paula, O.B., Vidotti, R.M., n.d. Estimativa da Descontinuidade de Mohorovicic a partir de dados gravimétricos - Costa Leste Brasileira, VII Cong. Int. Soc. Bras. Geof., Salvador, BA. Exp. Abs., SBGf.
De Wit, M.J., de Brito Neves, B.B., Trouw, R.A.J., Pankhurst, R.J., 2008. Pre-Cenozoic correlations across the South Atlantic region: (the ties that bind). Geol. Soc. London, Spec. Publ. 294, 1–8.

Demercian, L.S., 1996. A halocinese na evolucão do Sul da Bacia de Santos do Aptiano ao Cretáceo Superior. Universidade Federal do Rio Grande do Sul, Porto Alegre, Brazil.

Direen, N.G., Borissova, I., Stagg, H.M.J., Colwell, J.B., Symonds, P.A., 2007. Nature of the continent-ocean transition zone along the southern Australian continental margin: A comparison of the Naturaliste Plateau, SW Australia, and the central Great Australian Bight sectors, in: KARNER, G.D., MANATSCHAL, G., PINHEIRO, L.M. (Eds.), Imaging, Mapping and Modelling Continental Lithosphere Extension and Breakup. Geological Society, London, Special Publications, 282. Geological Society of London, pp. 235–261.

Direen, N.G., Stagg, H.M.J., Symonds, P.A., Colwell, J.B., 2011. Dominant symmetry of a conjugate southern Australian and East Antarctic magma-poor rifted margin segment. Geochemistry, Geophys. Geosystems 12, n/a–n/a.

Direen, N.G., Stagg, H.M.J., Symonds, P.A., Norton, I.O., 2012. Variations in rift symmetry: cautionary examples from the Southern Rift System (Australia-Antarctica). Geol. Soc. London, Spec. Publ. 369, 453–475.

Doglioni, C., Carminati, E., Bonatti, E., 2003. Rift asymmetry and continental uplift. Tectonics 22, n/a–n/a.

Driscoll, N.W., Hogg, J.R., Christie-Blick, N., Karner, G.D., 1995. Extensional tectonics in the Jeanne d'Arc Basin, offshore Newfoundland: implications for the timing of break-up between Grand Banks and Iberia, The tectonics, sedimentation and palaeoceanography of the North Atlantic region. Geological Society, London; Special Publication, 90.

Dupré, S., 2003. Integrated tectonic study of the South Gabon Margin. Insights on the rifting style from seismic, well and gravity data analysis and numerical modelling. Netherlands Research School of Sedimentary Geology Thesis, 90-9017055-3 Vrije Universiteit, Amsterdam.

Dupré, S., Bertotti, G., Cloetingh, S., 2007. Tectonic history along the South Gabon Basin: Anomalous early post-rift subsidence. Mar. Pet. Geol. 24, 151–172.

Ebinger, C., 2005. Continental break-up: The East African perspective. Astron. Geophys. 46, 2.16–2.21.

Ebinger, C., 2005. Continental break-up: The East African perspective. Astron. Geophys. 46, 16–21.

EBINGER, C.J., 1989. Tectonic development of the western branch of the East African rift system. Geol. Soc. Am. Bull. 101, 885–903.

Ebinger, C.J., Deino, A.L., Drake, R.E., Tesha, A.L., 1989. Chronology of volcanism and rift basin propagation: Rungwe volcanic province, East Africa, Journal of Geophysical Research.

Einsele, G., 1992. Sedimentary Basins - Evolution, Facies, and Sediment Budget, 1st ed. Springer-Verlag, New York.

Faccenna, C., Davy, P., Brun, J.P., Funiciello, R., Giardini, D., Mattei, M., Nalpas, T., 1996. The dynamics of back-arc extension: An experimental approach to the opening of the Tyrrhenian Sea. Geophys. J. Int. 126, 781–795.

Fadaie, K., Ranalli, G., 1990. Rheology of the lithosphere in the East African Rift System, Geophysical Journal International.

Faulds, J.E., Varga, R.J., 1998. Special Paper 323: Accommodation zones and transfer zones; the regional segmentation of the Basin and Range Province, Special Paper of the Geological Society of America. Geological Society of America.

Ferreira, J.M., Bezerra, F.H.R., Sousa, M.O.L., do Nascimento, A.F., Sá, J.M., França, G.S., 2008a. The role of Precambrian mylonitic belts and present-day stress field in the coseismic reactivation of the Pernambuco lineament, Brazil. Tectonophysics 456, 111–126.

Ferreira, J.M., Bezerra, F.H.R., Sousa, M.O.L., do Nascimento, A.F., Sá, J.M., França, G.S., 2008b. The role of Precambrian mylonitic belts and present-day stress field in the coseismic reactivation of the Pernambuco lineament, Brazil. Tectonophysics 456, 111–126.

Fletcher, R.J., 2009. Mechanisms of Continental Lithosphere Thinning and Rifted Margin Formation. (PhD thesis) University of Liverpool.

Fossen, H., 2010. Structural Geology. Cambridge University Press.

Fraser, S.I., Fraser, A.J., Lentini, M.R., Gawthorpe, R.L., International, C., Post, T., Central, O., Boulevard, P.O., 2007. Return to rifts – the next wave : fresh insights into the petroleum geology of global rift basins.

Garcia, S.F. de M., Letouzey, J., Rudkiewicz, J.-L., Danderfer Filho, A., Frizon de Lamotte, D., 2012. Structural modeling based on sequential restoration of gravitational salt deformation in the Santos Basin (Brazil). Mar. Pet. Geol. 35, 337–353.

Gawthorpe, R.L., Leeder, M.R., 2000. Tectono-sedimentary evolution of active extensional basins. Basin Res. 12, 195–218.

Gibbs, A.D., 1983. Balanced cross-section construction from seismic sections in areas of extensional tectonics. J. Struct. Geol. 5, 153–160.

Gladczenko, T.P., Skogseid, J., Eldhom, O., 1998. Namibia volcanic margin. Mar. Geophys. Res. 20, 313–341.

Gomes, P.O., Kilsdonk, B., Minken, J., Grow, T., Barragan, R., 2009. The outer high of the Santos Basin, southern São Paulo Plateau, Brazil: pre-salt exploration outbreak, paleogeographic setting, and evolution of the syn-rift structures, in: Search and Discovery, 10193.

Gomes, P.O., Parry, J., Martins, W., 2002. EXTENDED ABSTRACT: The Outer High of the Santos Basin, Southern São Paulo Plateau, Brazil: Tectonic Setting, Relation to Volcanic Events and some Comments on Hydrocarbon Potential; #90022 (2002).

Gray, D.R., Foster, D. a., Meert, J.G., Goscombe, B.D., Armstrong, R., Trouw, R. a. J., Passchier, C.W., 2008. A Damara orogen perspective on the assembly of southwestern Gondwana. Geol. Soc. London, Spec. Publ. 294, 257–278.

Groshong, R.H., 2006. Structural Validation, Restoration and Prediction: 3-D Structural Geology-A Practical Guide to Surface and Subsurface Map Interpretation.

Guiraud, M., Buta-Neto, A., Quesne, D., 2010. Segmentation and differential post-rift uplift at the Angola margin as recorded by the transform-rifted Benguela and oblique-to-orthogonal-rifted Kwanza basins. Mar. Pet. Geol. 27, 1040–1068.

Haralyi, N.L.E., Hasui, Y., 1982. The gravimetric information and the Archean-Proterozoic structural framework of eastern Brazil, in: ISAP, Salvador, R. (Eds.), Brasileira Geocie Paulo, 12, Nos. 1–3,. pp. 160–166.

Heilbron, M., Mohriak, W.U., Valeriano, C.M., Milani, E.J., Almeida, J., 2000. From collision to extension: the roots of southeastern continental margin of Brazil, in: Mohriak, W.; Taiwani, M. (Ed.), Atlantic Rifts and Continental Margins -

Geophysical Monograph Series Vol. 115 P. 1-354. pp. 1 – 32.
Heilbron, M., Pedrosa-Soares, A., Neto, M., da Silva, L., Trouw, R., Janasi, V., 2004. Brasiliano Orogens in Southeast and South Brazil. J. Virtual Explor. 17.
Heilbron, M., Valeriano, C.M., Tassinari, C.C.G., Almeida, J., Tupinamba, M., Siga, O., Trouw, R., 2008. Correlation of Neoproterozoic terranes between the Ribeira Belt, SE Brazil and its African counterpart: comparative tectonic evolution and open questions. Geol. Soc. London, Spec. Publ. 294, 211–237.
Heine, C., Zoethout, J., Müller, R.D., 2013. Kinematics of the South Atlantic rift. Solid Earth 4, 215–253.
Hoffman, P.F., 1991. Did the breakout of Laurentia turn Gondwanaland inside-out? Science (80-.). 252, 1409–1412.
Hopper, J.R., Buck, W.R., 1998. Styles of extensional decoupling.
Hubbert, M.K., 1937. Theory of scale models as applied to the study of geologic structures. Geol. Soc. Am. Bull. 48, 1459–1519.
Huismans, R.S., Beaumont, C., 2008. Complex rifted continental margins explained by dynamical models of depth-dependent lithospheric extension. Geology 36, 163.
Jackson, J.A., White, N.J., 1989. Normal faulting in the upper continental crust: observations from regions of active extension. J. Struct. Geol. 11, 15–36.
Jacopo, N.L., 2001. Don't worry child. in: Work hard, play harder, eds. Lagomarsino, D., Special Pubblication, Roma. 1-∞
Karner, G.D., Driscoll, N.W., 1999. Tectonic and stratigraphic development of the West African and eastern Brazilian Margins: insights from quantitative basin modelling. Geol. Soc. London, Spec. Publ. 153, 11–40.
Karner, G.D., Gamboa, L. a. P., 2007. Timing and origin of the South Atlantic pre-salt sag basins and their capping evaporites. Geol. Soc. London, Spec. Publ. 285, 15–35.
Kirby, S.H., 1983. Rheology of the lithosphere. Rev. Geophys. 21, 1458.
Kusznir, N.J., Karner, G.D., 2007. Continental lithospheric thinning and breakup in response to upwelling divergent mantle flow: application to the Woodlark, Newfoundland and Iberia margins. Geol. Soc. London, Spec. Publ. 282, 389–419.
Lavier, L.L., Manatschal, G., 2006. A mechanism to thin the continental lithosphere at magma-poor margins. Nature 440, 324–8.
Lagomarsino, D., 2004. Rise and fall of an accademic drifting. Pers. Comm.
Lentini, M.R., Fraser, S.I., Sumner, H.S., Davies, R.J., 2010. Geodynamics of the central South Atlantic conjugate margins: implications for hydrocarbon potential. Pet. Geosci. 16, 217–229.
Lezzar, K.E., Tiercelin, J.-J., Le Turdu, C., Cohen, A.S., Reynolds, D.J., Le Gall, B., Scholz, C.A., 2002. Control of normal fault interaction on the distribution of major Neogene sedimentary depocenters, Lake Tanganyika, East African rift. Am. Assoc. Pet. Geol. Bull. 86, 1027–1059.
Ligi, M., Bonatti, E., Bortoluzzi, G., Cipriani, A., Cocchi, L., Caratori Tontini, F., Carminati, E., Ottolini, L., Schettino, A., 2012. Birth of an ocean in the Red Sea: Initial pangs. Geochemistry, Geophys. Geosystems 13, n/a–n/a.
Lima Filho, M.F.D., Barbosa, J.A., Souza, E.M., 2006. EVENTOS TECTÔNICOS E SEDIMENTARES NAS BACIAS DE PERNAMBUCO E DA PARAÍBA: IMPLICAÇÕES NO QUEBRAMENTO DO GONDWANA E CORRELAÇÃO COM A BACIA DO RIO

MUNI. Geociências 25, 117–126.
Lima, M.G., 2008. The weathering history of the Oriental Borborema Province, Northeastern Brazil: Paleoclimatic and tectonic implications. (PhD Thesis). Univ. Fed. Rio Grande do Norte, Natal, Brazil.(in Portuguese).
Lima Neto, H.C., Ferreira, J.M., Bezerra, F.H.R., Assumpção, M.S., do Nascimento, A.F., Sousa, M.O.L., Menezes, E.A.S., 2013. Upper crustal earthquake swarms in São Caetano: Reactivation of the Pernambuco shear zone and trending branches in intraplate Brazil. Tectonophysics 608, 804–811.
Lin, A.T., Watts, A.B., Hesselbo, S.P., 2003. Cenozoic stratigraphy and subsidence history of the South China Sea margin in the Taiwan region. Basin Res. 15, 453–478.
Lister, G.S., Etheridge, M.A., Symonds, P.A., 1986. Detachment faulting and the evolution of passive continental margins., Geology.
Litak, R.K., Barazangi, M., Brew, G., Sawaf, T., Al-Imam, A., Al-Youssef, W., 1998. Structure and evolution of the petroliferous Euphrates graben system, southeast Syria. Am. Assoc. Pet. Geol. Bull. 82, 1173–1190.
Lopes, A.E. V., Assumpção, M., do Nascimento, A.F., Ferreira, J.M., Menezes, E. a. S., Barbosa, J.R., 2010. Intraplate earthquake swarm in Belo Jardim, NE Brazil: reactivation of a major Neoproterozoic shear zone (Pernambuco Lineament). Geophys. J. Int. 180, 1303–1312.
Lundin, E.R., Dore, A.G., 2011. Hyperextension, serpentinization, and weakening: A new paradigm for rifted margin compressional deformation. Geology 39, 347–350.
Manatschal, G., Bernoulli, D., 1999. Architecture and tectonic evolution of nonvolcanic margins: Present-day Galicia and ancient Adria. Tectonics 18, 1099–1119.
Mart, Y., Dauteuil, O., 2000. Analogue experiments of propagation of oblique rifts. Tectonophysics 316, 121–132.
Matos, R.M.D. de, 1992. The Northeast Brazilian Rift System. Tectonics 11, 766–791.
McClay, K.R., Dooley, T., Whitehouse, P., Mills, M., 2002. 4-D evolution of rift systems: Insights from scaled physical models. Am. Assoc. Pet. Geol. Bull. 86, 935–959.
McClay, K.R., White, M.J., 1995. Analogue modelling of orthogonal and oblique rifting. Mar. Pet. Geol. 12, 137–151.
McKenzie, D., 1978. Some remarks on the development of sedimentary basins. Earth Planet. Sci. Lett. 40, 25–32.
Meisling, K.E., Cobbold, P.R., Mount, V.S., 2001. Segmentation of an obliquely rifted margin, Campos and Santos basins, southeastern Brazil. Am. Assoc. Pet. Geol. Bull. 85, 1903–1924.
Menzies, M.A., Klemperer, S.L., Ebinger, C.J., Baker, J., 2002. Characteristics of volcanic rifted margins 1–14.
Michon, L., Merle, O., 2003. Mode of lithospheric extension: Conceptual models from analogue modeling. Tectonics 22, n/a–n/a.
Michon, L., Sokoutis, D., 2005. Interaction between structural inheritance and extension direction during graben and depocentre formation: An experimental approach. Tectonophysics 409, 125–146.
Mohriak, W., Nemcok, M., Enciso, G., 2008. South Atlantic divergent margin evolution: rift-border uplift and salt tectonics in the basins of SE Brazil. Geol. Soc. London, Spec. Publ. 294, 365–398.

Mohriak, W.U., Lira Rabelo, J., De Matos, R.D., De Barros, M.C., 1995. Deep seismic reflection profiling of sedimentary basins offshore Brazil: Geological objectives and preliminary results in the Sergipe Basin. J. Geodyn. 20, 515–539.
Mohriak, W.U., Nobrega, M., Odegard, M.E., Gomes, B.S., Dickson, W.G., 2010. Geological and geophysical interpretation of the Rio Grande Rise, south-eastern Brazilian margin: extensional tectonics and rifting of continental and oceanic crusts. Pet. Geosci. 16, 231–245.
Mohriak, W.U., Rosendahl, B.R., 2003. Transform zones in the South Atlantic rifted continental margins. Geol. Soc. London, Spec. Publ. 210, 211–228.
Morley, C.K., 1999a. How successful are analogue models in addressing the influence of pre-existing fabrics on rift structure? J. Struct. Geol. 21, 1267–1274.
Morley, C.K., 1999b. Patterns of displacement along large normal faults: Implications for basin evolution and fault propagation, based on examples from east Africa. AAPG Bull. (American Assoc. Pet. Geol. 83, 613–634.
Morley, C.K., Haranya, C., Phoosongsee, W., Pongwapee, S., Kornsawan, A., Wonganan, N., 2004. Activation of rift oblique and rift parallel pre-existing fabrics during extension and their effect on deformation style: examples from the rifts of Thailand. J. Struct. Geol. 26, 1803–1829.
Morley, C.K., Nelson, R.A., Patton, T.L., Munn, S.G., 1990. Transfer zones in the East African rift system and their relevance to hydrocarbon exploration in rifts. Am. Assoc. Pet. Geol. Bull. 74, 1234–1253.
Moulin, M., Aslanian, D., Olivet, J.-L., Contrucci, I., Matias, L., Géli, L., Klingelhoefer, F., Nouzé, H., Réhault, J.-P., Unternehr, P., 2005. Geological constraints on the evolution of the Angolan margin based on reflection and refraction seismic data (ZaïAngo project). Geophys. J. Int. 162, 793–810.
Moulin, M., Aslanian, D., Rabineau, M., Patriat, M., Matias, L., 2012. Kinematic keys of the Santos-Namibe basins. Geol. Soc. London, Spec. Publ. 369, 91–107.
Moulin, M., Aslanian, D., Unternehr, P., 2010. A new starting point for the South and Equatorial Atlantic Ocean. Earth-Science Rev. 98, 1–37.
Müller, R.D., Sdrolias, M., Gaina, C., Roest, W.R., 2008. Age, spreading rates, and spreading asymmetry of the world's ocean crust. Geochemistry, Geophys. Geosystems 9, n/a–n/a.
Müller, R.D., Sdrolias, M., Gaina, C., Steinberger, B., Heine, C., 2008. Long-term sea-level fluctuations driven by ocean basin dynamics. Science 319, 1357–62.
Nelson, R.A., Patton, T.L., Morley, C.K., 1992. Rift-segment interaction and its relation to hydrocarbon exploration in continental rift systems, American Association of Petroleum Geologists Bulletin.
Nestola, Y., Storti, F., Bedogni, E., Cavozzi, C., 2013. Shape evolution and finite deformation pattern in analog experiments of lithosphere necking. Geophys. Res. Lett. 40, 5052–5057.
Nielsen, T.K., Hopper, J.R., 2004. From rift to drift: Mantle melting during continental breakup. Geochemistry, Geophys. Geosystems 5, n/a–n/a.
Nogueira, F.C., Bezerra, F.H.R., Fuck, R.A., 2010. Quaternary fault kinematics and chronology in intraplate northeastern Brazil. J. Geodyn. 49, 79–91.
Ojeda, H.A.O., 1982. Structural Framework, Stratigraphy, and Evolution of Brazilian Marginal Basins. Am. Assoc. Pet. Geol. Bull. 66, 732–749.
Oreiro, S.G., Cupertino, J.A., Szatmari, P., Filho, A.T., 2008. Influence of pre-salt alignments in post-Aptian magmatism in the Cabo Frio High and its

surroundings, Santos and Campos basins, SE Brazil: An example of non-plume-related magmatism. J. South Am. Earth Sci. 25, 116–131.
Paul, D., Mitra, S., 2013. Experimental models of transfer zones in rift systems. Am. Assoc. Pet. Geol. Bull. 97, 759–780.
Pedrosa-Soares, A.C., Noce, C.M., Alkmim, F.F., Silva, L.C., Babinski, M., Cordani, U., Castañeda, C., 2007. Orógeno Araçuaí: síntese do conhecimento 30 anos após Almeida 1977. Geonomos 15, 1–16.
Pereira, R., Alves, T.M., 2011. Margin segmentation prior to continental break-up: A seismic–stratigraphic record of multiphased rifting in the North Atlantic (Southwest Iberia). Tectonophysics 505, 17–34.
Peres, G.G., Alkmim, F.F., Jordt-Evangelista, H., 2004. The southern Araçuaí belt and the Dom Silvério Group: Geologic architecture and tectonic significance. An. Acad. Bras. Cienc. 76, 771–790.
Peron-Pinvidic, G., Manatschal, G., 2010. From microcontinents to extensional allochthons: witnesses of how continents rift and break apart? Pet. Geosci. 16, 189–197.
Péron-Pinvidic, G., Manatschal, G., Minshull, T.A., Sawyer, D.S., 2007. Tectonosedimentary evolution of the deep Iberia-Newfoundland margins: Evidence for a complex breakup history. Tectonics 26, n/a–n/a.
Peron-Pinvidic, G., Manatschal, G., Osmundsen, P.T., 2013. Structural comparison of archetypal Atlantic rifted margins: A review of observations and concepts. Mar. Pet. Geol. 43, 21–47.
Péron-Pinvidic, G., Van Wijk, J., Shillington, D.J., Gernigon, L., 2009. An introduction to the Tectonophysics Special Issue "Role of magmatism in continental lithosphere extension". Tectonophysics 468, 1–5.
Prosser, S., 1993. Rift-related linked depositional systems and their seismic expression. Geol. Soc. London, Spec. Publ. 71, 35–66.
Quirk, D.G., Schodt, N., Lassen, B., Ings, S.J., Hsu, D., Hirsch, K.K., Von Nicolai, C., 2012. Salt tectonics on passive margins: examples from Santos, Campos and Kwanza basins. Geol. Soc. London, Spec. Publ. 363, 207–244.
Ramberg, H., 1981. Gravity, Deformation and the Earth's Crust in Theory, Experiments and Geologic Application, Second. ed. Academic Press, London.
Ranalli, G., 1995. Rheology of the Earth,, 2nd ed. ed. London, Glasgow, Weinheim, New York, Tokyo, Melbourne, Madras: Chapman & Hall.
Ranalli, G., Murphy, D.C., 1987. Rheological stratification of the lithosphere. Tectonophysics 132, 281–295.
Ranero, C.R., Pérez-Gussinyé, M., 2010. Sequential faulting explains the asymmetry and extension discrepancy of conjugate margins. Nature 468, 294–9.
Ravnas, R., Nottvedt, A., Steel, R.J., Windelstad, J., 2000. Syn-rift sedimentary architectures in the Northern North Sea. Geol. Soc. London, Spec. Publ. 167, 133–177.
Reston, T.J., 2007. Extension discrepancy at North Atlantic nonvolcanic rifted margins: Depth-dependent stretching or unrecognized faulting? Geology 35, 367.
Reston, T.J., 2009. The structure, evolution and symmetry of the magma-poor rifted margins of the North and Central Atlantic: A synthesis. Tectonophysics 468, 6–27.
Reston, T.J., 2010. The opening of the central segment of the South Atlantic:

symmetry and the extension discrepancy. Pet. Geosci. 16, 199–206.
Reston, T.J., Leythaeuser, T., Booth-Rea, G., Sawyer, D., Klaeschen, D., Long, C., 2007. Movement along a low-angle normal fault: The S reflector west of Spain. Geochemistry, Geophys. Geosystems 8, n/a–n/a.
Reston, T.J., Pérez-Gussinyé, M., 2007. Lithospheric extension from rifting to continental breakup at magma-poor margins: rheology, serpentinisation and symmetry. Int. J. Earth Sci. 96, 1033–1046.
Reynisson, R.F., Ebbing, J., Lundin, E., Osmundsen, P.T., 2010. Petroleum Geology: From Mature Basins to New Frontiers—Proceedings of the 7th Petroleum Geology Conference, Geological Society, London, Petroleum Geology Conference series. Geological Society of London.
Rosenbaum, G., Weinberg, R.F., Regenauer-Lieb, K., 2008a. The geodynamics of lithospheric extension. Tectonophysics 458, 1–8.
Rosenbaum, G., Weinberg, R.F., Regenauer-Lieb, K., 2008b. The geodynamics of lithospheric extension. Tectonophysics 458, 1–8.
Rosenbaum, G., Weinberg, R.F., Regenauer-Lieb, K., Tsikalas, F., Faleide, J.I., Kusznir, N.J., 2008c. Along-strike variations in rifted margin crustal architecture and lithosphere thinning between northern Vøring and Lofoten margin segments off mid-Norway. Tectonophysics 458, 68–81.
Rosendahl, B.R., 1986. Structural expressions of rifting: lessons from Lake Tanganyika, Africa., Sedimentation in the African Rifts. Blackwell Scientific; Geological Society Special Publication, 25.
Rosendahl, B.R., 1987. Architecture of continental rifts with special reference to East Africa., Annual review of earth and planetary sciences. Vol. 15. Annual Reviews Inc.
Rosendahl, B.R., Mohriak, W.U., Odegard, M.E., Turner, J.P., Dickson, W.G., 2005. West African and Brazilian conjugate margins: crustal types, architecture, and plate configurations, in: Petroleum Systems of Divergent Continental Margin Basins. 25th Gulf Coast Section, SEPM Research Conference.
Rossetti, D.F., Bezerra, F.H.R., Dominguez, J.M.L., 2013. Late Oligocene–Miocene transgressions along the equatorial and eastern margins of Brazil. Earth-Science Rev. 123, 87–112.
Rossetti, D.F., Bezerra, F.H.R., Góes, A.M., Valeriano, M.M., Andrades-Filho, C.O., Mittani, J.C.R., Tatumi, S.H., Brito-Neves, B.B., 2011. Late Quaternary sedimentation in the Paraíba Basin, Northeastern Brazil: Landform, sea level and tectonics in Eastern South America passive margin. Palaeogeogr. Palaeoclimatol. Palaeoecol. 300, 191–204.
Rowley, D.B., Sahagian, D., 1986. Depth-dependent stretching: A different approach. Geology 14, 32–35.
Ruppel, C., 1995. Extensional processes in continental lithosphere. J. Geophys. Res. 100, 24187.
Salvini, F., Brancolini, G., Busetti, M., Storti, F., Mazzarini, F., Coren, F., 1997. Cenozoic geodynamics of the Ross Sea region, Antarctica: Crustal extension, intraplate strike-slip faulting, and tectonic inheritance. J. Geophys. Res. 102, 24669.
Sandwell, D.T., Smith, W.H.F., 1997. Marine gravity anomaly from Geosat and ERS 1 satellite altimetry. J. Geophys. Res. 102, 10039.
Sawyer, D.S., Coffin, M.F., Reston, T.J., Stock, J.M., Hopper, J.R., 2007. COBBOOM: The Continental Breakup and Birth of Oceans Mission. Sci. Drill. 5, 13–25.

Schlische, R.W., Withjack, M.O., 2009. Origin of fault domains and fault-domain boundaries (transfer zones and accommodation zones) in extensional provinces: Result of random nucleation and self-organized fault growth. J. Struct. Geol. 31, 910–925.

Schreurs, G., Buiter, S.J.H., Boutelier, D., Corti, G., Costa, E., Cruden, A.R., Daniel, J.-M., Hoth, S., Koyi, H.A., Kukowski, N., Lohrmann, J., Ravaglia, A., Schlische, R.W., Withjack, M.O., Yamada, Y., Cavozzi, C., Del Ventisette, C., Brady, J.A.E., Hoffmann-Rothe, A., Mengus, J.-M., Montanari, D., Nilforoushan, F., 2006. Analogue benchmarks of shortening and extension experiments. Geol. Soc. London, Spec. Publ. 253, 1–27.

Scotchman, I.C., Gilchrist, G., Kusznir, N.J., Roberts, A.M., Fletcher, R., 2010. Petroleum Geology: From Mature Basins to New Frontiers—Proceedings of the 7th Petroleum Geology Conference, Geological Society, London, Petroleum Geology Conference series. Geological Society of London.

Sibuet, J.-C., Srivastava, S., Manatschal, G., 2007. Exhumed mantle-forming transitional crust in the Newfoundland-Iberia rift and associated magnetic anomalies. J. Geophys. Res. 112, B06105.

Smith, M., Mosley, P., 1993. Crustal heterogeneity and basement influence on the development of the Kenya Rift, East Africa. Tectonics 12, 591–606.

Sokoutis, D., Corti, G., Bonini, M., Pierre Brun, J., Cloetingh, S., Mauduit, T., Manetti, P., 2007. Modelling the extension of heterogeneous hot lithosphere. Tectonophysics 444, 63–79.

Srivastava, S.P., Sibuet, J.-C., Cande, S., Roest, W.R., Reid, I.D., 2000. Magnetic evidence for slow seafloor spreading during the formation of the Newfoundland and Iberian margins. Earth Planet. Sci. Lett. 182, 61–76.

Stewart, J., Watts, A.B., Bagguley, J.G., 2000. Three-dimensional subsidence analysis and gravity modelling of the continental margin offshore Namibia. Geophys. J. Int. 141, 724–746.

Storti, F., Salvini, F., Rossetti, F., Phipps Morgan, J., 2007. Intraplate termination of transform faulting within the Antarctic continent. Earth Planet. Sci. Lett. 260, 115–126.

Strummer, J., 19xx. The future is unwritten

Suguio, K., Bezerra, F.H.R., Barreto, A.M.F., 2011. Luminescence dated Late Pleistocene wave-built terraces in northeastern Brazil. An. Acad. Bras. Cienc. 83, 907–920.

Sun, Z., Zhong, Z., Keep, M., Zhou, D., Cai, D., Li, X., Wu, S., Jiang, J., 2009. 3D analogue modeling of the South China Sea: A discussion on breakup pattern. J. Asian Earth Sci. 34, 544–556.

Sykes, L.R., 1978. Intraplate seismicity, reactivation of preexisting zones of weakness, alkaline magmatism, and other tectonism postdating continental fragmentation. Rev. Geophys. 16, 621.

Szatmari, P., 2000. Habitat of Petroleum Along the South Atlantic Margins, in: Mello, M.R., Katz, B.J. (Eds.), Petroleum Systems of South Atlantic Margins: AAPG Memoirs 73. AAPG, pp. 69–75.

The GEBCO_08 Grid, version 20100927, http://www.gebco.net [WWW Document], n.d. URL http://www.gebco.net

Tommasi, A., Vauchez, A., 2001. Continental rifting parallel to ancient collisional belts : an e ¡ ect of the mechanical anisotropy of the lithospheric mantle. Earth

Planet. Sci. Lett. 185, 199 – 210.
Torsvik, T.H., Rousse, S., Labails, C., Smethurst, M.A., 2009. A new scheme for the opening of the South Atlantic Ocean and the dissection of an Aptian salt basin. Geophys. J. Int. 177, 1315–1333.
Trudgill, B.D., 2002. Structural controls on drainage development in the Canyonlands grabens of southeast Utah. Am. Assoc. Pet. Geol. Bull. 86, 1095–1112.
Tsikalas, F., Eldholm, O., Faleide, J.I., 2005. Crustal structure of the Lofoten–Vesterålen continental margin, off Norway. Tectonophysics 404, 151–174.
Tsikalas, F., Faleide, J.I., Eldholm, O., Antonio Blaich, O., 2012. The NE Atlantic conjugate margins, in: Regional Geology and Tectonics: Phanerozoic Passive Margins, Cratonic Basins and Global Tectonic Maps. pp. 140–201.
Tsikalas, F., Inge Faleide, J., Eldholm, O., 2001. Lateral variations in tectono-magmatic style along the Lofoten–Vesterålen volcanic margin off Norway. Mar. Pet. Geol. 18, 807–832.
Turcotte, D.L., Schubert, G., 2002. Geodynamics (2nd ed.). Cambridge University Press, Cambridge, New York, Melbourne.
Unternehr, P., Peron-Pinvidic, G., Manatschal, G., Sutra, E., 2010. Hyper-extended crust in the South Atlantic: in search of a model. Pet. Geosci. 16, 207–215.
Van der Beek, P., Cloetingh, S., Andriessen, P., 1994. Mechanisms of extensional basin formation and vertical motions at rift flanks: Constraints from tectonic modelling and fission-track thermochronology. Earth Planet. Sci. Lett. 121, 417–433.
Van Wijk, J.W., 2005. Role of weak zone orientation in continental lithosphere extension. Geophys. Res. Lett. 32, L02303.
Vauchez, A., Neves, S., Caby, R., Corsini, M., Egydio-Silva, M., Arthaud, M., Amaro, V., 1995. The Borborema shear zone system, NE Brazil. J. South Am. Earth Sci. 8, 247–266.
Vauchez, A., Tommasi, A., 2003. Wrench faults down to the asthenosphere: geological and geophysical evidence and thermomechanical effects. Geol. Soc. London, Spec. Publ. 210, 15–34.
Vendeville, B., Cobbold, P.R., Davy, P., Choukroune, P., Brun, J.P., 1987. Physical models of extensional tectonics at various scales. Geol. Soc. London, Spec. Publ. 28, 95–107.
Watts, A.B., Fairhead, J.D., 1999. Process-oriented approach to modeling the gravity signature of continental margins. Lead. Edge (Tulsa, OK) 18.
Watts, A.B., Ryan, W.B.F., 1976. Flexure of the lithosphere and continental margin basins. Tectonophysics 36, 25–44.
Watts, A.B., Steckler, M.S., 1979. Subsidence and eustacy at the continental margin of eastern North America, in: Talwani, M., Hay, W., Ryan, W.B.F. (Eds.), Deep Drilling Results in the Atlantic Ocean: Continental Margins and Paleoenvironments, Maurice Ewing Series 3,. AGU, Washington, D. C., pp. 218–234.
Watts, A.B., Stewart, J., 1998. Gravity anomalies and segmentation of the continental margin offshore West Africa. Earth Planet. Sci. Lett. 156, 239–252.
Watts, A.B., Torné, M., 1992. Subsidence history, crustal structure, and thermal evolution of the Valencia Trough: A young extensional basin in the western Mediterranean. J. Geophys. Res. 97, 20021.
WDMAM, W.D.M.A.M., 2007. World Digital Magnetic Anomaly Map (WDMAM),

in: IAGA, International Association of Geomagnetism and AeronomyIUGG, Perugia, Italy (2007).
Weijermars, R., Schmeling, H., 1986. Scaling of Newtonian and non-Newtonian fluid dynamics without inertia for quantitative modelling of rock flow due to gravity (including the concept of rheological similarity). Phys. Earth Planet. Inter. 43, 316–330.
Wernicke, B., 1981. Low-angle normal faults in the Basin and Range Province: nappe tectonics in an extending orogen. Nature 291, 645–648.
Wernicke, B., 1985. Uniform-sense normal simple shear of the continental lithosphere., Canadian Journal of Earth Sciences.
Whitmarsh, R.B., Miles, P.R., 1995. Models of the development of the West Iberia rifted continental margin at 40°30′ N deduced from surface and deep-tow magnetic anomalies. J. Geophys. Res. 100, 3789.
Whitmarsh, R.B., Sawyer, D.S., 1996. The Ocean/Continent Transition beneath the Iberia Abyssal Plain and Continental-Rifting to Seafloor-Spreading Processes. Proc. Ocean Drill. Progr. Sci. Results 149, 713–733.
Whitmarsh, R.B., White, R.S., Horsefield, S.J., Sibuet, J.-C., Recq, M., Louvel, V., 1996. The ocean-continent boundary off the western continental margin of Iberia: Crustal structure west of Galicia Bank. J. Geophys. Res. 101, 28291.
Wilson, J.T., 1965. A New Class of Faults and their Bearing on Continental Drift. Nature 207, 343–347.
Wyer, P., Watts, A.B., 2006. Gravity anomalies and segmentation at the East Coast, USA continental margin. Geophys. J. Int. 166, 1015–1038.
Younes, A.I., McClay, K., 2002. Development of accomodation zones in the gulf of Suez-Red Sea rift, Egypt. Am. Assoc. Pet. Geol. Bull. 86, 1003–1026.
Yuri, N.L., 2010. Il mondo prima, in: The future is unwritten, eds. Lagomarsino, D. , Special Pubblication, Bologna, 1-∞
Zalán, P.V., Severino, M.C.G., Rigoti, C.A., Magnavita, L.P., de Oliveira, J.A.B., Viana, A.R., 2011. An entirely new 3D-view of the crustal and mantle structure of a South Atlantic passive margin — Santos, Campos and Espírito Santo Basins, Brazil, in: AAPG Annual Conference and Exhibition. Making the Next Giant Leap in Geosciences. April 10–13, 2011, Houston, Texas (2011) (AAPG, Search and Discovery Article, 90124. World Wide Web Address:
Ziegler, P. a., Cloetingh, S., 2004a. Dynamic processes controlling evolution of rifted basins. Earth-Science Rev. 64, 1–50.
Ziegler, P. a., Cloetingh, S., 2004b. Dynamic processes controlling evolution of rifted basins. Earth-Science Rev. 64, 1–50.

a Daniela
e a i nostri figli.